

**The author(s) shown below used Federal funds provided by the U.S. Department of Justice and prepared the following final report:**

**Document Title:           Quantitative Assessment of the Individuality of Friction Ridge Patterns**

**Author:                     Sargur N. Srihari**

**Document No.:           227842**

**Date Received:          August 2009**

**Award Number:          2005-DD-BX-K012**

**This report has not been published by the U.S. Department of Justice. To provide better customer service, NCJRS has made this Federally-funded grant final report available electronically in addition to traditional paper copies.**

**Opinions or points of view expressed are those of the author(s) and do not necessarily reflect the official position or policies of the U.S. Department of Justice.**

# *Quantitative Assessment of the Individuality of Friction Ridge Patterns*

## FINAL REPORT

**Award Number: 2005-DD-BX-K012**

**SUBMITTED TO:**

U.S. Department of Justice  
Office of Justice Programs  
National Institute of Justice  
810 Seventh Street N.W.  
Washington, DC 20531

**AWARDEE:**

Research Foundation of the State University of New York

**Author:**

Sargur N. Srihari  
520 Lee Entrance, Suite 202  
University at Buffalo, State University of New York  
Buffalo, New York 14260  
Tel: 716-645-6164 ext 113  
Email: srihari@cedar.buffalo.edu

March 20, 2009

## Abstract

The goal of this project was to increase understanding of the discriminative power of friction ridge patterns using computational approaches. A three-pronged approach was taken: (i) a study of the fingerprints of twins using automatic fingerprint matching algorithms, (ii) modeling the probability distribution of fingerprints from which the probability of random correspondence of fingerprints is determined— this is the generative approach to individuality, and (iii) new algorithms for feature extraction and classification are used to determine error probabilities— this is the discriminative approach to individuality. The main conclusion of the twins' study is that although friction ridge patterns of twins are more similar than in the general population, they are still discriminable. The twins' findings strengthen the argument of fingerprint individuality. Taking the generative approach the individuality of a forensic modality can also be established by computing the probability of random correspondence of two pieces of evidence directly from the underlying probability distribution of evidence features. The distribution can be modeled as a mixture distribution whose parameters can be determined from a database of fingerprints. First a model consisting of only minutiae was considered and then expanded to include ridge information as well. It was found that the probability of random correspondence with ridges is much lower than with minutiae alone. These probabilities were quantified in terms of the available number of minutiae and ridge points. In the discriminative approach two new approaches to automatic fingerprint comparison were developed: use of likelihood methods instead of ROC-based methods, and using ridge information in addition to minutiae in fingerprint comparison. Both discriminative studies point to improved performance particularly when there are fewer minutiae available in the input as in the case of latent prints.

# Contents

<b>1</b>	<b>Executive Summary</b>	<b>2</b>
<b>2</b>	<b>Final Report Narrative</b>	<b>4</b>
2.1	Introduction . . . . .	4
2.1.1	Statement of the problem . . . . .	4
2.1.2	Literature citation and review . . . . .	5
2.1.3	Rationale for the research . . . . .	9
2.2	Methods . . . . .	10
2.2.1	Discriminability of Twin’s Fingerprints . . . . .	10
2.2.2	Generative Model of Fingerprints . . . . .	15
2.2.3	Likelihood-based Methods for Fingerprint Comparison . . . . .	25
2.2.4	Use of Ridge Information in Fingerprint Comparison . . . . .	31
2.3	Results . . . . .	45
2.3.1	Statement of Results . . . . .	45
2.3.2	Tables . . . . .	48
2.3.3	Figures . . . . .	56
2.4	Conclusions . . . . .	86
2.4.1	Discussion of Findings . . . . .	86
2.4.2	Implications for Policy and Practice . . . . .	86
2.4.3	Implications for Further Research . . . . .	86
<b>3</b>	<b>References</b>	<b>87</b>
<b>4</b>	<b>Dissemination</b>	<b>93</b>
4.1	Publications . . . . .	93
4.1.1	Journal Papers . . . . .	93
4.1.2	Papers in Conference Proceedings . . . . .	93
4.2	Presentations . . . . .	94
4.2.1	Conferences . . . . .	94
4.2.2	General . . . . .	94

# Chapter 1

## Executive Summary

The central focus of the project was to study the discriminability of friction ridge patterns using computational approaches. Computational approaches provide large scale testing and evaluation that are not feasible using manual approaches. They also provide a method for evaluating probabilities of interest. The approach was a three-pronged one: (i) a study of the fingerprints of twins using automatic fingerprint matching algorithms, (ii) determining the probability distribution of fingerprints using different feature sets which can then be used to determine the probability of random correspondence of fingerprints, and (iii) determining error rates of automatic fingerprint matching algorithms. There were two efforts focusing on the classification and feature extraction parts of discrimination: improving automatic fingerprint comparison using a likelihood based approach (instead of the standard receiver operating characteristics (ROC) approach), and use of ridge information in automatic fingerprint comparison.

**1. Twin's Study.** The use of a cohort groups such as twins to study various physiological and behavioral characteristics is well-known. The data used in this study was of higher quality and quantity compared to previous limited such studies of fingerprints. The data set consisted of prints of predominantly young subjects— with 298 pairs of twins, whose ten prints were captured (by the International Association for Identification) using a live scan device. Fingerprint discriminability using level 1 and level 2 features were independently determined. The level 1 study was to visually classify, by humans, each fingerprint into one of six categories (right loop, left loop, whorl, arch, twin loop and tented arch). It was found that twins are much more likely (55%) to have similar level 1 classification when compared to to the general population of fingerprints (32%). The level 2 study was to compare minutiae (ridge endings and bifurcations) using a minutiae-based automatic fingerprint identification algorithm which provided match scores (0-350) for fingerprint pairs. Distributions of scores were computed for corresponding fingers of twins and non-twins. Five distributions of scores were computed: twins, non-twins, identical twins, fraternal twins and genuine scores for the same finger. Using statistical tests to compare distributions, the following inferences were made: twin pairs are different from genuine pairs, twins are different from non-twins, identical twins are the same as fraternal twins, and similarity of twins is different from similarity between arbitrary fingers. The main conclusion is that although friction ridge

patterns of twins are more similar than in the general population, they are still discriminable. The findings strengthen the argument of fingerprint individuality.

**2. Probability Distributions of Fingerprints.** Generative models of pattern recognition attempt to represent the distribution of observed quantitative features by learning parameters from a database. When the distributions are learnt and validated they can be used for several purposes, e.g., generate samples to evaluate algorithms, determine the probability of two random patterns being the same (thereby providing a measure of individuality for the modality), determine the uniqueness of a given pattern, etc. The joint probability of minutiae location, minutiae orientation and ridge point location and orientation was modeled as a mixture distribution. The parameters of the distribution were estimated using a database of fingerprints. Given the distribution (model) several probabilities were evaluated, principally the *probability of random correspondence (PRC)*, which is the probability that two independently drawn samples have the same value. Given the PRC, the probability that given  $n$  fingerprints the probability that at least two among them have the same value can be directly computed. Finally, the probability that a specific fingerprint has a match, within a certain tolerance, with at least one among  $n$  can also be computed. Motivated by the fact that ridges have not been modeled in generative models, and using representative ridge points in fingerprint matching, ridge information was incorporated into the generative model by using the distribution for ridge point location and orientation. It was found that the PRC with ridges is much lower than with minutiae alone. As a consequence of this study a general mathematical approach to determining the degree of individuality of any forensic modality has been formulated.

**3. Error Rates of Fingerprint Comparison Algorithms.** An alternative computational approach to evaluating discriminability is to evaluate error rates of fingerprint comparison algorithms. Two main components of any automatic fingerprint comparison algorithm are the features extracted and the method of classification. The error rates are dependent on these two choices. Two algorithm development tasks focusing on each of these components were undertaken and their error rates were evaluated:

1. **Use of likelihood methods.** The use of likelihood methods was seen to improve fingerprint matching results when compared with traditional receiver operation characteristics (ROC)-based methods. This improvement was particularly significant when there are few minutiae in the input image, as would be likely in the case of latent prints.
2. **Use of ridge features.** Ridge information used in conjunction with minutiae was seen to improve performance over using minutiae alone. An algorithm was proposed to incorporate ridge information into existing minutiae-based algorithms without significant degradation in speed.

# Chapter 2

## Final Report Narrative

### 2.1 Introduction

The use of fingerprint evidence in the justice system has been based on two premises, that, (i) they do not change with time and (ii) they are unique for each individual. Until recently, fingerprint evidence has been accepted by the courts without question as a legitimate means of identification. However, after a series of rulings in United States courts, beginning with *Daubert v Merrell Dow* in 1993 [1] and particularly in *USA vs Mitchell* in 1999 [2], a need has been felt to scientifically test the premises stated above. While the first premise has been accepted, the second premise on individuality has been questioned. This latter is the subject of this investigation.

This project is an effort to increase existing knowledge of the discriminatory power of fingerprints. Although there have been dozens of such studies in the past, the present effort is to use newly developed computational methods such as scanning technologies and machine learning methodologies to study the issues on a scale that was not possible earlier.

The terms class characterization and individualization are commonly used in forensics. In addition terminology from the biometric domain, such as verification and identification are also present. Thus it is useful to first define these terms. Class-characterization is the narrowing down of the evidence into a sub-class within the forensic modality, e.g., ethnicity. Individualization is sometimes defined as the exclusion of all other sources for the given evidence. Verification is the determination of whether a given evidence is from a given source and is a binary decision. Identification is the determination of the best match of the evidence given a finite set of sources for that evidence. Finally individuality of a forensic modality or of a piece of forensic evidence is the degree of distinctiveness of that type of evidence in a population.

#### 2.1.1 Statement of the problem

The central focus of the project is to study the discriminability of fingerprints using computational approaches. Computational approaches provide large scale testing and evaluation that are infeasible using manual approaches. They also provide a means of evaluating various probabilities of interest in fingerprint comparison.

The effort was a three-pronged one. The first was to study the discriminability of a cohort group such as twins. The second was to model the statistical distributions of fingerprint features so that different probabilities of interest can be evaluated, e.g., probability of random correspondence of full and partial fingerprints; where the features considered were minutiae as well as ridge flow. The third was to determine error rates of automatic fingerprint comparison algorithms such as those used in fingerprint identification systems (AFIS) type; both standard algorithms and their improvements were considered.

### 2.1.2 Literature citation and review

The approach of fingerprint analysis is described in several text-books on the subject, including the early classics [3, 4, 5] and more recent ones [6, 7, 8]. In the following we give a brief overview and literature survey, dividing the discussion into four parts: (A) fingerprint features, (B) AFIS algorithms for minutiae detection and comparison, (C) twin's studies, and (D) individuality models. Throughout the discussion the focus is on AFIS type approaches. However the goal is to provide results of value for forensic analysis of latent prints and ten prints.

#### A. Fingerprint Features

The premise of fingerprint verification and identification is that the local ridge structures of fingers are unique given a sufficient amount of detail. Eighteen types of local ridge descriptions have been identified [9, 10].

Features for representing fingerprints are usually grouped into three types [8]. Level 1 features provide class-characterization of fingerprints based on ridge flow. They are divided into five primary classes: whorl, left loop, right loop, arch and tent (Figure 2.1). Some of the primary classes have secondary classes resulting in more than five class types. Level 1 features are useful only to exclude possibilities and are insufficient for individualization.

Level 2 features, which are more useful for individualization are also known as minutiae. Fingerprints such as those shown in Figure 2.1 are first aligned. This is done manually where core points are identified and then the image is centered. The minutiae correspond to ridge endings and ridge bifurcations. Automatic fingerprint matching algorithms use minutiae as the salient features, e.g., [11], since they are stable and are reliably extracted. A minutia is represented by its location and direction; direction is determined by the ridge ending at the location (Figure 2.2). The type of minutiae (either bifurcation or ending) is not distinguished since this information is not as reliable as the information on location and direction. Level 3 features, such as pores and scars are ancillary features.

Ridge endings and ridge bifurcations (Fig. 2.2(a)) are the two most prominent structures which are usually called minutiae. Normally, minutiae detection algorithms [11, 12] firstly define a set of template patterns that ridge endings or bifurcations would present like, and then compare local patterns with these template patterns while scanning the binary image of a fingerprint. With candidate minutiae indicated by the pattern matching stage, a post-process to remove false minutiae are performed with various criteria [11]. Figure 2.2(b) displays detected minutiae on a skeleton fingerprint image.

Motivated by the fact that human examiners use general ridge information as well as minutiae, several algorithms [13, 14, 15, 16, 17, 18] have been proposed to utilize ridges for automatic fingerprint matching. However, existing algorithms mostly suffer from (i) sensitivity to non-linear deformation, (ii) much higher computational complexity and (iii) unscalable to partial fingerprint matching.

## B. AFIS Algorithms

The most important part of the study involves level 2 features since they are what are primarily used by AFIS systems. Level 2 features consist of minutiae which are either ridge endings or ridge bifurcations. Each minutia is represented by a 3-tuple  $(x, y, \theta)$  representing its position and orientation in the fingerprint image.

When an input print is to be matched against the database two types of minutiae are extracted: ridge endings and ridge bifurcations. Both minutiae are represented as triples  $(x, y, \theta)$  where  $x$  and  $y$  are the two-dimensional coordinates and  $\theta$  is the angle made by a short line segment representing the minutiae. The direction of the line segment is determined by the direction of the ridge in the case of a ridge ending. In the case of a bifurcation the direction is determined by the bisector of the angle between the two bifurcating ridges.

**Minutia Detection.** Several algorithms and software for detecting minutiae in friction ridge images are available. A program available from NIST known as MINDTCT (pronounced “min-detect” for minutiae detector) takes as input a friction ridge image file, generates image maps, binarizes the image, detects minutiae, removes false minutiae, counts neighbor ridges, assesses minutiae quality and outputs a minutiae file. The MINDTCT program performed well in a recent competitive test (known as FPVTE [19]) conducted for the US Visit program; the best was a product from NEC. An advantage of the MINDTCT program is that the source code is freely available and therefore modifiable for research purposes. Yet for the purpose of latent print examination it may be relevant that a program such as MINDTCT may miss detecting some minutiae and detect false minutiae. When many minutiae (30 to 40) are correctly located, the fact that a few are missing or that a few are false may be inconsequential.

**Minutia Matching.** With detected minutiae, fingerprint matching could be achieved with point pattern matching (minutiae matching). A number of minutiae-based matching algorithms with varying accuracy and efficiency are described in the literature. The capability of a fingerprint matcher to find true correspondences between prints of the same finger while minimizing mismatches is the measure of performance of a matching algorithm. Due to frequent non-linear deformation in fingerprint images, directly ensuring global correspondence is very difficult. Most matching algorithms tend to first compute local similarity and then perform global consolidation. The result of comparing two fingerprints is expressed as a similarity or distance measure. It signifies the strength of match between two fingerprints each of which is represented by a feature set. The similarity measure converts the data from feature space to *distance* space.

## 2.1. INTRODUCTION

## CHAPTER 2. FINAL REPORT NARRATIVE

When fingerprints are characterized by minutiae a value in distance space is the result of comparing two sets of minutiae. Each minutia is characterized by a triplet  $\{x, y, \theta\}$ , corresponding to the  $(x, y)$  coordinates of the minutia and its angular direction  $\theta$ . The following procedure can be used to compute a distance measure between two fingerprint imprints. Let  $T$  be a template image with  $M$  minutiae and  $I$  be the input image with  $N$  minutiae:

$$T = \{m_1, m_2, \dots, m_M\} \quad \text{where} \quad m_i = \{x_i, y_i, \theta_i\}, \quad i = 1, \dots, M. \quad (2.1)$$

$$I = \{m_1', m_2', \dots, m_N'\} \quad \text{where} \quad m_j' = \{x_j', y_j', \theta_j'\}, \quad j = 1, \dots, N. \quad (2.2)$$

The distance between a minutia  $m_j'$  in  $I$  and a minutia  $m_i$  in  $T$  can be calculated using *spatial distance* ( $sd$ ) and *direction difference* ( $dd$ )

$$sd(m_j', m_i) = \sqrt{(x_j' - x_i)^2 + (y_j' - y_i)^2} \quad (2.3)$$

$$dd(m_j', m_i) = \min(|\theta_j' - \theta_i|, 360^\circ - |\theta_j' - \theta_i|) \quad (2.4)$$

Note that  $sd$  is the Euclidean distance and  $dd$  lies in the interval  $[0, \pi]$ .

Fingerprint matching algorithms are based on the structure of minutiae within a given fingerprint. This structure can be captured by pairs of minutiae, triples of minutiae or even a set of  $k$  minutiae. Each of these is briefly described below.

*Pair of Minutiae* The simplest local model is to define a minutia pair, as in the case of the Bozorth algorithm [11]. An intra-fingerprint minutiae pair table is constructed to capture relative position and orientation of a pair of minutiae. For each pair  $m_i, m_j$  where  $i$  and  $j$  are the index of minutiae, the local model vector is maintained as  $[d_{ij}, \beta_i, \beta_j, \theta_{ij}, i, j]$ . Here  $d_{ij}$  indicates the relative distance between minutiae  $m_i$  and  $m_j$ .  $\beta_i$  and  $\beta_j$  measure the relative angle of the minutiae with respect to the connecting line. Besides these relative measurements, absolute orientation of the connecting line  $\theta_{ij}$  is maintained for later global consolidation. (See Figure 2.3(a)). These pairwise measurements are made for each pair of minutiae where the connecting distance  $d_{ij}$  is less than a fixed threshold. In global consolidation, for a fingerprint pair, the Bozorth algorithm constructs a third table from the two intra-fingerprint tables. This inter-fingerprint compatibility table has potential associations between the two intra-fingerprint minutiae pair tables. The inter-fingerprint compatibility table is searched for the longest path of linked compatible associations.

The *Bozorth matcher* algorithm is designed to be rotation and translation invariant. There are three main steps in the matcher: (i) construct an intra-fingerprint minutiae comparison table, (ii) construct an Inter-fingerprint compatibility table, (iii) traverse the inter-fingerprint compatibility table. A score corresponding to this longest path is then generated. The Bozorth score is typically in the range 0-50 for impostor scores and can be as high as 350 for genuine scores. Other AFIS algorithms have similar scores but different ranges.

*Minutia Triplet* The next level of complexity of a local model is to use a central minutia and two nearest neighbors, which together constitute a triplet. The triplet can be characterized by a feature vector that contains minutiae information as well as ridge counts (No.

of ridges between two minutiae). An eleven dimensional feature vector was proposed in [54]. This can be simplified to include only minutiae information, thereby reducing the feature vector to a five-dimensional one [52]. This vector can be written as:  $[d_{i0}, d_{i1}, \phi_{ij}, \phi_{ik}, \theta_i]$  where  $d_{i0}$  and  $d_{i1}$  respectively represents the distance from minutiae  $M_i$  to its nearest neighbors  $N_0$  and  $N_1$ ;  $\phi_{ik}$  is the orientation difference between  $M_i$  and  $N_k$  ( $k$  is 0 or 1); and  $\theta_i$  represents the acute angle between the line segments  $M_iN_0$  and  $M_iN_1$ . (See Fig. 2.3(b)). In global consolidation, after the potentially corresponding triplet pairs have been identified, a histogram of the global rotation parameter is constructed. The peak of the histogram corresponds to the optimal rotation angle. Potentially corresponding triplet pairs are pruned by checking the differences between their individual rotation parameters and the optimal one. In the end, Minimum Cost Flow (MCF) [55] technique is used to find optimal correspondence between two fingerprints.

*k Minutiae* The most general local model is to use a central minutia and a set of  $k$  nearest neighbors. One such local model[53] includes a central minutia  $m_i$  and  $k$  other minutiae  $m_1, m_2, \dots, m_k$  chosen from its local neighborhood. The feature vector for each central-neighbor minutiae pair is  $(\phi_{ij}, \theta_{ij}, \gamma_{ij})$  (See Figure 2.3(c)), where  $\phi_{ij}$  represents the direction of the edge connecting the two minutia  $m_i$  and  $m_j$  ( $j = 1, \dots, k$ ), which is measured relative to orientation of minutia  $m_i$ ;  $\theta_{ij}$  is the relative orientation of minutia  $m_j$  ( $j = 1, \dots, k$ ) with respect to the central minutia  $m_i$ ; and  $\gamma_{ij}$  represents the distance between minutiae  $m_i$  and  $m_j$  ( $j = 1, \dots, k$ ). In global consolidation, the method of [53] first converts a fingerprint represented by local  $k$ -minutiae models to an adjacency graph and then performs coupled breadth first search (CBFS) to search for minutiae correspondence between two fingerprints.

## C. Twin's Studies

The study of twins has been important in various physiological [20, 21, 22] and behavioral [23] settings. Genetic and environmental similarities of twins allow studies such as the effectiveness of drugs, presence of psychological traits, etc. By examining the degree to which twins are differentiated, a study may determine the extent to which a particular trait is influenced by genetics or by the environment.

In forensics and biometrics, few twin studies have been carried out in any modality due to the lack of sufficient data. Such studies are important since any modality needs to be evaluated in conditions under which the possibility of error is maximum, i.e., the worst-case scenario. Satisfactory performance with twins strengthens the reliability of the method. It also establishes the degree of individuality of the the particular trait. Such an individuality measure is relevant from the viewpoint of Daubert challenges in forensic testimony [1].

A significant number of twin pairs (206) have been studied for handwriting [24]. These samples were processed with features extracted and conclusions drawn by comparing verification performances with twins and non-twins. In that study the conclusion was that twins are discriminable but less so than an arbitrary pair of individuals.

A fingerprint twin study has been previously reported with a small data set of 94 pairs of index fingers [25]. Using a state-of-the-art fingerprint verification system it was concluded that identical twins are discriminable with lower accuracy than non-twins. The slight difference was attributed to the dependence of minutiae distribution on fingerprint class. The

present study involves a much larger set of nearly 3,000 pairs of fingers.

The question to be answered is whether there exists a higher degree of match between individuals who are twins rather than when the individuals are not twins. The goal is to determine if friction ridge patterns from cohorts (twins) are more difficult to tell apart.

## D. Individuality Models

Fingerprint individuality studies started in the late 1800s. A critical analysis of the models proposed up to about 2000 has been made by Stoney [26, 27]. The goal of this part of the project was to place this work in the context of Stoney's work— by providing a new organization of the models— and focus on some of the newer generative models.

About twenty models have been proposed trying to establish the improbability of two different fingers having the same fingerprint. The models, which are mostly based on minutiae, try to quantify the uniqueness property. The models are used to find out the probability of false correspondence, i.e., probability that a wrong person is identified given a latent fingerprint collected from a crime scene from a set of previously recorded whole fingerprints. A match here does not necessarily mean an exact match but a match within given tolerance levels. The models can be classified into different categories based on the approach taken. The models typically establish the probability of two samples being identified as the same based on their fingerprint features— which is referred to as the *probability of random correspondence (PRC)*.

The models can be classified for better understanding based on the different approaches taken. Figure 2.3.3 shows such a taxonomy of different individuality models. There are five different model categories: grid-based, ridge-based, fixed probability, relative measurement and generative. Grid-based models include Galton[3] and Osterburg[28] which were proposed in the late 80s and the early 90s respectively. Ridge-based models include the Roxburgh model[29, 30]. Fixed probability models contain the class of Henry-Balthazard[4, 31] models. Relative measurement models include the Champod model[32] and the Trauring model[33].

Statistical models in pattern recognition can be divided into those that are discriminative and those that are generative [34]. In discriminative models the probability of classification error is computed and used as a measure of individuality[35]. In generative models a distribution of the features is inferred from the data which is then used to compute the probability of random correspondence. In the case of fingerprints, the distribution of fingerprint features is modeled from a database from which the PRC can then be computed [36, 37, 38] .

### 2.1.3 Rationale for the research

The individuality study has a three-fold complementary approach: a study of the fingerprints of twins using automatic fingerprint matching algorithms and a computational evaluation of the individuality of fingerprints using generative and discriminative approaches.

Cohort studies involving twins are commonly used in physiological and behavioral sciences because they are likely to provide two samples having the maximum likelihood of being similar. In the case of comparing forensic evidence cohort studies can provide an upper bound on the error that could be expected.

The generative approach to measuring individuality is based on sound statistical principles. It involves a two-step process in which a statistical model is first inferred and it is then used to derive a probability. There are several advantages in using a generative model over a discriminative model, e.g., assumptions made in deriving the model are explicit, models derived from different data sets can be compared without dependence on the particular classification method used.

The discriminative approach to measuring fingerprint individuality directly addresses the issue of error rates. Any discriminative approach involves two aspects: feature extraction and classification. Both of these were addressed in this research. The use of likelihood-based approaches is an effort to improve classification methods and the use of ridge information is an effort to improve feature extraction.

## 2.2 Methods

Description of methods used in this research are divided into four parts: discriminability of twin's fingerprints (Section 2.2.1), generative model of fingerprint individuality (Section 2.2.2), use of likelihood-based methods in fingerprint comparison (Section 2.2.3) and use of ridge information in fingerprint comparison (Section 2.2.4).

### 2.2.1 Discriminability of Twin's Fingerprints

#### A. Data Set and Methodology

Two data sets were used in this study. The principal data set consisted of friction ridge patterns of over six hundred pairs of twins. This data set was collected by the International Association for Identification (IAI) at a twins festival held in Twinsburg, Ohio in August 2003. The friction ridge images of 610 individuals corresponds to: 297 sets of twins, 5 pairs of twins along with their families, 5 sets of twins with inconclusive or no DNA analysis results, and three sets of triplets. For each individual there are ten fingerprints, thus making available 2,970 pairs of twin's fingers. In addition there are writer palm prints. The twins' images were all obtained using a live-scan device at 500 dpi. Fig. 2.5 shows a sample of pairs of twin fingerprints. Fig. 2.6 shows 10 rolled fingerprints from one individual.

Another data set that was used in the study was a standard data set (non-twin) available from NIST. The FVC2002 DB1 was collected by using optical sensor "TouchView II" by Identix. The database is 110 fingers wide and 8 samples per finger in depth (it consists of 880 fingerprint images in total). The database is partitioned in two disjoint subsets A and B. The subset DB1-A, which contains the first 100 fingers (800 images), is used for the algorithm performance evaluation; the subset DB1-B, containing the last 10 fingers (80 images), is for parameter tuning if necessary. The image format is TIF, 256 gray-level, uncompressed. The image resolution is about 500 dpi and the size is  $388 \times 374$  (142K pixels) The orientation of fingerprint is approximately in the range  $[-15, +15]$  degrees w.r.t the vertical orientation.

**Twin Demographics.** A meta-data table accompanying each folder of fingerprint images gives the demographic information for the individual, code for the individual and a pointer to

his/her twin. The demographic information consists of age, gender, hair color, racial characteristics, whether twins are identical or fraternal, and handedness. The distribution of ages of the twins is given in Fig. 2.7– which shows that the twins in the study are predominantly in their adolescent years and therefore the quality of the prints can be expected to be good. Other meta data details include the hair color, sex, race and handedness(left/right). The corresponding distribution in the database for each is illustrated in Fig. 2.8.

**Study Methodology.** The goal of this study is to determine whether the fingerprints of twins are more similar to each other than in the case of the general population. Friction ridge patterns contained in fingerprints can be analyzed at several levels of features. Level 1 features correspond to visually observable characteristics such as whorl, arch, loop, double whorl, etc. Level 2 features correspond to minutiae, which are points corresponding to ridge endings and ridge bifurcations, that are represented as a triple consisting of  $(x,y)$  coordinates and a direction  $\theta$ . Level 3 features include pores within ridges and other marks.

The analysis reported here was done using only level 1 and level 2 features. The level 1 analysis was done manually and the level 2 analysis was done using algorithms such as those used in an automatic fingerprint identification system (AFIS). In the case of fingerprints we need to ensure some overlap between different portions of the images to always not get an exclusion. For non-twins (and different fingers) test cases can be generated.

## B. Twins' Level 1 Comparison

The first study was to determine the similarities at Level 1. An interface was created to present one fingerprint at a time to the subject on a screen. The observer was asked to determine whether the given print belonged to one of six categories: arch, tented arch, right loop, left loop, whorl and twin loop.

Two individuals independently performed the Level 1 classification. Their individual classifications were then compared. When there was a disagreement in their decision, a third individual did an arbitration to determine the correct classification. Finally, the classification decisions were validated by two professional friction ridge examiners. The overall distribution of the six level 1 features are shown in the chart of Figure 2.9. Level 1 fingerprint classification is known to be somewhat error prone [39]. However the distribution obtained provides an indication of how frequently each class is encountered, i.e., right loop (30%), left loop (27%), whorl (19%), arch (13%), twin loop (7%) and tented arch (5%).

The analysis consisted of determining as to how often the the prints of the same finger in a pair of twins matched and a comparison with the case of non-twins. Examples of pairs of prints when they belonged to identical twins and fraternal twins (same hand and finger) are given in Table 2.2.

The results were as follows. The percentage of times twins had the same level 1 label for a given finger was 54.68%. The percentage of times non-twins had the same level 1 label was 31.76%. Thus we can conclude that twins are nearly twice as likely as non-twins in matching level 1 features. Further, considering only identical twins, the percentage of same level 1 was 56.92% as against 39.44% for fraternal twins.

## 2.2. METHODS

## CHAPTER 2. FINAL REPORT NARRATIVE

Level 1 features are used only as a coarse method of eliminating candidates from a large database as in AFIS. However it has no implication on the discriminability of twins since level 1 features are not used in fingerprint identification.

### C. Twin's Level 2 Comparison

The question to be examined is as to whether the fingerprints match when minutiae are used as features. For this purpose we can use an AFIS type of algorithm which extracts minutiae and performs an identification as being the same or different when given the fingerprint images of twins. The twin and non-twin level 2 error rates are given in Table 2.1.

The scores of corresponding fingers provides a score distribution. We can do this for the fingers of twins. However we will be left with deciding on a threshold of the scores to determine whether it was match or a non-match. Instead, we can obtain a distribution of the scores of non-twins and compare the two distributions. This will help us determine whether they are the same or whether they are different.

The design of statistical experiments for the testing of samples originating from twin pairs is important. The goal is to compare the matching score distribution of twins fingerprints to that of non-twins (see Figure 2.10). How different the distribution of scores of identical twins are from those of fraternal twins is considered.

The approach taken was to use an AFIS type algorithm to quantify the results. The MIN-DTCT algorithm for detecting minutiae and the Bozorth matcher [11], which provides a score for the degree of match of a pair of fingerprints, both of which are available from NIST, was used to compare fingerprint pairs. The final step was to determine the similarity of the distributions. Below is described a brief summary of the algorithm.

Scores for the two populations of non-twins and twins, both for the same finger were obtained using the scenario depicted in Figure 2.10. The results were evaluated in two ways. The first was to simply place thresholds on the scores so as to make "hard" decisions whether the fingerprints had the same origin. The second was to make a "soft comparison" as to whether the score distributions were the same.

Fingerprints from a set of 297 pairs of twins was used to carry out the evaluation. The fingerprints were rolled fingerprints with 10 prints(corresponding to 10 fingers) per person. The total number of prints used were  $297 * 2 * 10 = 5,940$  (i.e., 2,970 twin pairs). Out of these 740 were prints of fraternal twins and the remaining 2,240 were those of identical twins.

Scores provided by the Bozorth matcher were thresholded to provide a hard decision as to whether the input fingerprints originated from the same finger. The thresholds are derived from the genuine and impostor distributions. The genuine distribution comes from multiple fingerprints of the same fingerprint as shown in Figure 2.11(e). The resulting error rates are shown in Table 2.1.

### D. Score Distributions

The error rates are dependent upon a choice of threshold, such as the equal error rate (EER) threshold used in Table 2.1. To remove this dependency, we can instead obtain a distribution

## 2.2. METHODS

## CHAPTER 2. FINAL REPORT NARRATIVE

of the scores and compare it with the distribution of non-twins. This will also help take into account the entire range of values rather than value relative to a single threshold.

The following five distributions were obtained.

1. Twins: The fingerprint of an individual was compared with the corresponding fingerprint of his/her twin. The number of comparisons made is 2,970. Let us denote the distribution of scores from matching twins as  $\mathcal{T}$ .
2. Non-Twins: In this case an individual's fingerprint was compared with the corresponding fingerprint of all other people who were not his/her twin. The total number of comparisons possible was 10 (ten prints)  $\times$  596 (total individuals who are twins)  $\times$  594 (leaving out the individual and his or her twin) = 3,540,240. Out of these 6,650 were used for the experiments based on computational considerations ( $133 \times 10 \times 5$ ). Let us denote the distribution of scores from matching twins as  $\mathcal{N}$ .
3. Identical Twins: This involved comparing fingerprints of identical twin and let us denote this with  $\mathcal{I}$ .
4. Fraternal Twins: This involved comparing fingerprints of fraternal twins and is denoted with  $\mathcal{F}$ .
5. Genuine: Pairs of fingerprints that belong to the same finger were compared against each other to obtain the Genuine distribution. The FVC2002 Db1 data set was used to obtain this particular distribution due to lack of multiple rolled fingerprint samples of the same finger in the twins' database. A total of 100 fingers with 8 samples of each finger constituting a total of 800 prints were present in the FVC2002 Db1 database. These were also obtained as lve scan images at 500 ppi, similar to the twins' dataset.

Histograms of the Bozorth scores for each of the five cases described are shown in Figure 2.11.

### E. Comparing Distributions

Many statistical tests exist to compare two distributions. These tests answer the question: "Can we disprove, with a certain required level of significance, the null hypothesis that the two distributions are drawn from the same population?" as stated in [40]. Some of the most common tests used in order to quantify the difference in the distributions are: chi-square, Kolmogorov-Smirnov (KS), student-T and ANOVA. Amongst these, the Kolmogorov-Smirnov test assumes nothing about the distribution and also can be used on unbinned distributions. Hence, it is chosen as the one that will be used for this statistical study.

The KS test was used to obtain a probability of similarity between two distributions. The KS test is applicable to unbinned distributions that are functions of a single independent variable, that is, to data sets where each data point can be associated with a single number[40]. The test first obtains the cumulative distribution function of each of the two distributions to be compared, and then computes the statistic,  $D$ , which is a particularly simple measure: it

## 2.2. METHODS

## CHAPTER 2. FINAL REPORT NARRATIVE

is defined as the maximum value of the absolute difference between the two cumulative distribution functions. Therefore, if comparing two different cumulative distribution functions  $S_{N_1}(x)$  and  $S_{N_2}(x)$ , the KS statistic  $D$  is given by  $D = \max_{-\infty < x < \infty} |S_{N_1}(x) - S_{N_2}(x)|$ . What makes the KS statistic useful is that its distribution in the case of the null hypothesis (data sets drawn from the same distribution) can be calculated, at least to useful approximation, thus giving the significance of any observed nonzero value of  $D$ . The significance level of an observed value of  $D$  is given approximately [40] by equation 2.5.

$$P_{KS} = \text{Probability}(D_i \text{ Observed}) = Q_{KS} \left( \sqrt{N_e} + 0.12 + (0.11/\sqrt{N_e})D \right), \quad (2.5)$$

where the  $Q_{KS}(\cdot)$  function is given by (see [40] for details):

$$Q_{KS}(\lambda) = 2 \sum_{j=1}^{\infty} (-1)^{j-1} e^{-2j^2\lambda^2}, \quad \text{such that: } Q_{KS}(0) = 1, \quad Q_{KS}(\infty) = 0, \quad (2.6)$$

and  $N_e$  is the effective number of data points,  $N_e = N_1 N_2 (N_1 + N_2)^{-1}$ , where  $N_1$  is the number of data points in the first distribution and  $N_2$  the number in the second. The following sections discuss other methods of comparing two distributions.

The KS test was performed to compare the distributions and to obtain a significance level that the distributions are drawn from the same population. Table 2.3 summarizes the results. The value shown in each of the cell of table 2.3 indicates the significance level with which it can be said that the two distributions are drawn from the same population. The hypothesis tested and their significance and conclusion are given below.

### 1. Test 1

- **Hypothesis:** Similarity of fingerprints of twins is the same as the similarity between genuine prints of the same finger.
- **Significance level:** .1% (refer column 1 in Table 2.3).
- **Deduction:** Hypothesis is rejected since it lesser than 5% signifiacne. It is concluded that similarity of fingerprints of twins is different from that between genuine prints of the same finger.

### 2. Test 2

- **Hypothesis:** Similarity of fingerprints of identical twins is the same as the similarity between fingerprints of fraternal twins.
- **Significance level:** 99.99% (refer column 2 in Table 2.3).
- **Deduction:** Hypothesis is accepted since it is stronger than 95% significance. It is concluded that similarity of fingerprints of identical twins is the same as the similarity between fingerprints of fraternal twins.

### 3. Test 3

- **Hypothesis:** Similarity of fingerprints of twins is the same as the similarity between arbitrary fingers.
- **Significance level:** 11.74% (refer column 3 in Table 2.3).
- **Deduction:** Significance is *not* lesser than 5% to reject the hypothesis. It can however be said that the conclusion is not in favour of the Hypothesis and hence the similarity of fingerprints of twins is different from the similarity between arbitrary fingers.

Further the distributions can also be compared by parametric methods. The distributions being positive can be modeled with Gamma distributions. The corresponding probability density functions are shown in Figure 2.12, which are gamma distributions corresponding to twins( $\mathcal{T}$ ), non-twins( $\mathcal{N}$ ), and same finger distributions  $\mathcal{G}$ .

A slight shift in the twins distribution in comparison to the non-twins distribution can be observed.

### 2.2.2 Generative Model of Fingerprints

Generative models are statistical models that represent the distribution of patterns of interest, where the patterns are represented quantitatively as a vector  $\mathbf{x}$ . They are referred to as being generative in that given the distribution, samples can be generated from them [34]. In these models, a distribution of  $\mathbf{x}$  is learnt through a training data set. There are several practical uses of generative models, e.g., generating samples to test algorithms, evaluating probabilities of random correspondence, evaluating the probability of a given pattern, etc. What training set is used to learn the distribution is immaterial as long as it is representative of the entire population.

Our goal is to model the distribution of fingerprints based on features. The distributions considered are those based on ridge flow types, minutiae only and a combination of minutiae and ridge flow information. In choosing parametric forms to represent distributions, methods for estimating distribution parameters are discussed. The resulting models are validated using goodness-of-fit tests.

#### A. Distribution of Ridge Flow Type

A simple distribution of the Level 1 ridge flow types is obtained by counting the relative frequency of each of the primary and secondary types in a fingerprint database. In our evaluation using the twin's database (Section 2.2.1) loops account for 64% of the fingers, with the secondary types being: 30% left loops, 27% right loops and 7% double loops. Arches account for 18% of the primary types, with the secondary types being: plain arches (13%) and tented arches (5%). Whorls account for the remainder of the Level 1 types (19%).

Level 1 features are clearly broad class characteristics which are useful for exclusion of individual fingers but not by themselves useful for the tasks of verification, identification and individualization.

## B. Distribution of Minutiae

Each minutia is represented as  $\mathbf{x} = (s, \theta)$  where  $s = (x_1, x_2)$  is its location and  $\theta$  its direction. The distribution of minutiae location conditioned on ridge flow is shown in Figure 2.13 where there were 400 fingerprints of each type. In the model we develop the combined distribution over all types is used (Figure 2.13(f)).

Since minutia location has a multimodal distribution, a mixture of  $K$  Gaussians is a natural approach. For the data set considered a value of  $K = 3$  provided a good fit, as validated by a goodness of fit test. Values of  $K = 4, 5$  do not fit the data as well. A Gaussian mixture with  $k = 3$  is shown in Figure 2.14.

Since minutiae orientation is a periodic variable, it is modeled by a *circular normal* or von Mises distribution which itself is derived from the Gaussian [34, 41]. Such a model is better than mixtures of hyper-geometric and binomial distributions [36, 37].

Such a model for minutiae distributions involves a random variable  $z$  that represents the particular mixture component from which the minutia is drawn. In this model both minutiae location and orientation depend on the component they belong to. Minutiae location and orientation are conditionally independent given the component. This is represented by

$$p(\mathbf{x}|z) = p(s, \theta|z) = p(s|z)p(\theta|z), \quad (2.7)$$

whose graphical model is shown in Figure 2.15 from which we have the joint distribution

$$p(\mathbf{x}, z) = p(z)p(\mathbf{x}|z). \quad (2.8)$$

Marginalizing over the components, we have the distribution of minutiae as

$$p(\mathbf{x}) = \sum_z p(z)p(\mathbf{x}|z). \quad (2.9)$$

Substituting (2.7) in (2.9) we have

$$p(\mathbf{x}) = \sum_z p(z)p(s|z)p(\theta|z). \quad (2.10)$$

Since minutiae location within each component is Gaussian and minutiae orientation within each component is von Mises we can write

$$p(\mathbf{x}|\Theta) = \sum_{k=1}^K \pi_k \cdot \mathcal{N}(s|\mu_k, \Sigma_k) \cdot \mathcal{V}(\theta|\nu_k, \kappa_k), \quad (2.11)$$

where  $K$  is the number of mixture components,  $\pi_k$  are non-negative component weights that sum to one,  $\mathcal{N}(s|\mu_k, \Sigma_k)$  is the bivariate Gaussian probability density function of minutia with mean  $\mu_k$  and covariance matrix  $\Sigma_k$ ,  $\mathcal{V}(\theta|\nu_k, \kappa_k)$  is the von Mises probability density function of minutiae orientation with mean angle  $\nu_k$  and precision (inverse variance)  $\kappa_k$ , and  $\Theta = \{\pi_k, \mu_k, \Sigma_k, \nu_k, \kappa_k, \rho_k\}$  where  $k = 1, 2, \dots, K$  is the set of all parameters of the  $k$  Gaussian and von Mises distributions.

Rather than using the standard form of the von Mises distribution for the range  $[0, 2\pi]$ , since minutiae orientations are represented as being in the range  $[0, \pi)$ , we use the alternate form [41] as follows

$$\mathcal{V}(\theta|\nu_k, \kappa_k, \rho_k) = \rho_k v(\theta) \cdot I\{0 \leq \theta < \pi\} + (1 - \rho_k) v(\theta - \pi) \cdot I\{\pi \leq \theta < 2\pi\} \quad (2.12)$$

where  $I\{A\}$  is the indicator function of the condition  $A$ ,

$$v(\theta) \equiv v(\theta|\nu_k, \kappa_k) = \frac{2}{I_0(\kappa_k)} \exp[\kappa_k \cos 2(\theta - \nu_k)], \quad (2.13)$$

minutiae arising from the  $k^{th}$  component have directions that are either  $\theta$  or  $\theta + \pi$  and the probabilities associated with these two occurrences are  $\rho_k$  and  $1 - \rho_k$  respectively.

Since fingerprint ridges flow smoothly with very slow direction changes, direction of neighboring minutiae are strongly correlated, i.e., minutiae that are spatially close tend to have similar directions with each other. However, minutiae in different regions of a fingerprint tend to be associated with different region-specific minutiae directions thereby demonstrating independence [42, 43]. The model allows ridge orientations to be different at different regions (different regions can be denoted by different components) while it makes sure that nearby minutiae have similar orientations (as nearby minutiae will belong to the same component).

### C. Distribution of minutiae and ridges

In the model just discussed, only minutiae was used in the framework of generative models for fingerprints. Models based purely on minutiae may be sufficient to model biometric scenarios where finger-prints are obtained in controlled conditions [36][37], but are insufficient to model forensic scenarios where latent prints are lifted off of surfaces. Due to the poor quality of latent prints, the detected minutiae are of low quantity and quality [44].

Ridge details provide vital information in latent fingerprints. Verification systems using minutiae together with ridge information are more accurate than using minutiae alone. Also, any generative model that makes use of ridge details can only be a better representation of the generative model for fingerprints. Ridge features are illustrated in Figure 2.16 where three different fingerprints are shown. In fingerprints 1 and 2, minutiae locations  $m_1$  and  $m_2$  are similar as well as the associated ridges  $r_1$  and  $r_2$ , are similar. In fingerprint 3, minutia location  $m_3$  is similar to  $m_1$  and  $m_2$  but the ridge  $r_3$  is dissimilar to  $r_1$  and  $r_2$ . Thus two minutiae matching with each other on location and orientation may actually have two very different ridge shapes. Thus, to make more reliable decisions on whether two fingerprints match, we use ridge information as well as minutiae location and orientation information. With this motivation, the distribution of ridge information is embedded into generative models.

The length of the ridge  $l_r$  is defined as the number of ridge points that could be sampled on the ridge. Three types of ridges are defined: (i) short:  $l_r \leq L/3$ , (ii) medium:  $L/3 < l_r \leq 2L/3$  and (iii) long:  $l_r > 2L/3$ , where  $L$  is the average ridge length of the top 10% longest representative ridges in the fingerprints database, e.g. in FVC2002,  $L$  is 18. By choosing the

## 2.2. METHODS

## CHAPTER 2. FINAL REPORT NARRATIVE

value of maximum ridge length  $L$  as the average of long ridges in the database, unusually long ridges caused by artifacts is avoided. The three possible ridge length types can be associated with any representative ridge. Without loss of generality, we can assume that there exist only three possible ridge length types corresponding to a representative ridge. The distribution of ridge length  $l_r$  is modeled as

$$p(l_r) = \frac{c_1}{c} \cdot I\{l_r \leq L/3\} + \frac{c_2}{c} \cdot I\{L/3 < l_r < 2L/3\} + \frac{c_3}{c} \cdot I\{2L/3 \leq l_r \leq L\} \quad (2.14)$$

where  $I\{C\}$  is the indicator function of condition  $C$ ,  $c_1$ ,  $c_2$  and  $c_3$  are the numbers of short, medium and long representative ridges, and  $c = c_1 + c_2 + c_3$ .

For ridges with different lengths, different ridge points are picked as anchors. For medium ridges,  $\lfloor L/3 \rfloor^{th}$  ridge point is picked and for long ridges, both  $\lfloor L/3 \rfloor^{th}$  and  $\lfloor 2L/3 \rfloor^{th}$  are picked. No ridge point is chosen for short ridges. The rationale for choosing these two ridge points is described in 2.2.4.

Let  $\mathbf{x} = \{\mathbf{x}_m, \mathbf{x}_r\}$  denote the feature vector of a representative ridge, where  $\mathbf{x}_m$  is a single minutia  $\{s_m, \theta_m\}$ , and  $\mathbf{x}_r$  consists of points along the ridge on which  $\mathbf{x}_m$  lies. Noting that the length of  $\mathbf{x}_r$  is  $l_r \leq L$  the points of  $\mathbf{x}_r$  are given by  $\{\mathbf{x}_{ri} : (i \in \{\lfloor L/3 \rfloor, \lfloor 2L/3 \rfloor\}) \& (i \leq l_r)\}$  where  $\mathbf{x}_{ri}$  is the  $i^{th}$  ridge point.

In contrast to the model for minutiae, ridge points are represented with respect to the minutiae defining the ridge. This is done naturally using the minutia as the origin and using polar coordinates to represent ridge points as shown in Figure 2.17. The location of ridge point  $s_{ri}$  is given by  $\{r_i, \phi_i\}$  and the direction of ridge point is  $\theta_i$ . Thus the ridge point  $\mathbf{x}_{ri}$  is represented as the combination of location and direction  $\{r_i, \phi_i, \theta_i\}$  where  $r_i$  is the distance from the  $i^{th}$  ridge point to the minutia,  $\phi_i$  is the positive angle required to reach the  $i^{th}$  ridge point from the polar axis.

A graphical model that represents the use of ridge information in addition to minutiae is given in Figure 2.18. The joint distribution of anchor minutia  $\mathbf{x}_m$  and associated ridge points  $\mathbf{x}_r$ , all located on a ridge of length  $l_r$ , can thus be written as

$$p(l_r, \mathbf{x}_m, \mathbf{x}_r) = p(l_r) \cdot p(\mathbf{x}_m | l_r) \cdot p(\mathbf{x}_r | \mathbf{x}_m, l_r) \quad (2.15)$$

where  $p(l_r)$  is the marginal distribution of ridge length,  $p(\mathbf{x}_m | l_r)$  is the conditional distribution of minutiae given the ridge length type and  $p(\mathbf{x}_r | \mathbf{x}_m, l_r)$  is the conditional distribution of ridge points given corresponding minutiae and ridge length type. For different ridge lengths, the conditional distribution of ridge points  $\mathbf{x}_r$  can be written as

$$p(\mathbf{x}_r | \mathbf{x}_m, l_r) = \begin{cases} 1 & l_r \leq \frac{L}{3} \\ p(\mathbf{x}_{r \lfloor \frac{L}{3} \rfloor} | \mathbf{x}_m, l_r) & \frac{L}{3} > l_r \leq \frac{2L}{3} \\ p(\mathbf{x}_{r \lfloor \frac{2L}{3} \rfloor} | \mathbf{x}_m, l_r) \cdot p(\mathbf{x}_{r \lfloor \frac{L}{3} \rfloor} | \mathbf{x}_m, l_r) & l_r > \frac{2L}{3} \end{cases} \quad (2.16)$$

where  $\mathbf{x}_{r \lfloor \frac{L}{3} \rfloor}$  and  $\mathbf{x}_{r \lfloor \frac{2L}{3} \rfloor}$  represent the  $\lfloor \frac{L}{3} \rfloor^{th}$  and  $\lfloor \frac{2L}{3} \rfloor^{th}$  ridge points.

The generative model is based on the distribution of representative ridges. Mixture distributions consisting of  $K_i$  components,  $i = 1, 2, 3$ , is used to model representative ridges of three ridge length types. Each component is distributed according the density of the

minutiae and density of ridge points. Assuming that the minutiae and ridge points are independent, representative ridge distribution is given by

$$p(\mathbf{x}|\Theta) = \begin{cases} p(l_r) \cdot \sum_{g=1}^{K_1} \pi_k p_k(s_m, \theta_m | \Theta_k) & l_r \leq \frac{L}{3} \\ p(l_r) \cdot \sum_{k=1}^{K_2} \pi_k p_k(s_m, \theta_m | \Theta_k) \cdot p_k(r_{\lfloor \frac{L}{3} \rfloor}, \phi_{\lfloor \frac{L}{3} \rfloor}, \theta_{\lfloor \frac{L}{3} \rfloor} | \Theta_k) & \frac{L}{3} < l_r < \frac{2L}{3} \\ p(l_r) \cdot \sum_{k=1}^{K_3} \pi_k p_k(s_m, \theta_m | \Theta_k) \cdot p_k(r_{\lfloor \frac{L}{3} \rfloor}, \phi_{\lfloor \frac{L}{3} \rfloor}, \theta_{\lfloor \frac{L}{3} \rfloor} | \Theta_k) \cdot p_k(r_{\lfloor \frac{2L}{3} \rfloor}, \phi_{\lfloor \frac{2L}{3} \rfloor}, \theta_{\lfloor \frac{2L}{3} \rfloor} | \Theta_k) & l_r \geq \frac{2L}{3} \end{cases} \quad (2.17)$$

The first condition corresponds to minutia alone, the second to minutia and one ridge point, and the third to minutia and two ridge points. In (2.17),  $p_k(s_m, \theta_m | \Theta_k)$  represents the distribution of the minutiae location  $s_m$  and the direction  $\theta_m$ ;  $p_k(r_i, \phi_i, \theta_i | \Theta_k)$  represents the distribution of the  $i^{\text{th}}$  ridge points. They are defined as in (2.18) and (2.19) respectively.

$$p_k(s_m, \theta_m | \Theta_k) = \mathcal{N}(s_m | \mu_{mk}, \Sigma_{mk}) \cdot \mathcal{V}(\theta_m | \nu_{mk}, \kappa_{mk}, \rho_{mk}) \quad (2.18)$$

$$p_k(r_i, \phi_i, \theta_i | \Theta_k) = p_k(r_i, \phi_i | \mu_{ik}, \Sigma_{ik}, \nu_{ik}^\phi, \kappa_{ik}^\phi, \rho_{ik}^\phi) \cdot \mathcal{V}(\theta_i | \nu_{ik}^\theta, \kappa_{ik}^\theta, \rho_{ik}^\theta) \quad (2.19)$$

where  $p_k(s_m, \theta_m | \Theta_k)$  can be calculated by Eq. 2.11 and  $p_k(r_i, \phi_i, \theta_i | \Theta_k)$  is the product of the probabilities of ridge point locations and directions, where  $\mathcal{V}(\theta_i | \nu_{ik}^\theta, \kappa_{ik}^\theta, \rho_{ik}^\theta)$  presents the distribution of the ridge point direction,  $\theta_i$  is the direction of the  $i^{\text{th}}$  ridge point and  $p_k(r_i, \phi_i | \mu_{ik}, \Sigma_{ik}, \nu_{ik}^\phi, \kappa_{ik}^\phi, \rho_{ik}^\phi)$  is the distribution of ridge point location given by

$$p_k(r_i, \phi_i | \mu_{ik}, \Sigma_{ik}, \nu_{ik}^\phi, \kappa_{ik}^\phi, \rho_{ik}^\phi) = \mathcal{N}(r_i | \mu_{ik}, \sigma_{ik}) \cdot \mathcal{V}(\phi_i | \nu_{ik}^\phi, \kappa_{ik}^\phi, \rho_{ik}^\phi) \quad (2.20)$$

where  $\mathcal{N}(r_i | \mu_{ik}, \sigma_{ik})$  is a univariate Gaussian distribution whose mean  $\mu_{ik}$  and variance  $\sigma_{ik}$  are learnt from a fingerprint database.

## D. Parameter Estimation

The parameter estimation problem for both minutiae and representative ridges are similar since the latter consists of only including additional points. Since the mixture distribution given in (2.11) and (2.17) cannot be directly maximized, due to the summations involved, an alternative approach is needed. We now develop an equivalent formulation of the mixture distribution given in (2.11) by involving an explicit latent variable. This will allow us to formulate the problem of parameter estimation in terms of the expectation maximization (EM) algorithm.

We define the joint distribution  $p(\mathbf{x}, \mathbf{z})$  in terms of a marginal distribution  $p(\mathbf{z})$  and a conditional distribution  $p(\mathbf{x} | \mathbf{z})$ , corresponding to the graphical model in Figure 2.19(a).

Given that the total number of minutiae observed in a finger is  $D$ , a joint distribution model is needed. The  $D$  minutiae are assumed to be independent of each other, with each minutiae, consisting of an  $\mathbf{x}(s, \theta)$  pair, being distributed according to a mixture of component densities. This is shown in Figure 2.19(b).

## 2.2. METHODS

## CHAPTER 2. FINAL REPORT NARRATIVE

The  $K$ -dimensional random variable  $\mathbf{z}$  has a 1-of- $K$  representation in which a particular element  $z_k$  is equal to 1 and all other elements are equal to 0, we can write

$$p(\mathbf{z}) = \prod_{k=1}^K \pi_k^{z_k} \quad (2.21)$$

Similarly the conditional distribution of  $\mathbf{x}$  given a particular value for  $\mathbf{z}$  is given by

$$p(\mathbf{x}|z_k = 1) = \mathcal{N}(\mathbf{x}|\mu_k, \Sigma_k) \cdot \mathcal{V}(\theta|\nu_k, \kappa_k, \rho_k) \quad (2.22)$$

which can also be written in the form

$$p(\mathbf{x}|\mathbf{z}) = \prod_{k=1}^K \mathcal{N}(\mathbf{x}|\mu_k, \Sigma_k)^{z_k} \cdot \mathcal{V}(\theta|\nu_k, \kappa_k, \rho_k)^{z_k}. \quad (2.23)$$

The joint distribution is given by  $p(\mathbf{z})p(\mathbf{x}|\mathbf{z})$ , and the marginal distribution of  $\mathbf{x}$  is obtained by summing the joint distribution over all possible states of  $\mathbf{z}$  to give

$$p(\mathbf{x}) = \sum_{\mathbf{z}} p(\mathbf{z})p(\mathbf{x}|\mathbf{z}) = \sum_{k=1}^K \pi_k \cdot \mathcal{N}(s|\mu_k, \Sigma_k) \cdot \mathcal{V}(\theta|\nu_k, \kappa_k, \rho_k) \quad (2.24)$$

where we have made use of (2.21) and (2.23). Thus the marginal distribution of  $\mathbf{x}$  is a mixture of the form (2.11). If we have several observed minutiae  $\mathbf{x}_1, \mathbf{x}_2, \dots, \mathbf{x}_D$  then, because we have represented the marginal distribution in the form  $p(\mathbf{x}) = \sum_{\mathbf{z}} p(\mathbf{z})p(\mathbf{x}|\mathbf{z})$ , it follows that for every observed minutia  $\mathbf{x}_n$ , there is a corresponding latent variable  $\mathbf{z}_n$ .

We are now able to work with the joint distribution  $p(\mathbf{x}, \mathbf{z})$  instead of the marginal distribution  $p(\mathbf{x})$ . To estimate the unknown parameters using the maximum likelihood approach, we use the EM algorithm. The number of components  $K$  for the mixture model was found after validation using  $k$ -means clustering.

**E-Step:** Using  $\gamma_{dk}$  is to denote the responsibility of component  $k$  for minutiae  $\mathbf{x}_d$ , its value can be found using Bayes's theorem

$$\begin{aligned} \gamma_{dk} \equiv p(z_k = 1|\mathbf{x}_d) &= \frac{p(z_k = 1)p(\mathbf{x}_d|z_k = 1)}{\sum_{k=1}^K p(z_k = 1)p(\mathbf{x}_d|z_k = 1)} \\ &= \frac{\pi_k \mathcal{N}(s_d|\mu_k, \sigma_k) \mathcal{V}(\theta_d|\nu_k, \kappa_k, \rho_k)}{\sum_{k=1}^K \pi_k \mathcal{N}(s_d|\mu_k, \sigma_k) \mathcal{V}(\theta_d|\nu_k, \kappa_k, \rho_k)} \end{aligned} \quad (2.25)$$

**M-Step:** The estimates of the Gaussian distribution parameters  $\pi_k$ ,  $\mu_{mk}$  and  $\Sigma_{mk}$  at the  $(n+1)$ th iteration, are given by

$$\pi_k^{(n+1)} = \frac{1}{D} \sum_{d=1}^D \gamma_{dk}^{(n)} \quad (2.26)$$

$$\mu_{mk}^{(n+1)} = \frac{\sum_{d=1}^D \gamma_{dk}^{(n)} s_m}{\sum_{d=1}^D \gamma_{dk}^{(n)}} \quad (2.27)$$

$$\Sigma_{mk}^{(n+1)} = \frac{\sum_{d=1}^D \gamma_{dk}^{(n)} (s_m - \mu_{mk}^{(n+1)}) (s_m - \mu_{mk}^{(n+1)})^T}{\sum_{d=1}^D \gamma_{dk}^{(n)}} \quad (2.28)$$

The parameters for orientation distributions are obtained using expectation maximization for the von Mises distribution [45]. The estimates of  $\nu_{mk}$  and  $\kappa_{mk}$  at the  $(n+1)th$  iteration are given by

$$\nu_{mk}^{(n+1)} = \frac{1}{2} \tan^{-1} \left( \frac{\sum_{d=1}^D \gamma_{dk}^{(n)} \sin 2\psi_d}{\sum_{d=1}^D \gamma_{dk}^{(n)} \cos 2\psi_d} \right) \quad (2.29)$$

$$\frac{I'_0(\kappa_{mk}^{(n+1)})}{I_0(\kappa_{mk}^{(n+1)})} = \frac{\sum_{d=1}^D r_{dk}^{(n)} \cos 2(\psi_d - \nu_k^{(n+1)})}{\sum_{d=1}^D r_{dk}^{(n)}}. \quad (2.30)$$

The solution for (2.30), which involves Bessel functions, obtained using an iterative method gives the estimate for  $\kappa_{mk}$ . The estimate of  $\rho_{mk}$  is then obtained as

$$\rho_{mk}^{(n+1)} = \frac{\sum_{d=1}^D I\{c_d^{(n+1)} = k, \theta_d \in [0, \pi)\}}{\sum_{d=1}^D I\{c_d^{(n+1)} = k\}} \quad (2.31)$$

where  $c_d^{(n+1)} = \arg \max_k \gamma_{dk}^{(n+1)}$  is the component label for the observation  $d$  at the  $(n+1)th$  iteration,  $\psi_j$  is the orientation of the minutiae  $m_j$ .

In the same way, the parameters for ridge point  $\nu_{ik}^\theta, \kappa_{ik}^\theta, \rho_{ik}^\theta$  and  $\nu_{ik}^\phi, \kappa_{ik}^\phi, \rho_{ik}^\phi$  can be estimated by Eq. (2.29), (2.30) and (2.31), when  $\psi_j$  is set as  $\theta_i$  and  $\phi_i$  respectively.

## E. Goodness of Fit

Goodness of fit means how well a sample of data agrees with a given distribution as its population. To test the goodness of fit, the chi-square statistical hypothesis test is applied. Chi-square goodness of fit test determines whether observed sample frequencies differ significantly from expected frequencies specified in the null hypothesis. The test is applied to binned data (i.e., data put into classes) and requires a sufficient sample size in each bin in order for the chi-square approximation to be valid [46]. In the case of fingerprint, we partitioned the minutiae location and direction space into  $16 \times 4$  non-overlapping blocks. The blocks are combined with adjacent blocks until both observed and expected numbers of minutiae in the block are greater than or equal to 5. The test statistic used here is a chi-square random variable  $\chi^2$  defined by the following equation.

$$\chi^2 = \sum_i \frac{(O_i - E_i)^2}{E_i} \quad (2.32)$$

where  $O_i$  is the observed minutiae count for the  $i$ th block, and  $E_i$  is the expected minutiae count for the  $i$ th block.

## 2.2. METHODS

## CHAPTER 2. FINAL REPORT NARRATIVE

The  $p$ -value, the probability of observing a sample statistic as extreme as the test statistic, associated with each test statistic  $\chi^2$  is then calculated based on the chi-square distribution and compared to the significance level. For the FVC2002 DB1, we chose significance level equal to 0.01. The numbers of fingerprints with  $p$ -values above (corresponding to accept the model) and below (corresponding to reject the model) the significance level are then computed. The results are given in Table 2.4. Of the 800 fingerprints, 679 are accepted with ridge model which is higher than 574 and 121 are rejected which is smaller than 226. The results imply that the mixture model with ridge information offers a better fit to the observed fingerprints compared to the model without ridge information. In addition, the independent assumptions between minutiae and between minutiae and ridge points are proved to be reasonable.

### F. Evaluation of PRCs

**Minutiae Only.** To compute the PRCs, we first define correspondence, or match, between two minutiae. Let  $\mathbf{x}_a = (s_a, \theta_a)$  and  $\mathbf{x}_b = (s_b, \theta_b)$  be a pair of minutiae. The minutiae are said to correspond if for tolerance  $\epsilon = [\epsilon_s, \epsilon_\theta]$ ,

$$|s_a - s_b| \leq \epsilon_s \text{ and } |\theta_a - \theta_b| \leq \epsilon_\theta \quad (2.33)$$

where  $|s_a - s_b|$ , the Euclidean distance between the minutiae location  $s_a = (x_{a1}, x_{a2})$  and  $s_b = (x_{b1}, x_{b2})$ , is given by

$$|s_a - s_b| = \sqrt{(x_{a1} - x_{b1})^2 + (x_{a2} - x_{b2})^2} \quad (2.34)$$

Then, the probability that a random minutia  $\mathbf{x}_a$  would match a random minutia  $\mathbf{x}_b$  is given by

$$\begin{aligned} p_\epsilon(\mathbf{x}) &= p(|\mathbf{x}_a - \mathbf{x}_b| \leq \epsilon | \Theta) \\ &= \int \int_{\mathbf{x}_a \mid |\mathbf{x}_a - \mathbf{x}_b| \leq \epsilon} p(\mathbf{x}_a | \Theta) p(\mathbf{x}_b | \Theta) d\mathbf{x}_a d\mathbf{x}_b \end{aligned} \quad (2.35)$$

where  $\Theta$  is the set of parameters describing the distribution of the minutiae location and direction.

Finally, the PRC, or the probability of matching at least  $\hat{m}$  pairs of minutiae within  $\epsilon$  between two randomly chosen fingerprint  $f_1$  and  $f_2$  is calculated as

$$p_\epsilon(\hat{m}, m_1, m_2) = \binom{m_1}{\hat{m}} \binom{m_2}{\hat{m}} \hat{m}! \cdot p_\epsilon(\mathbf{x})^{\hat{m}} (1 - p_\epsilon(\mathbf{x}))^{(m_1 - \hat{m}) \cdot (m_2 - \hat{m})} \quad (2.36)$$

where  $m_1$  and  $m_2$  are numbers of minutiae in fingerprints  $f_1$  and  $f_2$ ,  $p_\epsilon(\mathbf{x})^{\hat{m}}$  is the probability of matching  $\hat{m}$  specific pairs of minutiae between  $f_1$  and  $f_2$ ,  $(1 - p_\epsilon(\mathbf{x}))^{(m_1 - \hat{m}) \cdot (m_2 - \hat{m})}$  is the probability that none of minutiae pair would match between the rest of minutiae in  $f_1$  and  $f_2$  and  $\binom{m_1}{\hat{m}} \binom{m_2}{\hat{m}} \hat{m}!$  is the number of different match sets that can be paired up.

## 2.2. METHODS

## CHAPTER 2. FINAL REPORT NARRATIVE

Given  $n$  fingerprints and assuming that the number of minutiae in a fingerprint  $m$  can be modeled by the distribution  $p(m)$ , the general PRCs  $p(n)$  is given by

$$p(n) = 1 - \bar{p}(n) = 1 - (1 - p_\epsilon)^{\frac{n(n-1)}{2}} \quad (2.37)$$

where  $p_\epsilon$  is the probability of matching two random fingerprint from  $n$  fingerprints. If we set the tolerance in terms of number of matching minutiae to  $\hat{m}$ ,  $p_\epsilon$  is calculated by

$$p_\epsilon = \sum_{m'_1 \in M_1} \sum_{m'_2 \in M_2} p(m'_1)p(m'_2)p_\epsilon(\hat{m}, m'_1, m'_2) \quad (2.38)$$

where  $M_1$  and  $M_2$  contain all possible numbers of minutiae in one fingerprint among  $n$  fingerprints, and  $p_\epsilon(\hat{m}, m'_1, m'_2)$  can be calculated by Eq. 2.36.

Given a specific fingerprint  $f$ , the specific  $n$ PRCs can be computed by

$$p(f, n) = 1 - (1 - p(f))^{n-1} \quad (2.39)$$

where  $p(f)$  is the probability that  $\hat{m}$  pairs of minutiae are matched between the given fingerprint  $f$  and a randomly chosen fingerprint from  $n$  fingerprints.

$$\begin{aligned} p(f) &= \sum_{m' \in M} p(m') \binom{m'}{\hat{m}} \cdot \sum_{i=1}^{\binom{m_f}{\hat{m}}} p(f_i) \\ &= \sum_{m' \in M} p(m') \binom{m'}{\hat{m}} \cdot \sum_{i=1}^{\binom{m_f}{\hat{m}}} \prod_{j=1}^{\hat{m}} p(\mathbf{x}_{ij} | \Theta) \end{aligned} \quad (2.40)$$

where  $M$  contains all possible numbers of minutiae in one fingerprint among  $n$  fingerprints,  $p(m')$  is the probability of a fingerprint having  $m'$  minutiae in  $n$  fingerprints,  $m_f$  is the number of minutiae in the given fingerprint  $f$ , minutiae set  $f_i = (\mathbf{x}_{i1}, \mathbf{x}_{i2}, \dots, \mathbf{x}_{i\hat{m}})$  is the subset of the minutiae set of given fingerprint and  $p(f_i)$  is the joint probability of minutiae set  $f_i$  based on learned generative model.

**Minutiae with Ridge Points.** When ridge information is considered, a representative ridge is denoted by  $\mathbf{x} = \{\mathbf{x}_m, \mathbf{x}_r\}$ , where  $\mathbf{x}_r = \{\mathbf{x}_r^i : i \in \{[L/3], [2L/3]\} \wedge i \leq l_i\}$ . The representative ridge  $\mathbf{x}_a$  matches the representative ridge  $\mathbf{x}_b$  with tolerance  $\epsilon$  if

$$|\mathbf{x}_{ma} - \mathbf{x}_{mb}| \leq \epsilon_m \wedge |\mathbf{x}_{ra} - \mathbf{x}_{rb}| \leq \epsilon_r \quad (2.41)$$

where  $|\mathbf{x}_{ma} - \mathbf{x}_{mb}| \leq \epsilon_m$  is define by Eq.2.33 and  $|\mathbf{x}_{ra} - \mathbf{x}_{rb}| \leq \epsilon_r$  is defined as

$$|\mathbf{x}_{ra} - \mathbf{x}_{rb}| \leq \epsilon_r \equiv (\forall i \in A) |r_a^i - r_b^i| \leq \epsilon_r \wedge |\phi_a^i - \phi_b^i| \leq \epsilon_\phi \wedge |\theta_a^i - \theta_b^i| \leq \epsilon_\theta \quad (2.42)$$

## 2.2. METHODS

## CHAPTER 2. FINAL REPORT NARRATIVE

where  $A$  is the anchor point index set and the tolerance can be grouped together as  $\epsilon = \{\epsilon_s, \epsilon_\theta, \epsilon_r, \epsilon_\phi\}$ .

Then, the probability that a random representative ridge  $\mathbf{x}_a$  would match a random representative ridge  $\mathbf{x}_b$  is given by

$$\begin{aligned} p_\epsilon(\mathbf{x}) &= p(|\mathbf{x}_a - \mathbf{x}_b| \leq \epsilon | \Theta) \\ &= \int_{\mathbf{x}_a} \int_{|\mathbf{x}_a - \mathbf{x}_b| \leq \epsilon} p(\mathbf{x}_a | \Theta) p(\mathbf{x}_b | \Theta) d\mathbf{x}_a d\mathbf{x}_b \end{aligned} \quad (2.43)$$

where  $\Theta$  is the set of parameters describing the distribution of the representative ridges.

The  $n$ PRC and specific  $n$ PRC with ridge information can be calculated by Eq.2.37, 2.39 and 2.40.

### G. Evaluation with Fingerprint Databases

Parameters of the two fingerprint distribution models introduced in Sections 2.2.2 were evaluated using the fingerprint database FVC2002 DB1 [47]. The number of components  $G$  for the mixture model was found after validation using  $k$ -means clustering. The database has 100 different fingerprints with 8 impressions of the same finger. Thus, there are a total of 800 fingerprints using which the model has been developed.

Values of PRC  $p_\epsilon$  are calculated using the formula introduced in Section 2.2.2. For comparison, the empirical PRC  $\hat{p}_\epsilon(\mathbf{x})$  was calculated also. To compute  $\hat{p}_\epsilon(\mathbf{x})$ , the empirical probabilities of matching a minutiae pair or ridge pair between imposter fingerprints are calculated first by

$$\hat{p}_\epsilon(\mathbf{x}) = \frac{1}{I} \sum_{i=1}^I \frac{\hat{m}_i}{m_i \times m'_i} \quad (2.44)$$

where  $I$  is the number of the imposter fingerprints pairs,  $\hat{m}_i$  is the number of matched minutiae or ridge pairs and  $m_i$  and  $m'_i$  are the numbers of minutiae or pairs in each of the two fingerprints. Then, the empirical PRC  $\hat{p}_\epsilon$  can be calculated by Eq.2.36.

Both the theoretical and empirical PRCs are given in Table 2.5. The PRCs are calculated through varying number of minutiae or ridges in two randomly chosen fingerprint  $f_1$  and  $f_2$  and the number of matches between them. We can see that more minutiae or ridges the template and input fingerprint have, higher the PRC is. In experiments conducted on the FVC2002 DB1, there are some differences between the results obtained here and the results in [37]. This may result from use of different matching tolerance, which  $p_\epsilon(\mathbf{x})$  depends on. It should be noted that the PRC values with ridge information model are never greater than PRC values without ridge information, which indicates that ridge information strengthens individuality of fingerprints. Note that the theoretical PRC based on our model are close and have the same trend to empirical PRC. The consistency between the theoretical probabilities and empirical probabilities shows the validation of our generative model. The PRCs for the different  $m_1$  and  $m_2$  with 6, 16, 26 and 36 matches are shown in Figure 2.20. It is obvious to note that, when  $\hat{m}$  decreases or  $m_1$  and  $m_2$  increase, the probability of matching two random fingerprints is more.

Based on the PRC value,  $n$ PRC can be computed. Table 2.6 shows the  $n$ PRCs in 100,000 fingerprints through varying number of minutiae or ridges in each fingerprint  $m$  and number of matches  $\hat{m}$ .

The specific  $n$ PRCs are also computed by (2.39) and given by Table 2.7. Here three fingerprints are chosen as query prints and they are shown in Figure 2.21. The first one is a full print in good quality, the second one is a full print in low quality and the third one is a partial print. The specific  $n$ PRCs are calculated through varying number of minutiae/ridges in each template fingerprint ( $m$ ) and the number of matches ( $\hat{m}$ ), assuming that the number of fingerprints in template database ( $n$ ) is 100,000. The numbers of minutiae/ridges in 3 given query fingerprint  $m_f$  are 41, 26 and 13. In 100,000 randomly chosen fingerprints there is only  $1.1670 \times 10^{-23}$  probability that one of them have 12 matches with the fingerprint  $F_1$  if we consider both minutiae and ridge in matching. This probability is much smaller than previous minutiae only model which is  $5.7637 \times 10^{-14}$ .

### 2.2.3 Likelihood-based Methods for Fingerprint Comparison

A goal of most AFIS style methods is given an input fingerprint and a template fingerprint, to arrive at a binary decision of match/non-match. Along the way typically a score for the degree of match between the input and template is computed. This part of the project was to study the best way of obtaining such a score so that the decision can be expressed in terms of the strength of evidence.

There has been significant earlier work on automatic fingerprint verification/identification[39]. The three main operational steps of automatic fingerprint verification are: (i) feature extraction—where a set of features, typically minutiae, are determined from each fingerprint, (ii) matching—where a matcher determines the degree of match, or score, between the two sets of features and (iii) decision—where the score is used to make the classificatory decision of match/non-match. The robustness of the method of decision with respect to the quality of the previous two steps is pertinent when one or both of the fingerprints do not contain a sufficient number of minutiae. The focus here is on comparing the performance of two different methods of decision for fingerprint verification in the context of varying numbers of minutiae being available.

The commonly used method of making a decision with the score is to determine a threshold from the receiver operating characteristics (ROC), a term that originated from signal detection theory [48]. A score above this threshold indicates a matching pair of fingerprints and a score below indicates a non-match. The ROC-based strategy learns from a large general population of ensemble of pairs of fingerprint samples(training set) and decides on an operating point by analyzing the ROC curve. Such a method works well when there is a complete and well-registered fingerprint image.

On the other hand when there exists a partial imprint of a finger—as in the case of latent prints in forensics or due to limitations of the biometric device—a method based on probabilities may be justified. In such situations it is useful to consider decision methods based on computing the likelihood ratio of match/non-match. Likelihood ratio (LR) methods have a long history originating in statistical hypothesis testing [49]. LR methods considered here model the distribution of distances obtained by comparing the ensemble of pairs of

fingerprints using a Gaussian or a Gamma distribution.

## A. Decision Methods

We used the standard available *Bozorth matcher* to match two sets of minutiae. Other matching algorithms using ridge alignment and matching, such as those discussed in [50] are suited more for the 1:N verification problem and when the quality of fingerprint considered is good. The Bozorth matcher is superior to that discussed in [50] for the purpose of 1:1 verification on the FVC2002 dataset wherein the quality of the impressions is poor. By using the Bozorth score, one can arrive at a distance space representation of the data that characterizes the strength of match between two samples.

The decision task is to determine from the score of the matcher whether or not the two fingerprints belong to the same finger. The ROC method learns to operate at a particular threshold by analyzing the ROC curve obtained from comparing a large ensemble of pairs of fingerprint samples. The LR method models the distribution of distances obtained by comparing the ensemble of pairs of fingerprint samples using a statistical distribution. Both methods operate on a distribution of distances obtained by comparing the *features* of a pair fingerprint, which are described in the following section. This paper focuses on the methods for automatic fingerprint verification after a set of features have been extracted for each fingerprint sample. The features considered here are the set of minutiae extracted for each fingerprint sample. Before learning truly begins, these raw samples first need to be converted to feature space using a feature extractor.

### *ROC Learning*

The ROC curve is obtained for a two category problem by plotting the probability of a hit against the probability of false alarm. In a one-dimensional problem, such as a scalar-valued score or distance, such a plot can be obtained very simply by varying a threshold and determining the two probabilities for each value of the threshold.

The ROC method decides if a pair of fingerprints as belonging to the same finger or different, by learning from a large general population of ensemble of pairs. A pair of samples either belongs to the same finger or they are from different fingers. Features are extracted for each samples, and feature vectors between the two samples in a pair are compared using the Bozorth matcher described in Section 2.1.2. The result of such a matching is vector of distances, one distance value corresponding to every pair matched. The absolute value of these distances help classify whether the two samples in a pair belonged to the same finger or not. The ROC based method aims at deciding on a particular threshold in distance that separates the pairs that belonged to different fingers from those that belonged to the same finger. The score obtained from the Bozorth matcher are such that, generally when the samples from a pair truly came from the same finger, the score is higher than if they come from different finger. Figure 2.22(a) shows an example of a distance distribution obtained by comparing an ensemble of pairs. The threshold to decide for decision is obtained by moving the threshold from left to right, and at every point the number of pairs that were decided incorrectly is calculated. An incorrect decision can be of two types.

1. Pairs truly belonged to the different finger but classified as same(False Positive or False Alarm).

2. Pairs truly belonged to the same finger but classified as different(False Negative).

In a similar way a correct decision can be of two types.

1. Pairs truly belonged to the same finger and classified same(True Positive or Hit Rate).
2. Pairs truly belonged to different finger and classified different(True Negative).

As the threshold is moved from left to right on the distance scale, one can measure the four different variables mentioned above. A plot of Hit Rate(True Positive) against the False Alarm(False Positive) is called the ROC curve. Figure 2.22(b) shows a typical ROC curve. The best threshold, or the operating point is decided by choosing the threshold that gives the least average error. The average error is defined to be the average between False Negative and False positive. This definition of the average error gives equal importance to False Negative and False Positive. Thus the ROC method learns from a ensemble of pairs of training samples to obtain one threshold in distance that it can use to classify a pair as belonging to the same or different finger.

*LR Learning* This method of learning starts similar to the ROC method. Here again, a large ensemble of pairs of fingerprint samples are taken. This training set is divided into two categories. Set *one* consists of pairs of finger print samples where each pair truly belongs the same finger. Set *two* consists of a pairs of finger print samples where each pair truly belongs to different persons. Features are extracted for these samples and the Bozorth matcher computes a similarity score between the samples of each pair. Let  $\vec{D}_S$  denote the vector of distances between all pairs in set *one*, which represents the distribution of distances when samples truly came from the same finger. Similarly let  $\vec{D}_D$  denote the vector of distances between all pairs in set *two*, which represents the distribution of distances when samples truly came from different finger.

Figure 2.23 shows a histogram of these two different distributions. Note that this corresponds to the same data as in Figure 2.22(a) where the axes are turned around and the score values are flipped.

The next step in the likelihood ratio approach is to model the distributions respresented by the histograms. Modeling is essentially one of learning the true distributions underlying the data. If we take an approach of modeling the distribution using parametric forms then the parameters can be learnt accurately when there are a large number of available samples.

Two candidate parametric distributions are the Gaussian or Gamma distributions whose probability density functions (pdfs) in one dimension are given in equations (2.45) and (2.46) respectively:

$$\text{Gaussian pdf: } P(d|\mu, \sigma) = \frac{1}{\sqrt{2\pi\sigma^2}} e^{-\frac{(d-\mu)^2}{2\sigma^2}}, \quad -\infty < d < \infty \quad (2.45)$$

where  $\mu$  and  $\sigma^2$  are the mean and the variance of the distribution, respectively; and

$$\text{Gamma pdf: } P(d|\alpha, \theta) = \frac{1}{\Gamma(\alpha)\theta^{-\alpha}} e^{-\theta d} d^{\alpha-1}, \quad 0 < d < \infty \quad (2.46)$$

where  $\alpha$ (shape) and  $\theta$ (width) are the parameters of the Gamma distribution.

The Gamma distribution was chosen since the matcher always returns a positive score. On the other hand a Gaussian pdf assigns non-zero probabilities to negative scores. The parameters that need to be learnt for such a model( $\alpha$  and  $\theta$  for the Gamma distribution) are obtained from the mean and the variance of the distribution( $\mu$  (mean) and  $\sigma$  (variance)) and can be calculated using  $\mu = \alpha\theta$  and  $\sigma^2 = \alpha\theta^2$ . These distributions are the same- and different-finger distributions. Figure 2.24 shows the typical distribution p.d.f. curves obtained when the similarities are modeled using a Gaussian or a Gamma distribution.

## B. Comparison of Methods

The decision task answers the question whether or not a given pair of fingerprint samples came from the same finger or from different fingers. In forensics, typically one sample in the pair can be referred to as the known sample, e.g., from a ten-print card. The other is considered as the questioned sample. Each of the above mentioned learning strategies can provide their own decision answers. The ROC method uses threshold obtained by analyzing the ROC curves in the learning phase to answer whether two samples belong to the same finger. This task is called 1 : 1 verification. For the learning strategy, the corresponding decision tasks involves a pair of finger print samples and calculating the p.d.f. value under each distribution.

### *ROC Decision*

Once the optimum threshold has been obtained by analyzing the ROC the decision task is easy. For a new pair of finger print samples, features are extracted and a similarity score is obtained using the Bozorth matcher. If this score is greater than the threshold, the the pair is classified as belonging to the same finger or else different finger.

### *LR Decision*

Figure 2.25(a) shows two fingerprint imprint images that are to be verified if they belong to the same finger.

The process of such 1:1 verification starts with minutiae extraction and then computing the score  $d$  between the features using the Bozorth matcher. From the learning described, the likelihood ratio defined as  $\frac{P(D_S|d)}{P(D_D|d)}$  can be calculated, where  $P(D_S|d)$  is the probability density function value under the  $D_S$  distribution at the distance  $d$  and  $P(D_D|d)$  is the probability density function value under the  $D_D$  distribution at the distance  $d$ . If the likelihood ratio is greater than 1, then the decision answer is that the two samples do belong to the same finger and if the ratio is less than 1, they belong to different fingers. Figure 2.25(b) shows how the likelihood ratio is obtained. If we wish to do 1 :  $N$  verification, there are a total of  $N$  known samples from a finger(enrolled), then for one input sample,  $N$ , 1:1 verifications can be performed and the likelihood ratios multiplied. In these circumstances it is convenient to deal with log likelihood-ratios rather than with just likelihood ratios. The log likelihood-ratio (LLR) is given by  $\log P(D_S|d) - \log P(D_D|d)$ . The decision of same-finger is favored if  $\log P(D_S|d) - \log P(D_D|d) > 0$ , and the decision of different-finger chosen if  $\log P(D_S|d) - \log P(D_D|d) < 0$ . When  $N$  of these 1 : 1 verifications are performed these

LLR's are summed and then the decision is taken.

### C. Experiments and Results

The FVC2002 collection of database were used in the experiments. It contained four different datasets within it– Db1,Db2,Db3 and Db4. The four databases, contained fingerprint images acquired by different methods. Db3 contained very poor quality fingerprint images, whereas Db2 fingerprint image quality was the best. Each database contained a total of 800 fingerprint images comprising of 8 samples for each of 100 fingers. From this, a smaller derived dataset was made with a total of 80 fingerprint images images containing 8 samples for each of 10 fingers. Experiments were first performed on the derived smaller set and later on the full database. Additionally, experiments were also performed by varying the number of minutiae in each database. Figure 2.26(a) and 2.26(b) shows a few sample images from the database. For the task of verification, a number of pairs of fingers can be considered. For a given finger that has 8 samples, there are  $\binom{8}{2} = 28$  same finger pairs. Hence for all the 10 fingers together there are  $28 * 10 = 280$  same finger pairs. Similarly there are 2880 pairs of different finger samples. For the purpose of learning, half of the set was used as the training set and the remaining for testing, i.e. 140 samples from same finger pairs and 1440 pairs from different fingers were used for the purpose of training. Both the ROC based method and the likelihood methods used the same data set for training and testing, in order for them to be fairly compared. The first set of experiments were based on using all the minutiae available for each sample and the experiments and results are described in section 2.2.3. The second set of experiments were based on carrying out fingerprint verification with reduced number of minutiae in each sample. These are described in section 2.2.3.

**Experiments with all Minutiae preserved** For each of the 4 databases, the training set consisted of 140 pairs of same fingers and 1440 pairs of different fingers. Each of these pairs resulted in a similarity score as a result of matching the samples in the pair using the Bozorth matcher. The remaining pairs were used for testing the accuracy of the model. The average error rate, defined as average of False positives and False negatives, is used as a measure of the error rate for the model. Figure 2.29 shows the ROC curves learnt from the training set of the 4 different databases. Figure 2.30 shows the result of learning the distribution of the scores from the training set and modeling them as Gaussian distributions. After deciding on the operating point, the thresholds were used to classify the test data set. Similarly the log likelihood ratio was used to determine the decision for the likelihood method. Table 2.8 gives the error rates on the 4 different datasets for both the ROC based method and the likelihood method using Gaussian and Gamma distributions. The decision boundary is given by the sign of the log likelihood-ratio, LLR,  $\log P(D_S|d) - \log P(D_D|d)$ .

The results presented in Table 2.8 show that the likelihood methods, Gaussian and Gamma, outperformed the the ROC method. Higher error rates on database 3, is explained by the poor quality of fingerprint images in that database. The performance of modeling with Gaussian is slightly better than with modeling with Gamma. Although the difference is statistically insignificant, it can be explained by the fact that amongst the two models,

the Gaussian density for for the  $P(D_s/d)$  has a fatter tail towards the origin, and it accounts for greater uncertainty in that region.

**Experiments with reduced Minutiae** The number of available minutiae in the fingerprints directly affects the extent of match between two fingerprints. Partial fingerprints always account for fewer minutiae and we present an approach to simulate the reduced minutiae scenario, which are intended to simulate the effects arising from noisy image acquisition techniques. In this approach, minutiae are randomly removed from the set of total available. An alternative set of experiments, to consider only minutiae from a region as those available, was also performed but briefly discussed due to page limitations.

#### D. Randomly removing minutiae

In this experiment, the process of selecting the minutiae to be removed from the sample was done at random. Since the process of removing the minutiae were at random, the experiments discussed in this section were averaged over 5 different random seeds. The number of minutiae removed from each sample was proportional to the total amount of minutiae present in the sample.

The 80 samples of fingerprints in each of the 4 databases were tampered with by reducing the number of minutiae in each gradually. When the number of minutiae are reduced in the sample, the number of minutiae that match between a pair of fingerprints reduces significantly. As a result, there is more uncertainty in the decision. It is seen in our experiments that modeling uncertainty statistically proved better than the traditional ROC-based method. As the number of minutiae were reduced, the experiments mentioned in section 2.2.3 were carried out and the average error rate of the two methods were compared with the average number of minutiae per sample. 5 different experimental setups were created, each of which had on an average 5 minutiae less than the previous setup. Figure 2.27 shows the average error rate for each of the databases varying with the average number of minutiae present per sample. The size of the training and test set was fixed to be the same as discussed in the previous section. It is interesting to note from the figures that the likelihood methods perform better when there are fewer number of minutiae available on certain databases. The average difference between the error rates between the methods decreased non-linearly as minutiae were gradually removed. If more minutiae were included, the difference between the error rates of the two methods became smaller. In all cases, modeling the distribution statistically was never worse than the ROC-based method.

The above experiment was performed on a database of all available **800 fingerprint images**. This gives a better idea about the performance of the statistical methods against the ROC based method. The results for the same are shown in Figure 2.31(a). The error rates and the standard error of the mean are shown in the corresponding Table 2.9.

### E. Minutiae from a region

This experiment was based on the idea of simulating a partial fingerprint. One minutiae was chosen at random and  $N$  nearest minutiae to this chosen one (based on Euclidean distance on location) were said to be the available minutiae. Now when the first chosen minutiae is at the edge of the fingerprint, then only minutiae closest to that will be available, simulating the effect of having only edge of the fingerprint available for matching. Again here, the experimental results were averaged over 5 different positions of the chosen minutiae to simulate different regions of partial fingerprint. Figure 2.28 shows the average error rate for each of the databases varying with the average number of minutiae present per sample. Here again, the likelihood based methods performed consistently better than the ROC based methods. Also similar to the previous experiment the error rate increases non-linearly as the number of available minutiae are reduced. The experimental results on the 800 fingerprint database is shown in Figure 2.31(b). The experiment was carried over 6 different positions of the chosen minutiae. The error rates and the standard error of the mean are shown in Table 2.9. When very few minutiae are available (26 and 20), the error rate of the ROC method is fixed at 50% with no standard deviation.

### F. Experiments with 1:N Verification

The 1 :  $N$  Verification process consists of two steps (i) Enrollment: Here a known set of  $N$  impressions for a finger are enrolled and labeled so as to belong to that finger, and (ii) Authentication: The input impression is compared against all the  $N$  enrolled(templates), one by one to result in  $N$  different scores and the mean of the  $N$  score is taken to be the final score. Once again, the distribution of these scores can be used to model a Gaussian/Gamma distributions. The 80 fingerprint database consisting of 10 fingers, 8 impressions each was used as the data set and  $N = 4$  samples were enrolled for each finger. The input fingerprint could be of same or different finger. All the remaining fingerprints that were not used for enrollment were used for testing. Using the *Bozorth Matcher* score and with all minutiae preserved a verification accuracy of **99.8%** was achieved on DB1 of FVC2002. The accuracy was consistent across all models(ROC, Gaussian, Gamma) since all minutiae were considered. Using the *Alignment matching* method discussed in [36] along with a few modifications, the accuracy was found to be 98.5%. The presene of  $N$  templates instead of 1 makes the task of fingerprint verification that much easier, as indicated by the high verification accuracy rates. For the same DB1 FVC2002 dataset, in the 1 : 1 verification, an accuracy of 96.07% was achieved(reported in table 2.8 in section 2.2.3), whereas the 1 :  $N$  verification yielded 99.8%(reported above in this section).

#### 2.2.4 Use of Ridge Information in Fingerprint Comparison

Algorithms for fingerprint matching are used in human identification both in biometrics and in forensics (latent print and ten-print matching). The structures most widely used by fingerprint matching algorithms are minutiae– which are representations of ridge bifurcations and ridge endings. Minutiae-based algorithms with varying accuracy and efficiency are described in the literature on automatic fingerprint identification systems (AFIS) [11, 51, 52, 53, 54].

In several scenarios only a partial fingerprint image is available as input, e.g., compact silicon chip-based sensors that capture only part of the fingerprint, processing latent fingerprints from crime scenes, etc. The task in such cases is to match an incomplete input fingerprint against pre-enrolled full fingerprints. While some minutiae matchers are highly accurate in full fingerprint matching, their error rates dramatically increase with decreasing number of minutiae.

To overcome these three disadvantages, we proposed an effective algorithm for using ridges– based on utilizing representative ridge points (RRPs). A consideration was that an RRP have the same representation as minutiae so that existing minutiae matchers could be utilized with simple modifications to benefit from their well–developed tolerance to non-linear deformation. Since the addition of ridge points increases computation time significantly, a ridge point selection scheme is proposed, through which only one representative ridge point (RRP) is selected per ridge. Experiments demonstrated the effectiveness of using RRP for fingerprint matching as for the three disadvantages above.

The rest of this section is organized as follows: (i) relationship between available number of minutiae in the input, the number of matching minutiae and identification accuracy, (ii) alignment based on ridge similarity together with its drawbacks, (iii) RRP and how to utilize RRP on existing minutiae matchers, and (iv) results of comprehensive experiments performed to determine the effectiveness of the method for full and partial fingerprint matching.

### A. Partial Fingerprint Matching

Although some minutiae-based matching algorithms [11, 53, 52] are designed very well with satisfactory accuracy as well as efficiency, degradation in the performance of minutiae-only algorithms with decreasing number of minutiae is well-known [52]. In order to systematically study this effect one can generate fingerprint image snippets with progressively fewer numbers of minutiae as shown in Fig. 2.35(b)-(f)). In the last two of these there is also a loss of singular points (core and delta)(see Figs. 2.35(e) and (f)). In this effort our focus is on the effectiveness of using RRP for fingerprint matching when the number of available minutiae decreases in partial fingerprints with fair image quality, but not coping with the latent partial fingerprints in real forensic cases with very poor quality. So, we simulate partial fingerprints by cropping full-sized images with fair image quality.

The relationship between the number of available minutiae in the input to (i) the number of matching minutiae, and (ii) genuine error rate are illustrated in the chart of Figure 2.34. Partial images used to generate results shown in this chart were similar to those shown in Figure 2.35– which were generated from the NIST FVC2002 databases – using methods described in Section 2.2.4. The capacitive sensor resulted in more false minutiae and is therefore more similar to latent prints.

The average number of matched minutiae in DB1 and DB3 (when 15 minutiae are available) are only 10.92 and 7.98 respectively. From the “12 Point Rule” [56], the discriminative power of minutiae is insufficient for reliable verification. Although some commercial fingerprint scanners give a positive match with as few as eight minutiae [57], they require a high quality image– which is not always available in latent prints. Therefore, more features should be utilized in partial fingerprints to increase the discriminative power of fingerprints,

especially for partial ones. Since singular structures such as core and delta are unavailable in partial prints, general ridges need to be considered. Human examiners are known to utilize general ridges [58] which are always available in fingerprints. This leads to the consideration of using ridge information in addition to minutiae.

## B. Prior work in use of ridge information

### *Ridge related Symbol Definition*

In fingerprints, ridges are more general features than minutiae and singular points (e.g. core and delta). Firstly, we introduce some symbol definitions.

1.  $d$ : Average inter-ridge distance. Average distance between two directly nearby ridges. Normally,  $d$  is measured in pixel distance and could estimated from image samples in a fingerprint database (e.g. In FVC2002,  $d$  is about 11 pixel distance). Ridges are represented by points sampled at the average inter-ridge distance along the ridges(Figure 2.32(a)).  $d$  depends on the resolution of a fingerprint image.
2.  $L_i$ : Number of ridge points that could be sampled on the  $i^{th}$  ridge in a fingerprint.  $L_i$  could also be considered as the length of the  $i^{th}$  ridge (measured in units of  $d$ ).
3.  $L$ : Average number of ridge points that could be sampled on those longest ridges in fingerprints.  $L$  is defined for normalized ridge representation : on ridges whose  $L_i$  is larger than  $L$ , we sample up to  $L$  ridge points.  $L$  will play an important role in the selection of optimal ridge points. Like  $d$ ,  $L$  could also be estimated from image samples in a fingerprint database. However, unlike  $d$ ,  $L$  does not depend on image resolution, but depends on how much region of a finger is captured in a fingerprint image. Rolled full fingerprints will have larger  $L$  than flat full fingerprint. For flat full fingerprint,  $L$  could be considered as a constant, because the flat region of a finger that could be put on a sensor does not vary much. (e.g. In FVC2002,  $L$  is about 18).

A ridge associated with minutiae  $M_i$  is represented by points sampled at the average inter-ridge distance  $d$  from minutia  $M_i$  along the ridges as

$$R_i = \{P_{i1}, P_{i2}, \dots, P_{iL_i}\} \quad (2.47)$$

where  $P_{ij}$  represents the  $j^{th}$  ridge point sampled on ridge  $R_i$ .

## Previous Models Using Ridges

As minutiae pair, minutiae triplet and K-neighbors minutiae introduced in Section ??, ridges have also been utilized as local model [13, 14]. The following two measurements for ridge similarity are used in [14]:

$$Diff_{dist}(R_i, R_j) = \frac{1}{L_{min}} \sum_{k=1}^{L_{min}} |Dist(P_{ik}, M_i) - Dist(P_{jk}, M_j)| \quad (2.48)$$

$$Diff_{ang}(R_i, R_j) = \frac{1}{L_{min}} \sum_{k=1}^{L_{min}} |Ang(P_{ik}, M_i) - Ang(P_{jk}, M_j)| \quad (2.49)$$

where  $L_{min}$  is the minimum of  $L_i$  and  $L_j$ .  $Dist(P, M)$  represent the distance between ridge point  $P$  and minutiae  $M$ .  $Ang(P, M)$  represents the angle between the direction of the line segment  $MP$  and the orientation of the minutiae  $M$ . If the  $Diff_{dist}(R_i, R_j)$  and  $Diff_{ang}(R_i, R_j)$  are respectively within two thresholds, the two ridges  $R_i$  and  $R_j$  are considered to be similar enough. Such a ridge pair is used for fingerprint alignment. With the alignment decision, minutiae are converted into polar coordinates and then an adaptively compensating dynamic programming algorithm [13, 55] could decide the number of matched minutiae pairs. This model is efficient because the use of ridge similarity for alignment avoids an exponential search for point correspondence. Along with efficiency is the guarantee of reliable alignment, since minutiae matching depends on alignment. Although the matching stage could adaptively tolerate non-linear deformation and inexact pose transformation [13, 14], a sharp alignment error (Figure 2.32(b)), would exceed the tolerance of the minutiae matching stage and lead to a meaningless low score for an identical pair of prints.

A straight-forward solution is to use a tight threshold on ridge pair similarity. However, when there is a strong non-linear deformation of the fingerprint image, a tight threshold will result in no alignment— an identical pair will be assigned a zero score. Another approach is to use the most similar ridge pair— which may still offer a wrong ridge pair. This leads to the dilemma that a loose threshold would cause two similar but different ridges to be considered identical, while a tight threshold would not get an eligible ridge pair for alignment. Therefore, it is so difficult or impossible to find a proper threshold that could guarantee a true alignment and tolerate ridge deformation at the same time. One major cause is that the original alignment scheme [13] is based on a single ridge pair— with a risk that the pair of ridges chosen as being similar is wrong. The alignment scheme is improved by using multiple ridge pairs for alignment with a constraint that those pairs must share a similar transformation vector [13]. Although the modified matcher performs much better, it is still worse than Bozorth [11] and a compound minutiae matcher [53] which use minutiae only.

In [15], singular points such as delta and core are used to reduce the risk of false alignments resulting from unreliable ridge similarity. However, singular points are not guaranteed to exist in partial fingerprints, which limits the use of [15].

In [16], Hough Transform is used to approximate each ridge with a group of straight lines, all detected Hough space peaks are then used to estimate the rigid transformation parameters between the query and the template fingerprint images. After the alignment, a matching score is computed from a matrix of ridge alignments. Although the fingerprint verification accuracy in [16] is improved by this means, the matching run-time is, in the meanwhile, increased a lot.

In [17], ridges are not only used for fingerprint alignment, but also for later matching score computation. The computational complexity is very high because all sampled ridge points in a fingerprint are used for matching. What's more, the proposed algorithm requires a fairly high number of available minutiae in a fingerprint, so it will not be competent for partial fingerprint matchings.

In [18], a deformation model is developed for estimating the distortion effects in finger-

print impressions based on ridge curve correspondence. The proposed model was observed to result in a better performance compared to a model based on minutiae pattern correspondence. This fingerprint warping model is largely defined by the reliability of minutiae point correspondences generated by the algorithm. In partial fingerprint matching, minutiae matcher could not provide reliable minutiae correspondences, which will therefore limit the use of [18].

In the most recent work [59], ridge contours are used together with pores as level 3 features for more reliable matching of high resolution fingerprints. In this paper, we only focus on fingerprint matching with level 2 features.

There are three drawbacks in previous usages of ridge information:

1. Vulnerability under non-linear deformation, and not reliable for fingerprint alignment.
2. Trying to solve the first drawback mostly induce high computational complexity.
3. Unscalable for partial fingerprint matching.

**Vulnerability under Non-linear Deformation** Theoretically, increasing the number of features should not lead to worse performance. Practically, the method of utilizing ridge features is the key. Bozorth and the compound minutiae (or  $k$ -minutiae) matcher (also called CBFS [53] for coupled breadth first search) first compute local similarity and then perform global consolidation. The local features of Bozorth, compound minutiae matcher, and another based on triplets [52] are compared with the ridge similarity model in a fingerprint image in Figure 2.32(c). The boxes A, B, C and D could be considered as four types of local features. Clearly, an entire ridge such as D covers a large region. Conversely, the local similarity models defined as A, B and C are all within a relatively smaller region. In implementation, Bozorth only considers a minutiae pair if their distance is within a threshold [11]. The compound minutiae matcher uses  $k$  minutiae to control local region size and a variation uses only a triplet [52]. Several high accuracy minutiae matchers define local feature model within relatively small regions [60, 54]. Variety of non-linear deformation increases together with region size. So, local feature similarity defined on a larger region is more vulnerable to non-linear deformation. This essential weakness prevents ridge similarity model from better performance. A seeming solution is to divide entire ridges into several shorter ridges. However, a disadvantage is that, shorter ridges tend to be similar, because the longer a ridge is, the more variety it could have. Many shorter ridges divided from entire ridges tend to be short straight lines, thus could not be relied on for alignment decision. This is also why the ridge similarity model is not used in partial fingerprint matching. With the fact that using ridge similarity is blocking us from further improvement. An effective method is to utilize ridges for matching by means of representative ridge points (RRPs), which could avoid alignment using entire ridges.

**High Computational Complexity** In order to solve the first drawback, most previous use of ridge information tend to induce high computational complexity. In [16], Hough Transform brings on a large number of straight lines to approximate ridges in a fingerprint

and the computational complexity in the alignment stage is increased a lot. Minutiae matching is essentially a directed point pattern matching problem [13]. This implies that, if all sampled ridge points in a fingerprint are used for matching as in [17], the computational complexity in the matching stage will tend to be unacceptable.

**Unscalable for partial fingerprint matching** Ridge similarity models [13, 14, 16, 15] prefer long ridges in order to offer reliable alignment based on the decision that whether two ridge are similar or not. However, in partial fingerprints, most ridges are shorter than those in full prints. Therefore, ridge similarity will be further impaired and could not provide reliable alignment decision. The ridge warping algorithm [18] depends on a pre-computed minutiae correspondence, which implies that, in partial fingerprint matching, low number of available minutiae will weaken the effectiveness of the model. So, most previous algorithms using ridge information have not been designed to be unscalable for partial fingerprint matching.

*Our Motivation* Motivated by the above three drawbacks of previous works making use of ridges, the algorithm we are going to propose is specially designed to tolerate non-linear deformation. In the meanwhile, we try to realize the tolerance only by introducing acceptable run-time increment. What's more, our algorithm is also naturally competent for partial fingerprint matching.

## C. Representative Ridge Points

Minutiae represent only a portion of the discriminative information present in a fingerprint. Fig. 2.33 illustrates that, the match of two ridges is not reliable if we only use minutiae location and orientation as the criteria. Human examiners utilize general ridge information as described in the forensic friction ridge analysis literature [58]. As in Figure 2.36(a), two genuine fingerprints have not only matching minutiae but also matching ridges. However, there are no minutiae in each of the regions represented by the five boxes, which means minutiae could not capture the matching of two genuine fingerprints in these regions, where only ridges exists. In light of the discussion in Section 2.2.4, it is too risky to use ridge similarity in the alignment stage. Thus it was decided to try using ridge features in the matching stage. Some existing minutiae matchers have already been designed very well to tolerate non-linear deformation and make accurate decisions. So, it is expected that ridges could be input into such minutiae matchers. Ridges are represented as sampled ridge points as in Figure 2.32(a). If each ridge point is assigned a direction according to the ridge flow(towards minutiae) in the ridge point, ridge points will have exactly the same representation as minutiae. Although when both minutiae and ridge points could be directly input into minutiae matchers, unacceptable run-time will be an obvious problem. Apparently, it is not necessary to use all ridge points. A fingerprint is a smoothly flowing pattern of alternating ridges and valleys [61]. Ridge points that are close to each other tend to be implicated(infer position and orientation) from each other. Therefore a fingerprint feature called representative ridge point (RRP) is introduced– which only uses several or even one sparse representative ridge point(s).

**Basic RRP Selection Scheme** As defined earlier, a ridge associated with minutiae  $M_i$  is represented as  $R_i = \{P_{i1}, P_{i2}, \dots, P_{iL_i}\}$ . Starting from minutiae  $M_i$ , each ridge point is given an index  $i \in \{1, \dots, L_i\}$ . All the indices could be represented as a set  $I = \{1^{st}, 2^{nd}, \dots, L^{th}\}$  ( $L$  is defined in Section ??).

For all fingerprints, the RRPs are selected according to a pre-determined subset of  $I$ . We use  $I_{RRP}$  to represent this subset. For example, if  $I_{RRP}$  is decided to be  $\{k_1^{th}, k_2^{th}\}$ , then the  $k_1^{th}$  and  $k_2^{th}$  ridge point is selected from all ridges. The goal is to choose the indices such that a majority of ridges will contain these ridge points.

Under this selection scheme, through proper transformation (shift and rotation) [13], a genuine ridge pair will simultaneously have overlapping minutiae and overlapping RRPs. This is guaranteed by the fact that we use a pre-determined index subset  $I_{RRP}$  for all fingerprints. Suppose different indices are selected for different ridges, it is easy to imagine that genuine ridges would not be guaranteed to have overlapping RRPs. For two different ridges, with the pre-determined index subset  $I_{RRP}$ , it is less unlikely that they simultaneously have overlapping RRPs and overlapping minutiae, although they might occasionally have overlapping RRPs or overlapping minutia separately. “Overlap” is defined to be within a certain bounding box [13, 14] but not exactly overlapping because of non-linear deformation. Figure 2.36(a) illustrates the potential effectiveness of RRPs in a global view: when two fingerprints match, ridges will also match which means RRPs will match too. Although in some cases, two different fingerprints might have many occasionally overlapped minutiae, it will be difficult for this pair to also have many overlapping RRPs at the same time. Figure 2.36(b) is an example of RRPs, in which  $I_{RRP} = \{6^{th}, 12^{th}\}$ . Figure 2.36(b) also shows the regions that are originally ignored by minutiae (there are no minutiae inside any of the five boxes), currently could be characterized by RRPs. After the bringing RRPs as new fingerprint feature, a fingerprint contains ridge endings, ridge bifurcations and RRPs, while originally, only ridge endings, ridge bifurcations are defined (See Fig. 2.2). In other words, for ridges in two fingerprints, both minutiae and some predetermined RRP overlapping indicates a more possible match than just the minutiae overlapping. But too many RRPs could also add redundant information. Two key concerns about selection of RRP are:

1. How many RRPs should be selected per ridge?
2. Which ridge points should be selected as RRPs?

Extensive experiments were conducted to answer the two questions. Before that, the selection of RRPs is described from a theoretical perspective.

**How Many RRPs should be Selected per Ridge?** It can be shown that only one RRP needs to be selected per ridge. The reasons explained below highlight two basic points (i) fewer RRPs are required for lower time complexity and (ii) fewer RRPs (as low as just one) suffice since it is redundant to have many RRPs.

Theoretically, in order to assure accuracy, all the ridges points should be used with minutiae together as inputs to minutiae-based matcher. However, considering run-time, the number of selected ridge points should not be too high. Therefore RRP selection should be such that a satisfactory matching accuracy is obtained with the fewest RRPs per ridge.

## 2.2. METHODS

## CHAPTER 2. FINAL REPORT NARRATIVE

The time complexity of minutiae matching is no less than  $O(n^3)$  when both fingerprints to be matched have exactly  $n$  minutiae. This can be seen as follows. In the pairwise local model [11], each intra-table construction involves  $O(n^2)$  comparisons and the inter-table match has more than  $O(n)$  comparisons. The  $k$  minutiae model takes  $O(n)$  to build the local models and  $O(n^2)$  for coupled breadth-first search.

If  $|I_{RRP}| = k$ , which means, on each ridge,  $k$  ridge points are selected as RRP (for now, we temporarily assume that all ridges are long enough to have all the  $k$  ridge points), the overall number of inputs (minutiae and RRPs) to minutiae-based matcher is  $n + nk$  (number of ridges equals to number of minutiae). Therefore, the new time complexity of minutiae-based matcher will be no less than  $O((n(1+k))^3)$ . The effect of  $k$  should not be neglected because the number of minutiae  $n$  is around 50 and  $(1+k)^3$  will be on the same level when  $k$  increases. Table 2.10 displays both the theoretical and actual run-time increment according to the increases of  $k$  (number of RRPs selected per ridge). Even though the practical run-time is much less than the theoretical run-time (factors influencing practical run-time will be introduced in Section ??), it is clear to see that, there will be huge run-time increment when more than one RRP are used for matching. Therefore, we prefer to select only one RRP per ridge. Is one RRP sufficient to represent a whole ridge? Which RRP should be selected? We will show in the next section that an intelligent way to select this one RRP sufficing to approximately implicate(infer) the other RRP's.

**Which Ridge Points should be selected as RRPs?** A friction ridge pattern consists of smoothly flowing alternating ridges and valleys [61]. Ridge points tend to be implicated (position and orientation) by their neighbors on the same ridge. A ridge  $R_i$  as defined in Equ. 2.47 is shown in Fig. 2.37(a). Suppose the  $k^{th}$  ridge point is selected as RRP. Note that now only the minutia  $M_i$  and the ridge point  $P_{ik}$  are available (See Fig. 2.37(b)). The length of that ridge segment between  $M_i$  and  $P_{ik}$  is  $kd$  (ridge points are sampled at average inter-ridge distance  $d$  from minutia along ridge). It is possible to infer the approximate shape of the ridge between the minutia  $M_i$  and the selected ridge point  $P_{ik}$  : Fig. 2.37(c) shows four candidate types for the approximate shape of the ridge segment of length  $kd$  and fixed positions of both the two end points. Because fingerprint ridges are smoothly flowing patterns, so that only these four types are possible. Please note that, in (c), we are only considering the four possible candidates because we only care about the approximate ridge shape types. Slight shakes on ridge shapes are not interesting here because, given the existence of non-linear deformation in fingerprint impressions, it is irrational and impossible to use a strict criterion such as ridge similarity to say whether two ridges are identical or not. Instead, we use the basic ridge type (e.g. one/two turn) to classify all possible ridges connecting a minutia and a ridge point. Admittedly, there might be other possible ridge shape types, e.g. in core and delta region, ridges may have very sharp turns or more than two turns. However, in most cases, fingerprint ridges are smooth flowing patterns with seldom sharp turns, and unlikely have more than three turns. So, we are only considering the four possible candidates in Fig. 2.37(c). Among these four types, only one shape( $B$ ) satisfies the given orientations of both  $M_i$  and  $P_{ik}$  (See Figure 2.37(c)). Hence, minutiae  $M_i$  and ridge point  $P_{ik}$  suffice to approximately infer the shape  $B$  (Due to frequent non-linear deformations existing in

## 2.2. METHODS

## CHAPTER 2. FINAL REPORT NARRATIVE

fingerprint images, it is sufficient to infer only a approximate shape). The above statement holds good for each  $k \in [1, L_i]$ . Therefore, to approximately infer the entire ridge, the  $M_i$  and the last ridge point  $P_{iL_i}$  are needed.

The above example gives the intuition that by adding ridge point information (position/orientation), we can approximately infer the ridge shape together with the minutiae. Then we say that the index to be used for RRP selection should satisfy the following two conditions:

1. The index should be large so as to infer as many other ridge points (by inferring approximate shape of ridge segment up to that index) as possible, which has just been shown (from the view of a single ridge).
2. A common index will be used for all ridges in the fingerprints to be matched (it is *inconsistent* for matching if different indices are chosen for different ridges (as explained in Section 2.2.4). The index should not be too large because the majority of ridges are *not* expected to be long enough to have ridge points with the pre-determined index (from the view of a fingerprint with many ridges with different lengths).

*Procedure to Extract RRPs* The process of extracting RRPs from fingerprint images involves five operational steps: image enhancement, skeletonization, minutiae detection, ridge point detection, and RRP selection. The result of each operation is illustrated in Figure 2.38. Salient points of the five procedures are as follows.

1. *Fingerprint Image Enhancement*: Enhancement can amplify the effectiveness of RRPs because discontinuous ridges could be connected and therefore extracted ridge points and selected RRPs are more accurate. Many fingerprint image enhancement algorithms have been proposed [62, 63, 64, 65]. After the enhancement, binarization is performed as input to later skeletonization.
2. *Ridge Skeletonization*: Skeletonization is a process for reducing foreground regions in a binary image to a skeletal remnant that largely preserves the extent and connectivity of the original region while throwing away most of the original foreground pixels [66, 67]. Through skeletonization, foreground regions in a binary image or silhouette could be thinned to a one-pixel width spine. The Matlab image processing toolbox [68] provides support for skeletonization via the `bwmorph` function. Ridge skeletonization is preparation for ridge points detection.
3. *Minutiae Detection*: Introduced in Section 2.2.4.
4. *Ridge Point Detection*: Firstly, decide  $d$ -average inter-ridge distance and then sample ridge points starting from each minutia along ridge, each step goes  $d$  distance. Each ridge point ( $i^{th}$ ) is assigned a direction according to the ridge flow (towards minutia) in the ridge point, or could be approximated by the direction of the arrow from the  $i^{th}$  ridge point to the  $(i - 1)^{th}$  ridge point on the same ridge.
5. *RRP Selection*: With the scheme described in the first two parts of Section 2.2.4).

*Minutiae matcher modification* If minutiae and RRP(s) are directly used as input, a minutiae matcher will mistakenly consider a minutia and the selected RRP(s) in the same ridge as identical pair, which is wrong. Therefore, we modified the minutiae matcher into a two-phase matcher. The motivation for using a two phase matcher is from the fact that Ridge points strengthens individuality of fingerprints. For two fingerprints to match, its not necessary that some minutiae alone match, but also **their corresponding** ridge match. Hence, in the first phase we match only minutiae and in the second phase, we include additional constraint that the corresponding ridges of the matched minutiae must also match. Thus, three constraints should be modified in a minutiae matcher.

1. Minutiae could only match with minutiae.
2. An RRP could only match with an RRP with the same ridge point index. (e.g. A 6<sup>th</sup> RRP could only match with another 6<sup>th</sup> RRP, but not with a RRP with any other index.)
3. The RRP(s) should be matched only after the corresponding minutiae haven been matched.

With the guideline for RRP selection and matcher modification, a group of minutiae based minutiae could be improved to have more accurate performance conveniently.

## D. Experiments and Results

Bozorth and k-minutiae were designated as matchers that use only minutiae. For parameter  $k$  in k-minutiae matcher, 8 is used for matching with only minutiae, and 10 is used for matching with minutiae+RRP. The reason is that, when having more points,  $k$  should be increased so that k-minutiae model could still cover local regions of a similar area as originally covered only by minutiae. FVC2002 are used for full fingerprint matching. Each database consists of 800 images (100 distinct fingers, 8 impressions each). Before using MINDTCT [11] to detect minutiae, [62] is used for fingerprint image enhancement. Extensive experiment are conducted for both full fingerprints and partial fingerprints in this section. For full fingerprints:

A. Testing of varing performance of RRP by using different RRP index selection schemes that include:

1. Pre-determined RRP index
2. Dynamically selected RRP index
3. Empirical RRP index

B. Testing of efficiency performance of using RRP.

One important note is that, for an existing algorithm, we are comparing its performance with RRP and without RRP as input, but not between different algorithms. Even those state-of-the-arts algorithm that have not been tested in our paper are expected to have better accuracy than themselves when having RRP as input together with minutiae.

*Full fingerprint matching*

We mentioned earlier two key concerns about using RRP for fingerprint matching and theoretical analysis was perposed on how many RRP should selected and which one or ones should be selected. In this section, we will conduct experiment to explore the performance of RRP.

*Testing of Varing performance of RRP*

Due to the difference of fingerprint textures and image qualities among data sets, RRP selection is dependent on data sets. The average inter-ridge distance is about eleven pixels in FVC2002, and an entire ridge normally has more than 12 ridge points. Figure 2.39 showing the ridge length statistics for the FVC datasets. Besides the average ridge length for all 800 images in each data set, more robust median, complemented by the interquartile range (IQR) is also considered as a dispersion measure. Note that in fact, the levels induced by the medians sometimes differ from the ones based on means which are possibly biased by extremely short or long ridge. The statistical information could be a help to select RRP index which is thus based on the comprehensive consideration of the Mean and IQR. The median levels being above than means, indicates that the average ridge length might be biased by short ridges, for example in DB1, together with small lower IQR further prove that there exist relatively short ridges (with no more than 6 ridge points). Also for DB3, the ridge lengths are distributed more evenly (mostly short ridges means low image quality) due to comparative IQR and std range.

For Bozorth, the matching scores come directly from Bozorth's outputs when having both minutiae and RRP as input. For k-minutiae, a score-level fusion is used for both (i) k-minutiae outputs when having only minutiae as inputs, and (ii) k-minutiae outputs when having both minutiae and RRP as inputs, using the sum rule and min-max normalization [69]. RRP alone are not used for matching since they do not have as much discriminating power as minutiae. The RRP are used to assist matching originally done only by minutiae. For each database, 2800 genuine comparisons were selected (each impression of a finger is compared with the rest of the impressions resulting in  $(8 \times 7) / 2$  tests per finger) and 4950 impostor pairs (the first impression of each finger is compared against the first impression of all other fingers resulting in a total of  $(100 \times 99) / 2$  tests).

**Single RRP with pre-determined Index** Without lost of generality, we test the performance by selecting different RRP index at a time. In our experiment, RRP index ranges from 2 to 14. Equal Error Rate comparison on all the four databases in FVC2002 are shown in Table 2.11. In all four cases, both Bozorth and k-minutiae are improved by using minutiae and RRP together.

**Single RRP with Dynamically-selected RRP Index** From the experiment of using single RRP with pre-determined index, due to different qualities among fingerprint image data sets, the selection of RRP is not independent. Figure 2.40 shows the EER vs different RRP indices. Because of the varying length of ridges in the fingerprints images, the matching results could still be improved by selecting different RRP index on the fly. In other words, we avoiding choosing a common RRP index for all the 7750 comparisons (7750 pairs of

images). For every pair of fingerprint image, a particular RRP index is selected basing on the ridge information on both images. The advantage of this is that specific ridge information is considered for every pair of matching instead of using a general pre-selected RRP, the result should be better. There could be many ways to select one reasonable index for both images to be compared. For example, the minimal value of average ridge length for both fingerprint can be selected as the RRP index. However, there exists extreme short or long ridge, that could significantly affect the average ridge length. In Figure 2.39, for example in DB1, as we mentioned, except for few short ridges there are more ridges that have over 11 ridge points than those having less than 11 ridge points. Thus, to select a feasible RRP index, we use the upper quartile ridge together with the average length in both images to be compared. That is, for every comparison, we select the index  $i$  on the fly in equation 2.50

$$i = \left\lceil \frac{Mean + UpperIQR}{2} \right\rceil \quad (2.50)$$

And for all matchings hybrid RRP are used. Table 2.12 shows the Equal Error Rate is further improved compared to the best results from using a pre-determined RRP index. The ROCs curves are also shown in Figure 2.41 and the comparison will be given in the coming section.

**Single RRP with Empirical Index** The experiment of dynamically selecting RRP index demonstrate the significant power of using minutiae and RRP together. But a tradeoff has to be balanced between the two conditions above. By pre-determined RRP index, the sacrifice of a little bit accuracy wins a lot of time, since statistical ridge information needs to be extract beforehand if we want to selecting the RRP index dynamically. Together with another practical concern that the image quality is poorer in periphery of fingerprints than inner region, and that, ridges with large indices (those that are long ridges) mostly exists in periphery of fingerprints, we recommend to use an fix index  $i$  as given in equation 2.51

$$i = \left\lceil \frac{2}{3}L \right\rceil \quad (2.51)$$

This theoretical recommendation was also seen to be better empirically. In previous section, we propose the hybrid selection scheme base on the ridge statistic information in FVC2002 in Figure 2.47. The overall ridge length distribution for all four data sets indicates matching with minutiae and 12<sup>th</sup> RRP would be the best in FVC2002 databases (12 is just  $\lceil \frac{2}{3}L \rceil$  in FVC2002 where  $L = 18$ ). For full fingerprint matching, since  $L$  does not change very much among different databases (see the definition of  $L$ ), the 12<sup>th</sup> could be directly used. As for partial fingerprint matching, most fingerprints do not have the 12<sup>th</sup> RRP because of smaller sizes and therefore smaller  $L$ . It is more accurate to decide  $L$  for equation 2.51 according to each individual partial fingerprint. However, it implies recording in the template database, for each full fingerprint, all RRP. This is not feasible considering storage.

As a tradeoff, for template databases(database with full fingerprints), it was decided to only extract and store the 6<sup>th</sup> and the 12<sup>th</sup> RRP. The 12<sup>th</sup> RRP will be used when the input fingerprint is a full fingerprint and the 6<sup>th</sup> RRP will be used when the input fingerprint is partial. For special cases such as: partial fingerprints with only 10 available minutiae (most

## 2.2. METHODS

## CHAPTER 2. FINAL REPORT NARRATIVE

are too small to have even the 6<sup>th</sup> RRPs), RRPs with even smaller index such as the 4<sup>th</sup> have to be used. A course method to determine whether a fingerprint is full or partial, is by counting the number of minutiae available and compare to a threshold. The specific threshold depends on average number of minutiae of fingerprints in a particular scenario.

The Equal Error Rate comparison on all four databases in FVC2002 with using the hybrid RRPs and RRP with empirical index are already shown in Table 2.11. Both From the view of confidence interval [70], for Bozorth, all the four improvements resulting from utilizing RRPs are significant with 95% confidence, and for k-minutiae, the improvement on DB3 is significant with 95% confidence. Figure 2.41 shows the ROCs on each of the four databases with the 12<sup>th</sup> ridge points are used and also with dynamically selected RRP. It is observed that every ROC of using minutiae and RRPs together is totally above its corresponding ROC of using minutiae only. The coming partial fingerprint matching experiments demonstrate the even more significant effectiveness of using minutiae and RRPs together.

### *Testing of Efficiency performance of RRP*

As analyzed in Section ??, the theoretical time complexity of minutiae-based matcher having  $n$  minutiae and  $k$  RRPs per ridge as inputs is  $O((n(1+k))^3)$ , with the assumption that all ridges are long enough to have all the  $k$  RRPs. Besides the theoretical run-time computed by algorithm complexity, some other factors also influence actual run-time.

1. When minutiae and only one RRP ( $[\frac{2}{3}L]^{th}$ ) per ridge are used, experiments show that about half of ridges are long enough to have the  $[\frac{2}{3}L]^{th}$  RRP. Therefore the size of input to minutiae matchers, which is number of minutiae plus RRPs, will be  $n + \frac{1}{2}n = \frac{3}{2}n$ . When more and more one RRPs are selected per ridge, the chance for ridges to have those RRPs with small indices also increases together. Therefore, the size of input to minutiae matcher will be  $n + \frac{1}{2}n + (k-1)n = n(k - \frac{1}{2}n)$  for  $k > 1$ .
2. When selecting  $k$  RRPs per ridge, we do not have to input all minutiae and all RRPs together into a minutiae matcher. A better option is to input them in  $k$  rounds. In each round, we only input minutiae and RRPs with a single index. We then do score fusion [69] with the  $k$  outputs of the  $k$  rounds. RRPs alone are not used for matching since they do not have as much discriminating power as minutiae. RRPs are used to assist matching originally done only by minutiae. With this method, the run-time of using more than one RRPs per ridge will be reduced from  $O((n(1+k))^3)$  to  $O(k(2n)^3)$ . Although it is still unacceptable to use a large  $k$  in most usages requiring high efficiency, it is not a bad idea for some particular usages that do not care much about run-time, e.g. matching one fingerprint with several potential genuine candidates.
3. After the modification to minutiae matcher as described in Section ??, the actual run-time will be less because minutiae matcher will quickly deny some pairs to match such as one minuta with one RRP or two RRPs with different indices. The influence of this factor to actual run-time depends on how early an ineligible pair could be denied, and therefore depends on different minutiae-based matchers.

According to the three factors above, the actual run-times are listed in the last two rows of Table 2.10. Note that, the empirically actual run-time of using minutiae and only one

## 2.2. METHODS

## CHAPTER 2. FINAL REPORT NARRATIVE

RRP ( $[\frac{2}{3}L]^{th}$ ) per ridge is about twice of run-time of using only minutiae, which is acceptable. The practical run-time of using  $k$  ( $k > 1$ ) RRP's per ridge, is estimated to be  $O(\frac{1}{2}k(2n)^3)$  where  $k(2n)^3$  is explained in the second factor and  $\frac{1}{2}$  is an estimation from the third practical factors, which actually depends on different minutiae-based matching algorithms.

*Partial fingerprint matching* Firstly, it does not matter which fingerprint database we use, because every algorithm will be compared with itself on a number of partial fingerprint databases. Our highlight is the different performances when matching with or without RRP as input. Secondly, we are focusing on the effectiveness of using RRP for fingerprint matching when number of available minutiae decreases in partial fingerprints with fair image quality, but not coping with the latent partial fingerprints in real forensic cases. So, we simulate partial fingerprints by cropping full-sized images with fair image quality with the method designed to generate partial prints from full prints by cutting out portions of it: (i) To begin, a random minutiae is chosen. (ii) Next, its  $(N - 1)$  nearest neighbors are selected. (iii) Finally, a region is cut-out as a partial fingerprint with a bounding box that only contains  $N$  minutiae. The size of partial fingerprint is controlled by varying  $N$  (number of available minutiae in partial fingerprints). In the experiments,  $N$  increases from 15 to 35 with a step of 5.

Although the 4<sup>th</sup>, 5<sup>th</sup>, 6<sup>th</sup>, 7<sup>th</sup> and 8<sup>th</sup> RRP's for these five levels (recall  $[\frac{2}{3}L]$ ) should be used, with storage considerations (as discussed in section ??) the 6<sup>th</sup> RRP's were used for all five levels of partial fingerprint matching. Bozorth and k-minutiae are tested on partial fingerprint databases generated from FVC2002 Database, which have respectively the best and the worst image quality [44] in FVC2002. Because the initial minutiae when simulating partial fingerprint is randomly selected, three partial databases were generated for each value of  $N$  and then three EERs are averaged. In each database, number of genuine pairs and impostor pairs used for partial fingerprint matching are respectively 5600 and 9900 (twice the number in full fingerprint matching, because in partial fingerprint matching, fingerprint pair  $P_1$ (a partial print of fingerprint  $F_1$  and fingerprint  $F_2$ ) is different from fingerprint pair  $P_2$ (a partial print of fingerprint  $F_2$  and fingerprint  $F_1$ ).

Equal error rates (EERs) for partial fingerprint matching are shown in Table 2.13. All the EERs are plotted in Figure 2.42, from which it is seen that significant and stable improvements by using minutiae and RRP's together for partial fingerprint matching. Although some algorithms designed specially for partial fingerprint matching [52] have similar EERs using only minutiae, the highlight of this work is that, for a given minutiae matcher, improvement obtained by using both minutiae and RRP are even more significant in partial fingerprint matching than in full fingerprint matching.

## 2.3 Results

### 2.3.1 Statement of Results

#### Twin's Study

A study of the discriminability of the fingerprints of twins has been presented. Using a larger set of samples than used in previous studies, the similarities of the fingerprints of twins was studied. Live scans and younger ages of the subjects ensured good quality prints thereby allowing the focus to be on the inherent individuality of fingerprints and one that was not affected by image quality issues.

Two studies were conducted using fingerprint features at levels 1 and 2. The level 1 results, obtained by human visual comparison, show that twins finger's have a higher probability of having the same classification (42%) than in the case of non-twins (25%).

Level 2 features were studied using a minutiae-based matching algorithm which provides a similarity score. Distributions of scores were compared using the Kolmogorov-Smirnov test. The statistical inferences from the level 2 study are:

1. The distribution of the similarity of corresponding fingerprints of twins is different from that between genuine prints of the same finger.
2. The distribution of similarity of corresponding fingerprints of identical twins is the same as that between corresponding fingerprints of fraternal twins.
3. The distribution of similarity of fingerprints of twins is different from that between arbitrary fingers.

Although friction ridge patterns of corresponding fingerprints of twins are more similar than between two arbitrary fingerprints, they are still discriminable using minutiae-based algorithms.

#### Generative Model of Individuality

Generative models of individuality attempt to model the distribution of features and then use the models to determine the probability of random correspondence. We have proposed such models of individuality for birthdays, heights and fingerprints. Individuality is evaluated in terms of three probability measures: probability of random correspondence (PRC) between two individuals, general probability of random correspondence ( $n$ PRC) between two individuals among a group of  $n$  individuals and specific probability of random correspondence (specific  $n$ PRC) which is the probability of matching a given individual among  $n$  individuals.

We have proposed a generative model for both minutiae and ridge information, featured by ridge length and points. We used a mixture distribution to model ridge information. The generative model is then compared by implementation and experiments with a generative model without ridge information on the FVC2002 DB1. The PRC obtained for a fingerprint template and input with 36 minutiae each with 16 matching minutiae is  $1.4 \times 10^{-10}$ . This is a much stronger result than without using ridge information which is  $5.1 \times 10^{-6}$ . It has also

## 2.3. RESULTS

## CHAPTER 2. FINAL REPORT NARRATIVE

been observed that the  $n$ PRC and specific  $n$ PRC values with ridge information are much smaller than the PRC values without ridge information. Considering the case of 100000 fingerprints, the  $n$ PRC with ridge information where 26 out of 36 ridges are matched is  $1.5202 \times 10^{-14}$  instead of  $5.3414 \times 10^{-6}$  without ridge information. Similarly, given a specific fingerprint with 26 minutiae, the specific  $n$ PRC with ridge information where 14 out of 40 ridges are matched is  $1.1780 \times 10^{-58}$ , which is much smaller than  $7.3652 \times 10^{-23}$  where only minutiae is considered. The proposed ridge information model offers a more reasonable and more accurate fingerprint representation. The results provide a much stronger argument for the individuality of fingerprints in forensics than previous generative models.

### Likelihood Methods for Fingerprint Matching

Two different approaches to making a verification decision based on the score of a fingerprint matcher have been compared. The first, based on obtaining an ROC curve of scores, is a standard approach used by the biometrics community. The second is based on determining the likelihood ratio obtained from the distribution of scores conditioned upon whether the input pair belongs to the same finger or not. A comparison of the two approaches was empirically determined using standard fingerprint databases.

The study was in the context of a variable number of available minutiae. The decision methods involve mapping from feature space (minutiae) to distance space (similarity score). As the number of minutiae in the samples were reduced, the error rates increased, as expected, but with the likelihood methods performing significantly better than the ROC-based methods. This suggests that LR method for matching is a significantly superior method of choice over the ROC method, especially and most usefully so in the regime of small numbers of available minutiae. It should be noted that the results are with available numbers of minutiae rather than the number of matching minutiae which is expected to be a fraction of the available minutiae.

### Representative Ridge Points

Most automatic fingerprint matching algorithms are based on only using minutiae. Those that have been proposed for using ridge information have three major disadvantages : (i) sensitivity to non-linear deformation, (ii) high computational complexity and (iii) unscalable to partial fingerprint matching. To overcome these disadvantages, we proposed an algorithm to utilize ridge information more effectively— by choosing representative points along the ridges. In specific, the chosen ridge points are used, together with minutiae, in existing minutiae matching algorithms with modification to benefit from their well-developed tolerance to non-linear deformation (for disadvantage (i)). Since the addition of ridge points increases computation time significantly, a ridge point selection scheme is proposed, through which only one representative ridge point (RRP) is selected per ridge. The actual matching run-time is less than twice of original (for disadvantage (ii)). The performance of choosing fixed different RRP indices and dynamically selecting hybrid index were tested. Then an empirical RRP selection scheme is proposed. Extensive experiments on partial prints (cut from full-size prints) demonstrate the stable and significant accuracy improvement when

### 2.3. RESULTS

### CHAPTER 2. FINAL REPORT NARRATIVE

having a large range of numbers of available minutiae (10-35) as input (for disadvantage (iii)). Two caveats are: (1) the focus was on the effectiveness of using RRP for fingerprint matching when the number of available minutiae decreases in partial fingerprints with fair image quality, but not coping with the latent partial fingerprints. Partial fingerprints were simulated by cropping full-sized images with fair image quality, and (2) for an existing algorithm, we are comparing its performance with RRP and without RRP as input, but not between different algorithms. Even other state-of-the-arts algorithms not tested can be expected to have better accuracy than themselves when having RRP as input together with minutiae.

### 2.3.2 Tables

The following tables are referred to in the program narrative.

Table 2.1: False Positive Rate with Twins and Non-twins using Bozorth Matcher.

	FP Error Rate	EER Threshold
Non-Twins	2.91%	18
Twins	6.17%	26

Table 2.2: Samples of twins showing both similarity and dissimilarity at Level 1.

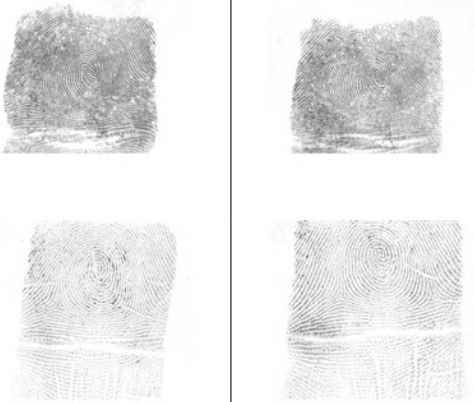
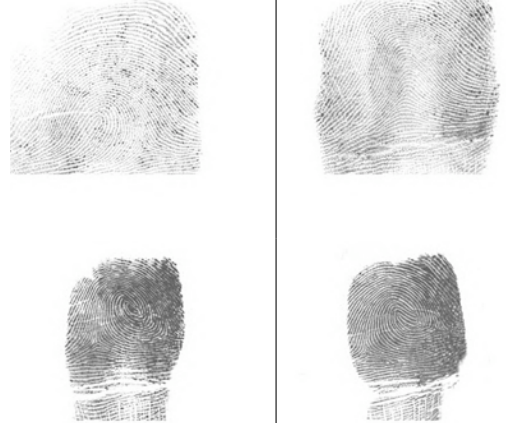
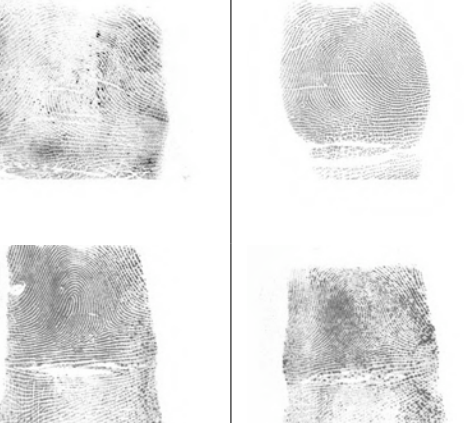
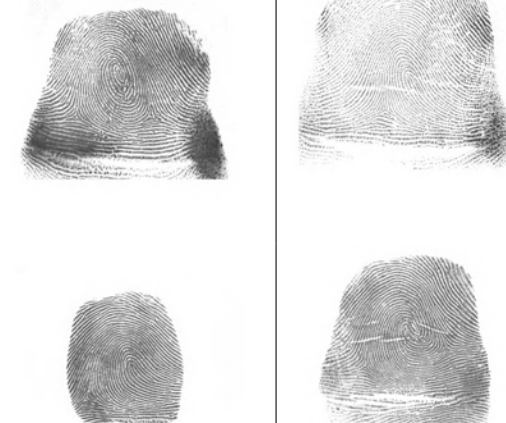
	
Matching Level 1: Identical twins	Non-matching Level 1: Identical twins
	
Matching Level 1 - Fraternal twins	Non-matching Level 1 - Fraternal twins

Table 2.3: Kolmogorov-Smirnov test between different distributions. All distribution pairs, except identical vs fraternal, were found to be different from each other.

	Gen v Twin	Ident v Frat	Twin v Non-Twin	Gen v Non-Twins
K-S(prob)	0.0010	0.9999	0.1174	0.0004

Table 2.4: Results from the Chi-square tests for testing the goodness of fit of the mixture models with and without ridge information. The total number of fingerprints in FVC2002 DB1 is 800.

<b>p-value</b>	<b>Without Ridge information</b>	<b>With Ridge information</b>
$p - value > 0.01$ (Model Accepted)	574	679
$p - value \leq 0.01$ (Model Rejected)	226	121

2.3. RESULTS

CHAPTER 2. FINAL REPORT NARRATIVE

Table 2.5: PRC for different fingerprint matches with varying  $m_1$  (number of minutiae/ridges in fingerprint  $f_1$ ),  $m_2$  (number of minutiae/ridges in fingerprint  $f_2$ ) and  $\hat{m}$  (number of matched minutiae/ridges) - With ridge information and without ridge information.  $p_\epsilon$  is the theoretical PRC for the general population and  $\hat{p}_\epsilon$  is the empirical PRC for FVC2002-DB1.

No. query $m_1$	No. temp $m_2$	No. match $\hat{m}$	Minutiae Only		Minutiae and Ridges	
			$p_\epsilon$	$\hat{p}_\epsilon$	$p_\epsilon$	$\hat{p}_\epsilon$
16	16	4	$2.1 \times 10^{-1}$	$2.1 \times 10^{-1}$	$3.9 \times 10^{-2}$	$1.6 \times 10^{-3}$
		8	$1.1 \times 10^{-2}$	$7.8 \times 10^{-3}$	$1.8 \times 10^{-5}$	$1.7 \times 10^{-8}$
		12	$1.2 \times 10^{-5}$	$5.7 \times 10^{-6}$	$2.0 \times 10^{-10}$	$3.7 \times 10^{-15}$
		16	$4.8 \times 10^{-11}$	$1.6 \times 10^{-11}$	$8.9 \times 10^{-18}$	$3.1 \times 10^{-24}$
26	26	6	$1.3 \times 10^{-1}$	$1.4 \times 10^{-1}$	$7.4 \times 10^{-3}$	$7.9 \times 10^{-4}$
		8	$3.5 \times 10^{-2}$	$4.3 \times 10^{-2}$	$3.0 \times 10^{-4}$	$1.2 \times 10^{-5}$
		12	$3.6 \times 10^{-4}$	$5.4 \times 10^{-4}$	$6.9 \times 10^{-8}$	$3.8 \times 10^{-10}$
		16	$3.2 \times 10^{-7}$	$6.0 \times 10^{-7}$	$1.4 \times 10^{-12}$	$1.1 \times 10^{-15}$
		20	$2.3 \times 10^{-11}$	$5.3 \times 10^{-11}$	$2.3 \times 10^{-18}$	$2.4 \times 10^{-22}$
		26	$6.7 \times 10^{-21}$	$2.1 \times 10^{-20}$	$2.2 \times 10^{-30}$	$1.2 \times 10^{-35}$
36	36	6	$1.5 \times 10^{-1}$	$1.7 \times 10^{-1}$	$1.8 \times 10^{-2}$	$4.1 \times 10^{-3}$
		8	$5.8 \times 10^{-2}$	$9.0 \times 10^{-2}$	$1.3 \times 10^{-3}$	$1.4 \times 10^{-4}$
		12	$1.5 \times 10^{-3}$	$4.3 \times 10^{-3}$	$1.1 \times 10^{-6}$	$2.9 \times 10^{-8}$
		16	$5.1 \times 10^{-6}$	$2.8 \times 10^{-5}$	$1.4 \times 10^{-10}$	$8.5 \times 10^{-13}$
		20	$3.1 \times 10^{-9}$	$3.2 \times 10^{-8}$	$3.1 \times 10^{-15}$	$4.2 \times 10^{-18}$
		26	$1.6 \times 10^{-15}$	$4.2 \times 10^{-14}$	$1.1 \times 10^{-23}$	$1.6 \times 10^{-27}$
		32	$5.5 \times 10^{-24}$	$3.8 \times 10^{-22}$	$2.4 \times 10^{-34}$	$4.2 \times 10^{-39}$
		36	$5.6 \times 10^{-32}$	$7.3 \times 10^{-30}$	$8.7 \times 10^{-44}$	$3.6 \times 10^{-49}$
46	46	6	$1.6 \times 10^{-1}$	$1.6 \times 10^{-1}$	$2.6 \times 10^{-2}$	$1.0 \times 10^{-2}$
		8	$8.1 \times 10^{-2}$	$1.2 \times 10^{-1}$	$2.5 \times 10^{-3}$	$5.5 \times 10^{-4}$
		12	$3.8 \times 10^{-3}$	$1.3 \times 10^{-2}$	$4.2 \times 10^{-6}$	$3.2 \times 10^{-7}$
		16	$2.9 \times 10^{-5}$	$2.4 \times 10^{-4}$	$1.2 \times 10^{-9}$	$3.3 \times 10^{-11}$
		20	$5.2 \times 10^{-8}$	$9.8 \times 10^{-7}$	$7.8 \times 10^{-14}$	$7.4 \times 10^{-16}$
		26	$2.8 \times 10^{-13}$	$1.8 \times 10^{-11}$	$2.9 \times 10^{-21}$	$5.9 \times 10^{-24}$
		32	$6.6 \times 10^{-20}$	$1.5 \times 10^{-17}$	$4.8 \times 10^{-30}$	$2.0 \times 10^{-33}$
		36	$3.5 \times 10^{-25}$	$1.8 \times 10^{-22}$	$9.3 \times 10^{-37}$	$1.3 \times 10^{-40}$
		42	$7.6 \times 10^{-35}$	$1.4 \times 10^{-31}$	$1.4 \times 10^{-48}$	$4.3 \times 10^{-53}$
		46	$1.4 \times 10^{-43}$	$6.1 \times 10^{-40}$	$9.9 \times 10^{-59}$	$1.0 \times 10^{-63}$

2.3. RESULTS

CHAPTER 2. FINAL REPORT NARRATIVE

Table 2.6: Fingerprint Probabilities:  $n$ PRCs with varying  $m$  and  $\hat{m}$  given  $n = 100,000$  fingerprints

No. of template minutiae/ridges $m$	No of matches $\hat{m}$	Minutiae only	Minutiae and Ridges
		$p(n)$	$p(n)$
46	46	$5.0680 \times 10^{-34}$	$6.7329 \times 10^{-49}$
	36	$1.3336 \times 10^{-15}$	$5.9220 \times 10^{-27}$
	26	$1.1842 \times 10^{-3}$	$1.7579 \times 10^{-11}$
	16	1	1
	6	1	1
36	36	$1.5551 \times 10^{-22}$	$7.5000 \times 10^{-35}$
	26	$5.3414 \times 10^{-6}$	$1.5202 \times 10^{-14}$
	16	1	$3.4852 \times 10^{-1}$
	6	1	1
26	26	$2.3517 \times 10^{-11}$	$5.9297 \times 10^{-20}$
	16	1	$1.8829 \times 10^{-2}$
	6	1	1
16	16	$1.3464 \times 10^{-1}$	$4.460 \times 10^{-8}$
	6	1	1

Table 2.7: Fingerprint Probabilities: Specific  $n$ PRCs for fingerprints in Figure 2.21 with  $n = 100,000$  fingerprints

Print $f$	No. query m/r $m_f$	No. temp m/r $m$	No. match matches $\hat{m}$	Minutiae only	Minutiae and Ridge
				$p(n, f)$	$p(n, f)$
$F_1$	41	40	31	$3.0327 \times 10^{-78}$	$8.5202 \times 10^{-190}$
		40	12	$5.7637 \times 10^{-14}$	$1.1670 \times 10^{-23}$
		20	12	$1.2995 \times 10^{-18}$	$2.6310 \times 10^{-28}$
		20	8	$8.3699 \times 10^{-8}$	$3.7832 \times 10^{-13}$
		10	8	$2.9899 \times 10^{-11}$	$1.3515 \times 10^{-16}$
		10	4	$6.2829 \times 10^{-1}$	$2.7439 \times 10^{-3}$
$F_2$	26	40	20	$3.0335 \times 10^{-43}$	$1.0602 \times 10^{-126}$
		40	14	$7.3652 \times 10^{-23}$	$1.1780 \times 10^{-58}$
		20	12	$1.1057 \times 10^{-21}$	$5.9308 \times 10^{-45}$
		20	8	$1.1077 \times 10^{-9}$	$7.4112 \times 10^{-16}$
		10	8	$3.9608 \times 10^{-13}$	$2.6501 \times 10^{-19}$
		10	4	$8.3675 \times 10^{-2}$	$6.6823 \times 10^{-4}$
$F_3$	13	40	12	$9.1311 \times 10^{-20}$	$6.2913 \times 10^{-72}$
		20	12	$2.0588 \times 10^{-24}$	$1.4185 \times 10^{-76}$
		20	8	$1.0564 \times 10^{-10}$	$2.8852 \times 10^{-25}$
		10	8	$3.7360 \times 10^{-14}$	$1.0204 \times 10^{-28}$
		10	4	$4.1707 \times 10^{-2}$	$1.2057 \times 10^{-3}$

2.3. RESULTS

CHAPTER 2. FINAL REPORT NARRATIVE

Database	ROC	Log-likelihood under	
	method	Gaussian	Gamma
1	4.16%	3.93%	3.93%
2	6.45%	2.57%	3.65%
3	14.43%	13.96%	13.96%
4	6.14%	6.14%	7.24%
overall	7.79%	6.65%	7.19%

Table 2.8: Error rates for 1:1 fingerprint verification on the 4 different database.

Randomly removed minutiae				Minutiae available in a region			
Available Minutiae	ROC Error Rate	Gamma Error Rate	Gaussian Error Rate	Available Minutiae	ROC Error Rate	Gamma Error Rate	Gaussian Error Rate
46	5.17±0.02	3.29±0.07	3.28±0.08	45	5.98±0.05	3.45±0.06	3.24±0.03
41	5.68±0.02	4.61±0.04	4.60±0.05	40	6.19±0.20	4.96±0.18	4.93±0.20
36	17.97±0.11	6.56±0.11	6.59±0.09	35	18.36±0.19	7.77±0.16	7.82±0.15
31	13.81±1.10	10.48±0.19	10.31±0.21	30	19.88±0.79	13.36±0.13	13.37±0.20
26	50.00±0.00	27.22±0.17	16.02±0.24	25	19.88±0.79	13.36±0.13	13.37±0.20
				20	50.00±0.00	29.55±0.30	29.72±0.35

Table 2.9: Mean and standard deviation of error rates for all available 800 fingerprint images with randomly removed minutiae.

Table 2.10: Theoretical and estimated run-times of minutiae-based matcher with both minutiae and RRP as inputs (In the last two rows, run-times for one and two RRPs per ridge are from experiments and for more than two RRPs are estimated).

No. of RRP selected per Ridge ( $k$ )	0	1	2	3	4	5	6
No. of Minutiae and RRP ( $n(1+k)$ )	n	2n	3n	4n	5n	6n	7n
Theoretical Ratio(RRP+Min:Min) $((1+k)^3)$	1	8	27	64	125	216	343
Estimated Ratio(RRP+Min:Min)	1	2	8	12	16	20	24
Actual Run-Time on Intel <sup>R</sup> Xeon <sup>TM</sup> 2.8GHz four processors (secs/match)	0.20	0.38	1.52	2.4	3.2	4.0	4.8

2.3. RESULTS

CHAPTER 2. FINAL REPORT NARRATIVE

Table 2.11: Equal Error Rates of Full Fingerprint Matching on all the four databases of FVC2002 using different RRP indices.

	EER on FVC2002 Database			
	DB1	DB2	DB3	DB4
k-minutiae using Minutiae	1.00 %	1.20 %	8.50 %	3.70 %
k-minutiae using Minutiae + 1 <sup>st</sup> RRP	0.97 %	1.22 %	7.83 %	3.50 %
k-minutiae using Minutiae + 2 <sup>nd</sup> RRP	0.79 %	1.05 %	7.08 %	3.43 %
k-minutiae using Minutiae + 3 <sup>rd</sup> RRP	0.80 %	1.06 %	7.21 %	3.43 %
k-minutiae using Minutiae + 4 <sup>th</sup> RRP	0.87 %	1.08 %	7.13 %	3.57 %
k-minutiae using Minutiae + 5 <sup>th</sup> RRP	0.87 %	1.08 %	7.13 %	3.47 %
k-minutiae using Minutiae + 6 <sup>th</sup> RRP	0.84 %	1.03 %	7.56 %	3.40 %
k-minutiae using Minutiae + 7 <sup>th</sup> RRP	0.86 %	1.03 %	7.44 %	3.39 %
k-minutiae using Minutiae + 8 <sup>th</sup> RRP	0.85 %	0.97 %	7.58 %	3.45 %
k-minutiae using Minutiae + 9 <sup>th</sup> RRP	0.81 %	1.05 %	7.27 %	3.39 %
k-minutiae using Minutiae + 10 <sup>th</sup> RRP	0.75 %	1.06 %	7.63 %	3.60 %
k-minutiae using Minutiae + 11 <sup>th</sup> RRP	0.76 %	1.10 %	7.36 %	3.44 %
k-minutiae using Minutiae + 12 <sup>th</sup> RRP	0.77 %	1.15 %	7.81 %	3.52 %
k-minutiae using Minutiae + 13 <sup>th</sup> RRP	0.74 %	1.17 %	7.99 %	3.43 %
k-minutiae using Minutiae + 14 <sup>th</sup> RRP	0.75 %	1.19 %	7.93 %	3.41 %
Bozorth using Minutiae	3.50 %	3.00 %	8.10 %	3.90 %
Bozorth using Minutiae + 1 <sup>st</sup> RRP	3.69 %	3.07 %	7.13 %	3.45 %
Bozorth using Minutiae + 2 <sup>nd</sup> RRP	2.69 %	3.02 %	5.57 %	3.38 %
Bozorth using Minutiae + 3 <sup>rd</sup> RRP	2.69 %	2.65 %	5.70 %	3.34 %
Bozorth using Minutiae + 4 <sup>th</sup> RRP	2.85 %	2.68 %	5.91 %	3.29 %
Bozorth using Minutiae + 5 <sup>th</sup> RRP	2.80 %	2.90 %	6.29 %	3.22 %
Bozorth using Minutiae + 6 <sup>th</sup> RRP	2.76 %	2.84 %	6.37 %	3.13 %
Bozorth using Minutiae + 7 <sup>th</sup> RRP	2.52 %	2.21 %	6.35 %	3.39 %
Bozorth using Minutiae + 8 <sup>th</sup> RRP	2.73 %	2.52 %	6.20 %	3.28 %
Bozorth using Minutiae + 9 <sup>th</sup> RRP	2.50 %	2.49 %	6.16 %	3.36 %
Bozorth using Minutiae + 10 <sup>th</sup> RRP	2.34 %	2.80 %	6.06 %	3.55 %
Bozorth using Minutiae + 11 <sup>th</sup> RRP	2.38 %	2.26 %	6.37 %	3.43 %
Bozorth using Minutiae + 12 <sup>th</sup> RRP	2.27 %	2.37 %	6.65 %	3.32 %
Bozorth using Minutiae + 13 <sup>th</sup> RRP	2.49 %	2.86 %	6.67 %	3.58 %
Bozorth using Minutiae + 14 <sup>th</sup> RRP	2.86 %	2.77 %	6.89 %	3.41 %

Table 2.12: Equal Error Rates of Full Fingerprint Matching on all the four databases of FVC2002 using hybrid RRP index.

	EER on FVC2002 Database			
	DB1	DB2	DB3	DB4
k-minutiae using Minutiae + hybrid RRP	0.70 %	0.95 %	6.37 %	3.37 %
Bozorth using Minutiae + hybrid RRP	2.20 %	2.18 %	6.10 %	3.14 %

2.3. RESULTS

CHAPTER 2. FINAL REPORT NARRATIVE

Table 2.13: Partial Fingerprint Verification EERs on simulated partial fingerprints generated from FVC2002 Databases. 'M' is used to denote minutiae in column 3.)

Selected Matcher	Data Set	Feature Used For Matching	Number of available minutiae in partial prints					
			10	15	20	25	30	35
Bozorth	DB 1	M	20.70%	14.55%	9.72%	8.02%	6.11%	5.13%
		M+RRP	19.39%	11.74%	7.95%	5.60%	4.80%	3.65%
	DB 2	M	21.90%	15.18%	12.74%	10.10%	8.17%	6.75%
		M+RRP	20.59%	14.57%	9.94%	8.61%	7.13%	5.09%
	DB 3	M	34.22%	25.28%	20.29%	17.80%	14.48%	12.76%
		M+RRP	32.30%	23.04%	18.09%	14.39%	11.08%	9.36%
DB 4	M	22.67%	17.55%	11.93%	9.05%	7.29%	6.25%	
	M+RRP	21.96%	15.04%	9.77%	7.05%	4.52%	3.77%	
K-Plet	DB 1	M	19.79%	11.23%	7.416%	4.84%	3.23%	2.41%
		M+RRP	17.33%	5.983%	3.914%	2.74%	1.92%	1.53%
	DB 2	M	21.75%	14.74%	9.96%	8.11%	6.59%	5.21%
		M+RRP	18.74%	12.11%	8.57%	6.40%	5.67%	4.51%
	DB 3	M	32.96%	27.74%	21.04%	16.3%	14.10%	10.76%
		M+RRP	31.21%	20.01%	15.2%	12.33%	10.21%	9.02%
DB 4	M	25.32%	17.90%	11.60%	7.97%	5.95%	5.01%	
	M+RRP	23.76%	15.80%	10.20%	6.99%	5.46%	4.95%	

### 2.3.3 Figures

Following are figures referred to in the narrative.

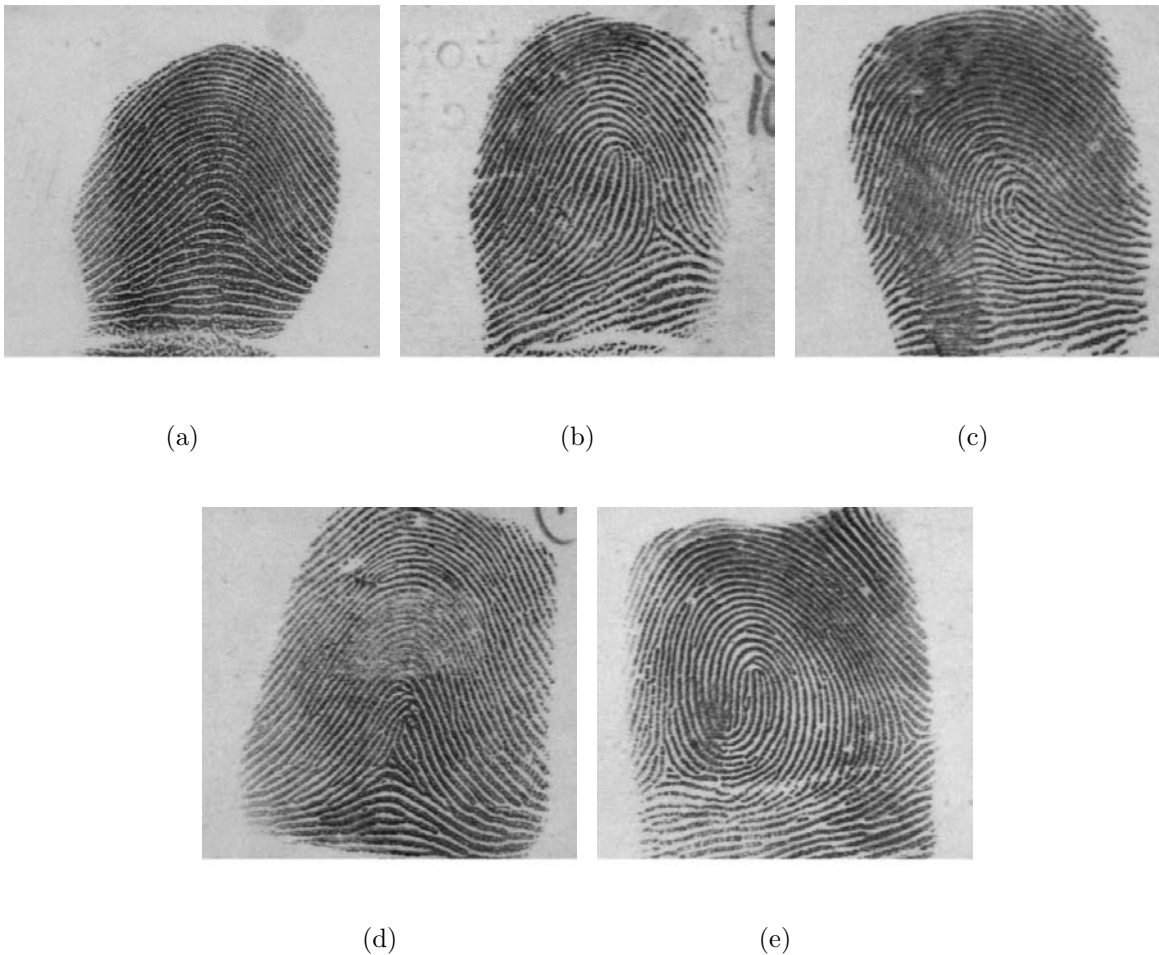


Figure 2.1: Examples of five main types of ridge flow in fingerprints, referred to as Level 1 features: (a) arch, (b) left loop, (c) right loop. (d) tented arch, and (e) whorl. From NIST Special Database 4.

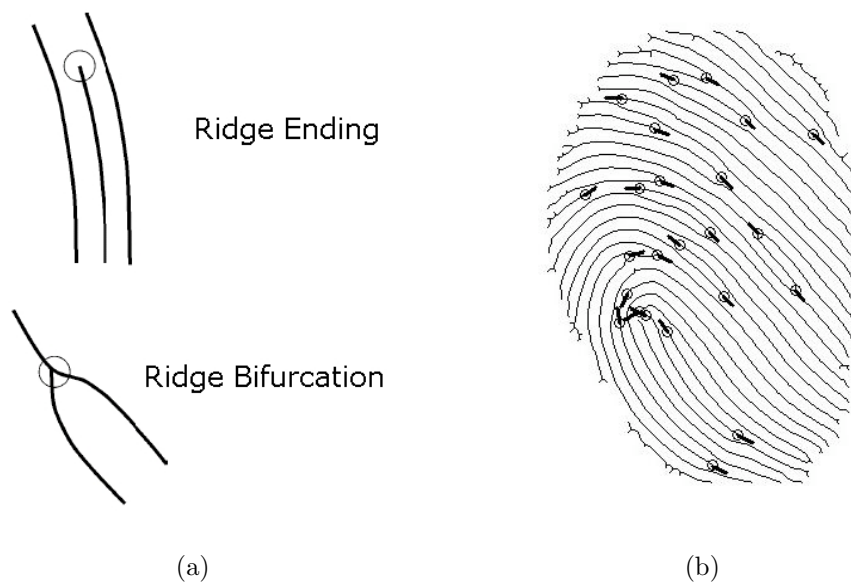


Figure 2.2: Representation of fingerprints using minutiae: (a) locations of ridge endings and ridge bifurcations are indicated by circles, and (b) minutiae directions are indicated by line segments in a skeletonized fingerprint image.

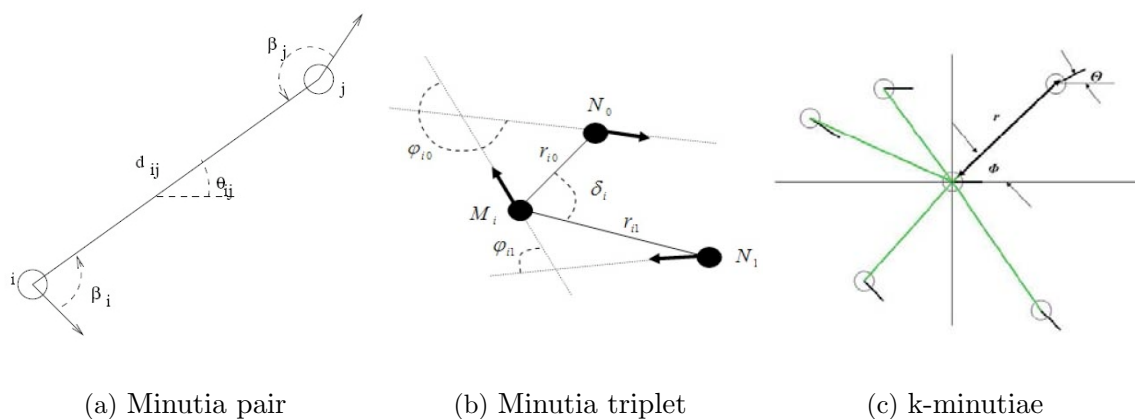


Figure 2.3: Local minutiae models consider the relative positions of: (a) pair of minutiae (b) triple of minutiae, and (c) k minutiae (5 in this case).

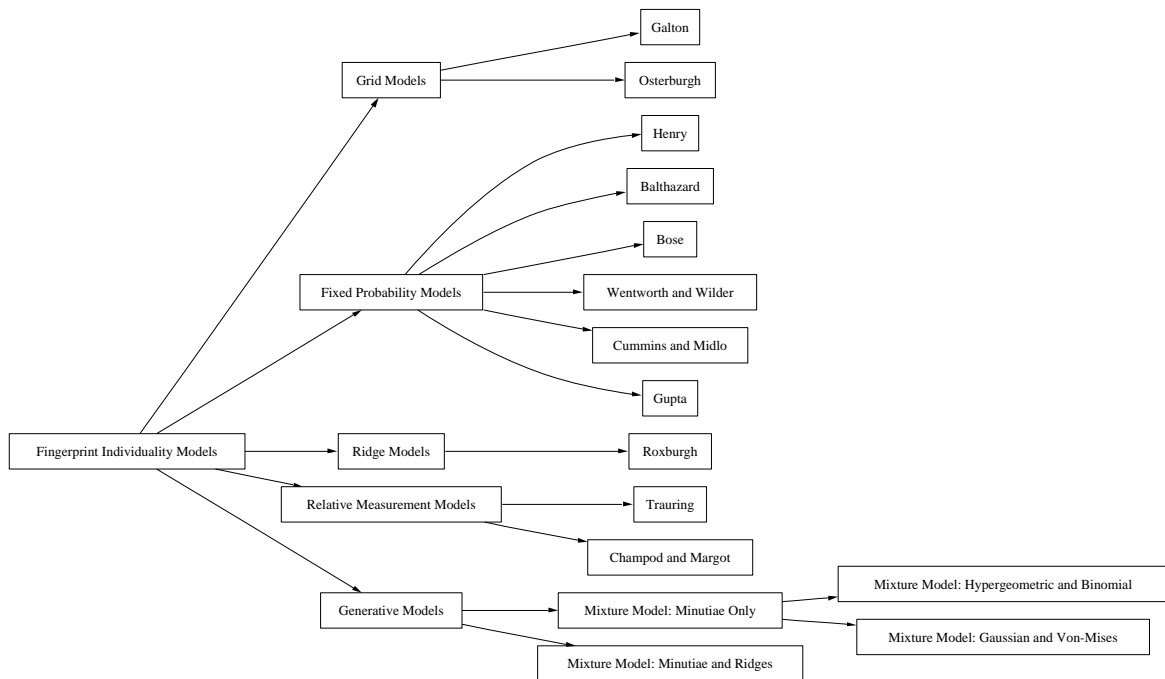


Figure 2.4: Taxonomy of fingerprint individuality models based on method of analysis. The generative models studied in this research are at the bottom right.

2.3. RESULTS

CHAPTER 2. FINAL REPORT NARRATIVE

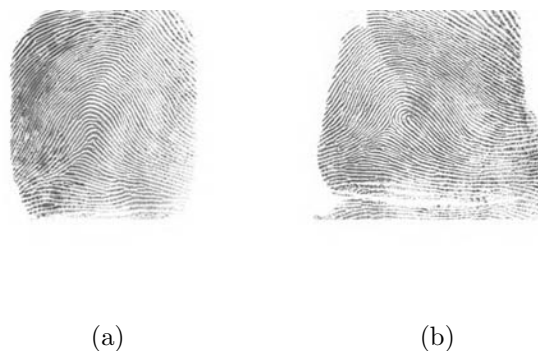


Figure 2.5: Fingerprints from a pair of twins.

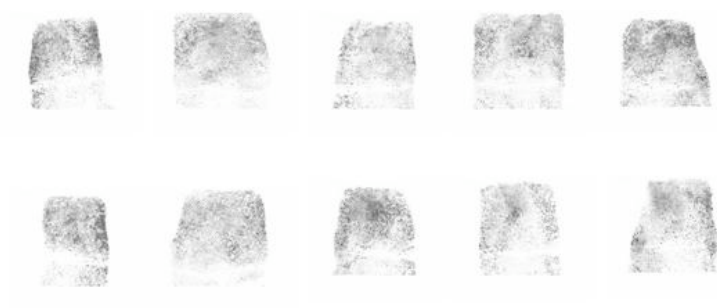


Figure 2.6: 10 Rolled fingerprints from one individual.

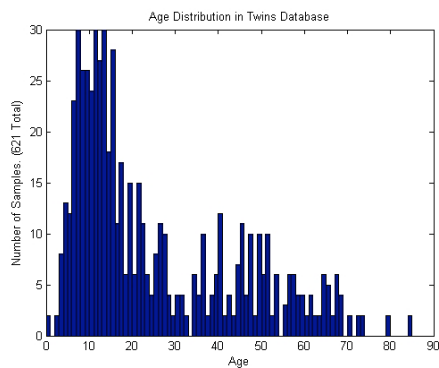
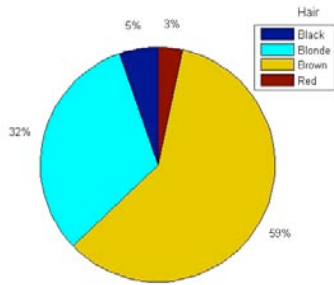


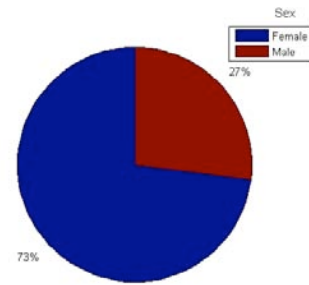
Figure 2.7: Distribution of ages of twins in database: a predominance of younger ages is seen.

2.3. RESULTS

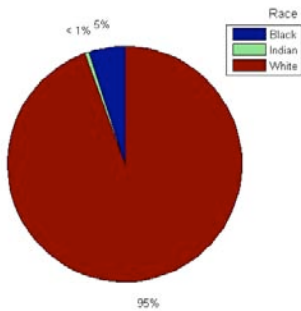
CHAPTER 2. FINAL REPORT NARRATIVE



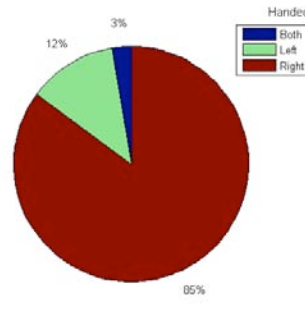
(a) Hair Color Distribution



(b) Gender Distribution



(c) Race Distribution



(d) Handedness Distribution

Figure 2.8: Distribution of twins meta data: (a) hair color (b) gender (c) race (d) handedness (left/right).

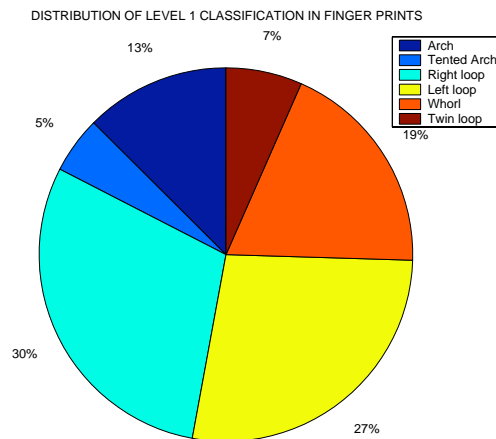


Figure 2.9: Distribution of level 1 features in database

2.3. RESULTS

CHAPTER 2. FINAL REPORT NARRATIVE

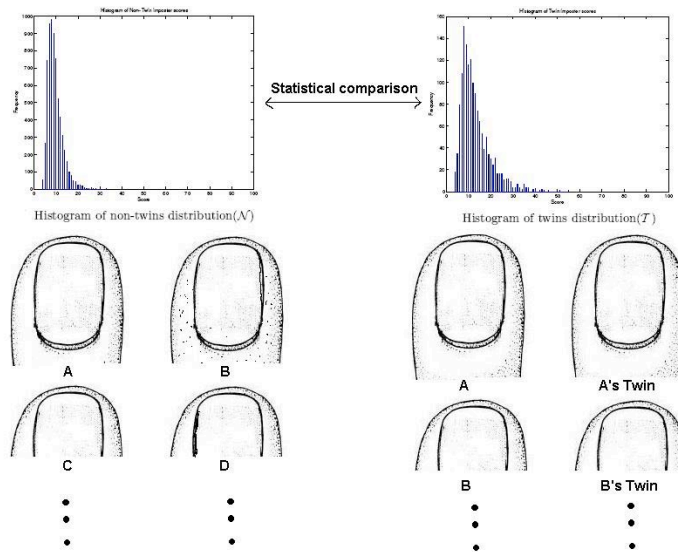
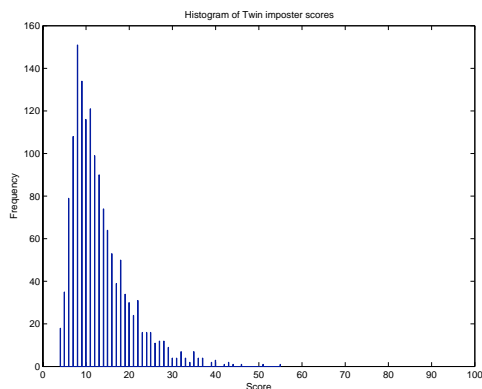


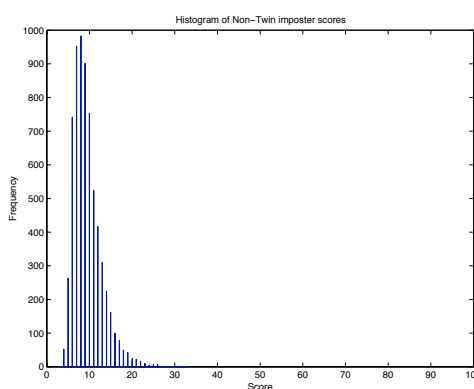
Figure 2.10: Methodology of comparing fingerprints of twins and non-twins using Level 2 features.

2.3. RESULTS

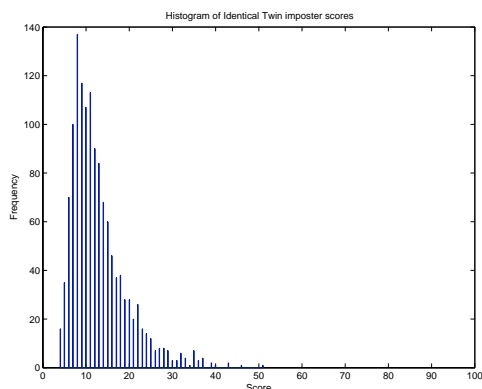
CHAPTER 2. FINAL REPORT NARRATIVE



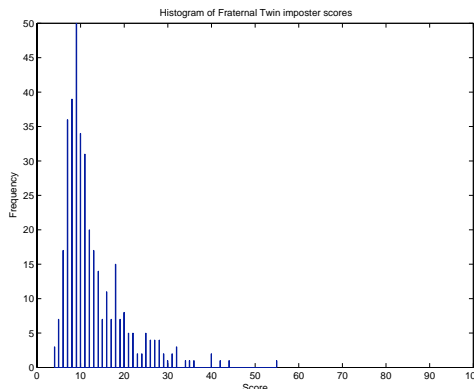
(a) Histogram of twins distribution( $\mathcal{T}$ )



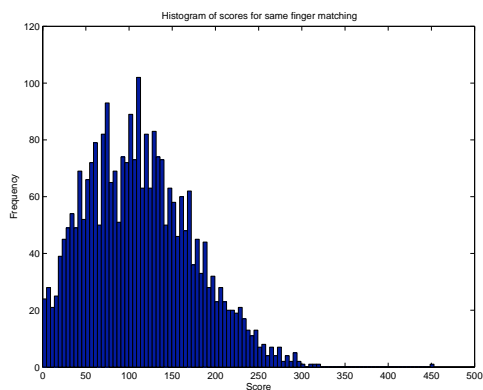
(b) Histogram of non-twins distribution( $\mathcal{N}$ )



(c) Histogram of identical twins distribution( $\mathcal{I}$ )



(d) Histogram of fraternal twins distribution( $\mathcal{F}$ )



(e) Histogram of genuine distribution( $\mathcal{G}$ )

Figure 2.11: Histograms of AFIS scores (using a Bozorth matcher): (a) twins, (b) non-twins (c) identical twins, (d) fraternal twins, and (e) genuine. Note that the first four (a),(b),(c) and (d) are impostor score distributions.

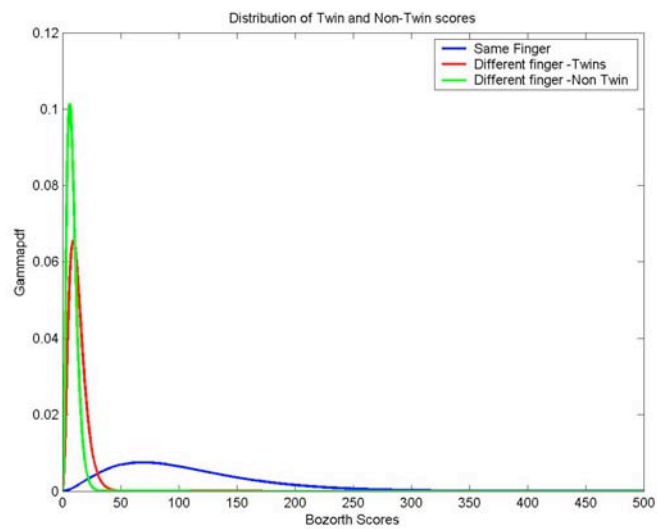


Figure 2.12: Probability density functions of fingerprint scores modeled as gamma distributions.

2.3. RESULTS

CHAPTER 2. FINAL REPORT NARRATIVE

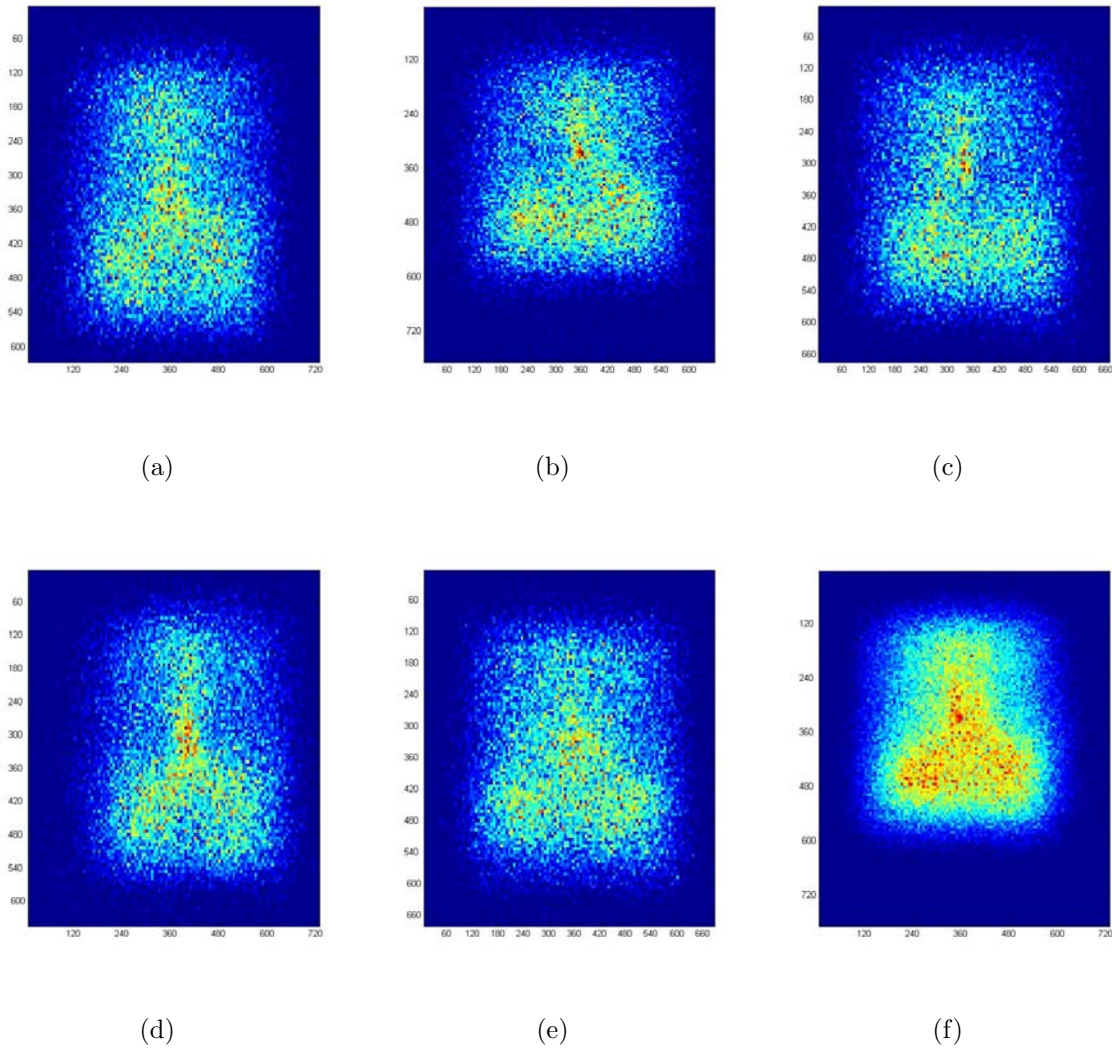


Figure 2.13: Distribution of minutia location for different types of ridge flow: (a) arch, (b) left loop, (c) right loop, (d) tent, (e) whorl, and (e) all types combined.

2.3. RESULTS

CHAPTER 2. FINAL REPORT NARRATIVE

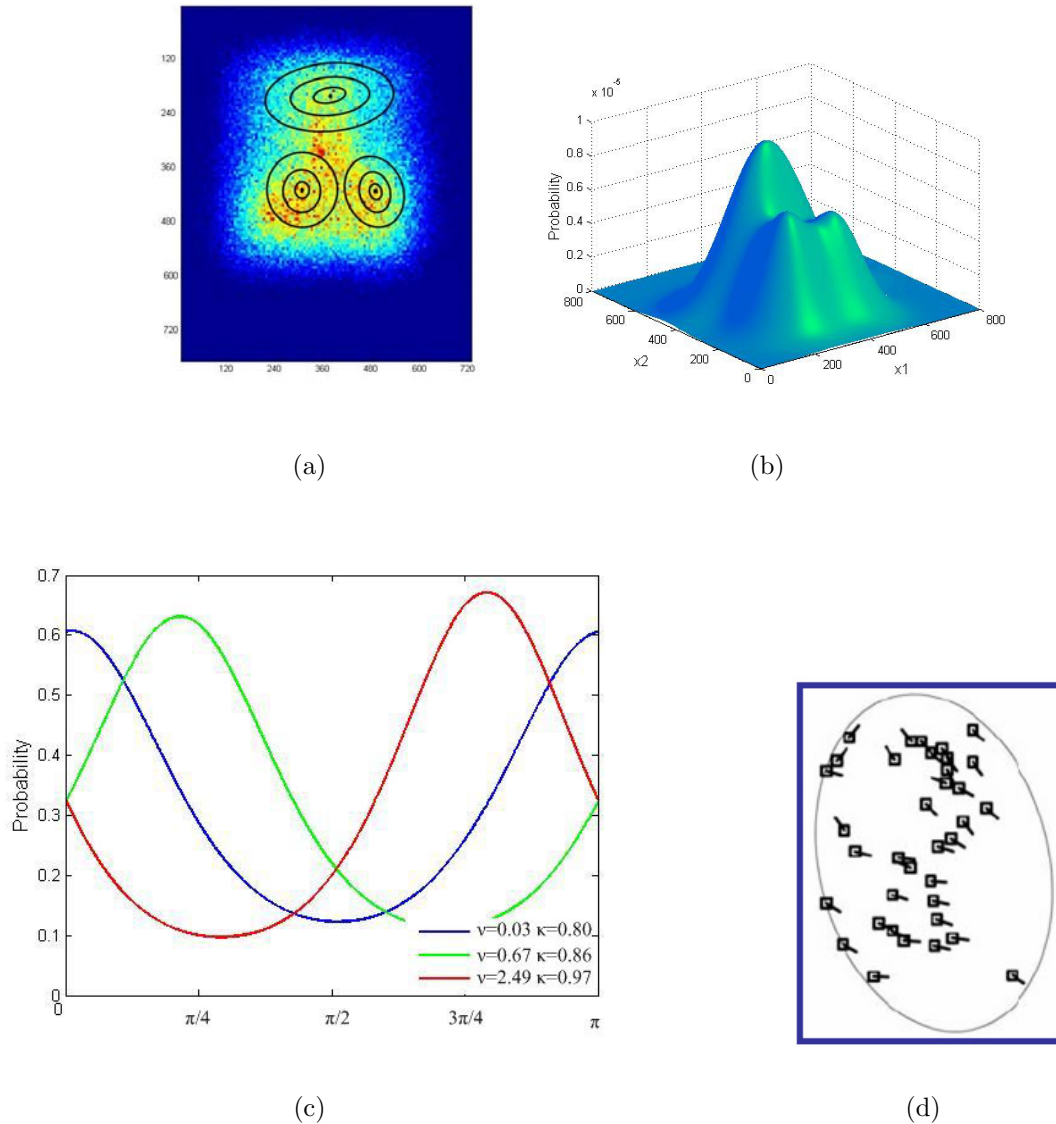


Figure 2.14: Model for minutiae distribution using Gaussian mixture for location and von Mises for direction: (a) Gaussian mixture model for minutia location with three components, (b) three-dimensional plot of mixture model, (c) von Mises distributions of minutiae orientation for each of the three components, where the green curve corresponds to the upper cluster, blue the lower left cluster and red the lower right cluster, and (d) sample generated from model.

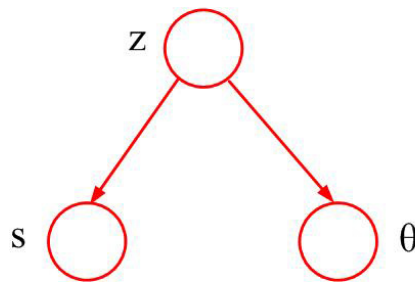


Figure 2.15: Mixture model for distribution of minutiae  $\mathbf{x} = (s, \theta)$ . The joint distribution of minutia location and orientation is given by  $p((s, \theta), z) = p(z)p(s|z)p(\theta|z)$ .

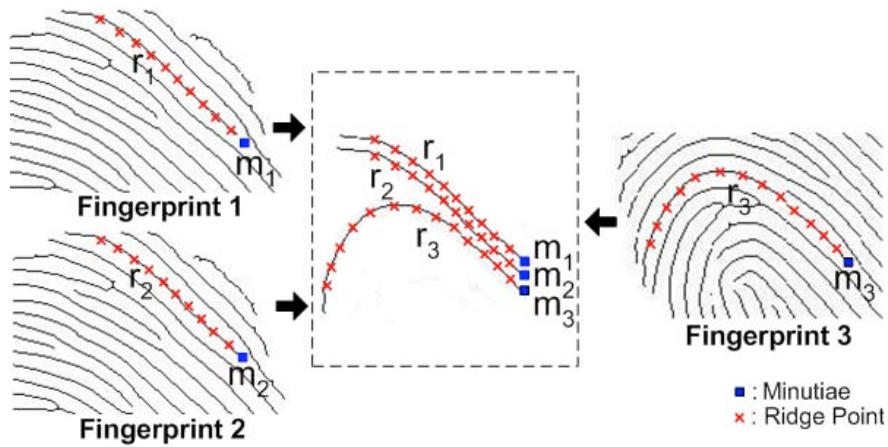


Figure 2.16: Representation of fingerprints using minutiae and ridge information: similarity of ridge shapes allows the matching of corresponding minutiae pair. Three fingerprints are shown, two of which are similar and one dissimilar. Minutiae  $m_1$  and  $m_2$  in fingerprints 1 and 2 are similar since not only their locations are similar but also the associated ridges  $r_1$  and  $r_2$  are similar. However, minutiae  $m_3$  in fingerprint 3 has a location similar to  $m_1$  and  $m_2$  but the associated ridge  $r_3$  is dissimilar to  $r_1$  and  $r_2$ .

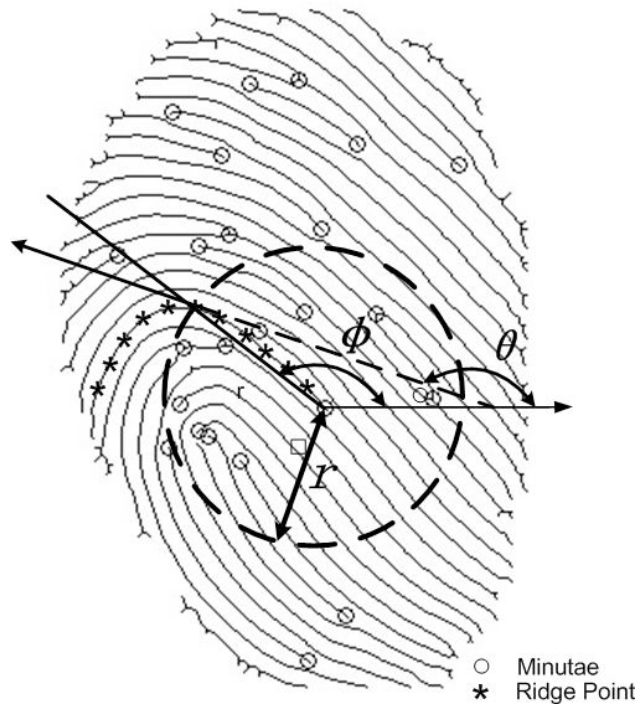


Figure 2.17: Representation of ridge points in polar coordinates. The minutia at the center is the origin. The sixth ridge point from the minutia is represented by  $((r, \phi), \theta)$ , where  $r$  and  $\phi$  are polar coordinates of its location and its direction  $\theta$  is the angle the tangent at the ridge point makes with the horizontal.

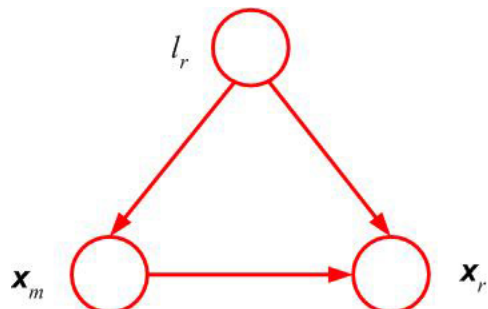


Figure 2.18: Graphical model for representative ridges. The distribution of ridge points  $\mathbf{x}_r$  are dependent on the defining minutia  $\mathbf{x}_m$ . Both are dependent on ridge length  $l_r$ .

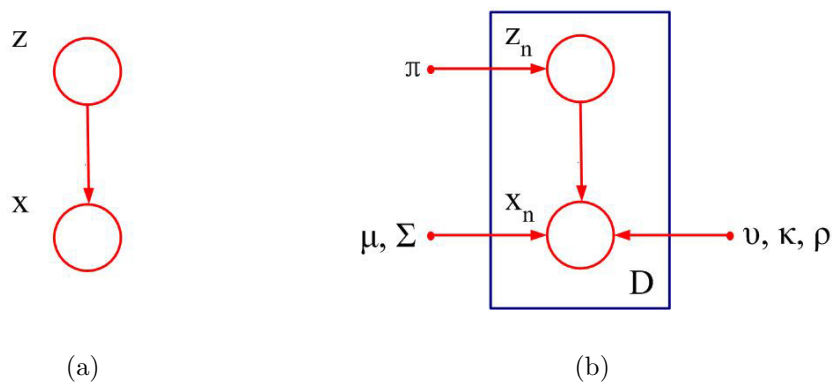


Figure 2.19: Graphical models representing mixture for: (a) single minutia whose distribution is expressed as  $p(\mathbf{x}, \mathbf{z}) = p(\mathbf{x})p(\mathbf{x}|\mathbf{z})$ , (b) set of  $D$  identically distributed minutiae with corresponding latent points  $\mathbf{z}_n$ , where  $n = 1, \dots, D$ .

2.3. RESULTS

CHAPTER 2. FINAL REPORT NARRATIVE

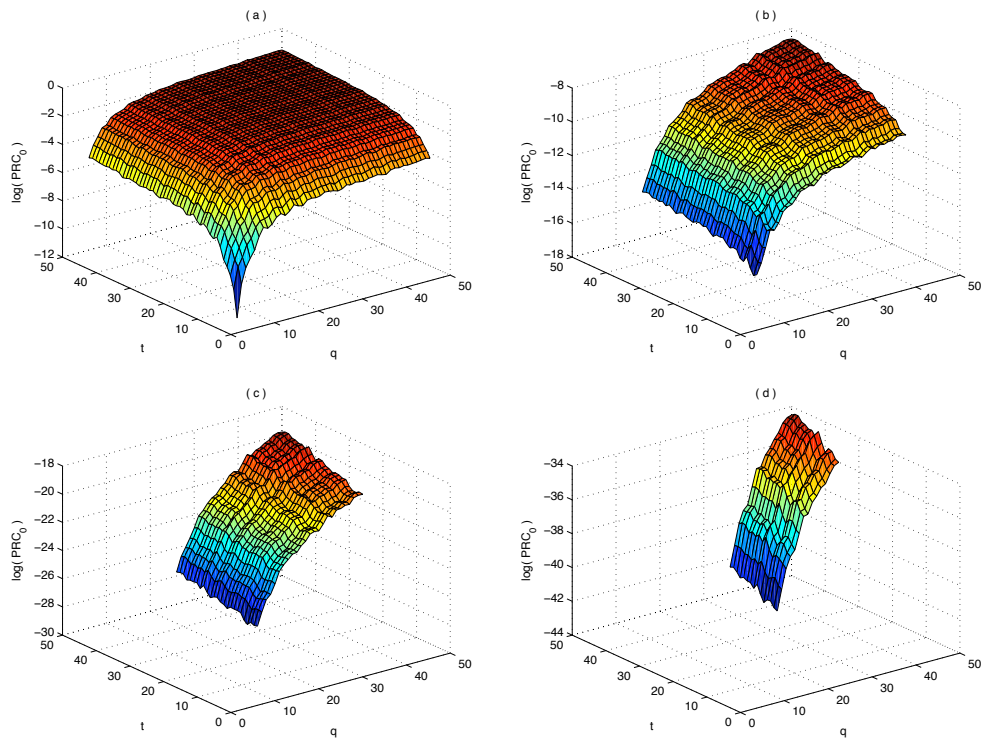


Figure 2.20: PRCs with different number of the matched ridges for (a)  $m = 6$ , (b)  $m = 16$ , (c)  $m = 26$ , and (d)  $m = 36$ .



Figure 2.21: Three specific fingerprints (from the same finger) used to calculate probabilities: (a) good quality full print, (b) low quality full print, and (c) partial print.

2.3. RESULTS

CHAPTER 2. FINAL REPORT NARRATIVE

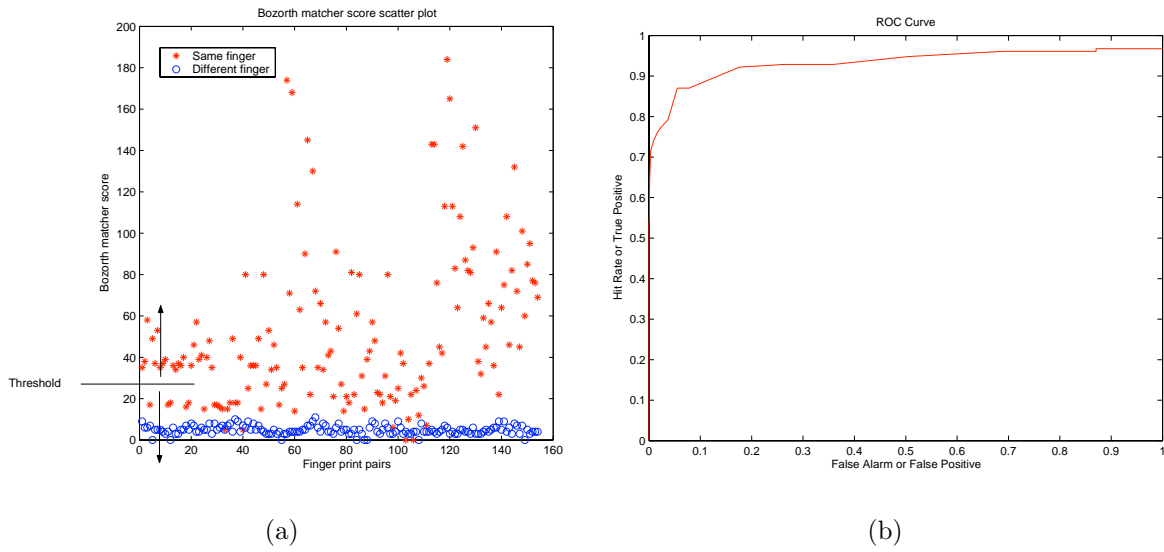


Figure 2.22: ROC Method: (a) Scatter plot of scores for large ensemble of pairs of samples using Bozorth matcher and (b) ROC obtained by moving the threshold in (a).

2.3. RESULTS

CHAPTER 2. FINAL REPORT NARRATIVE

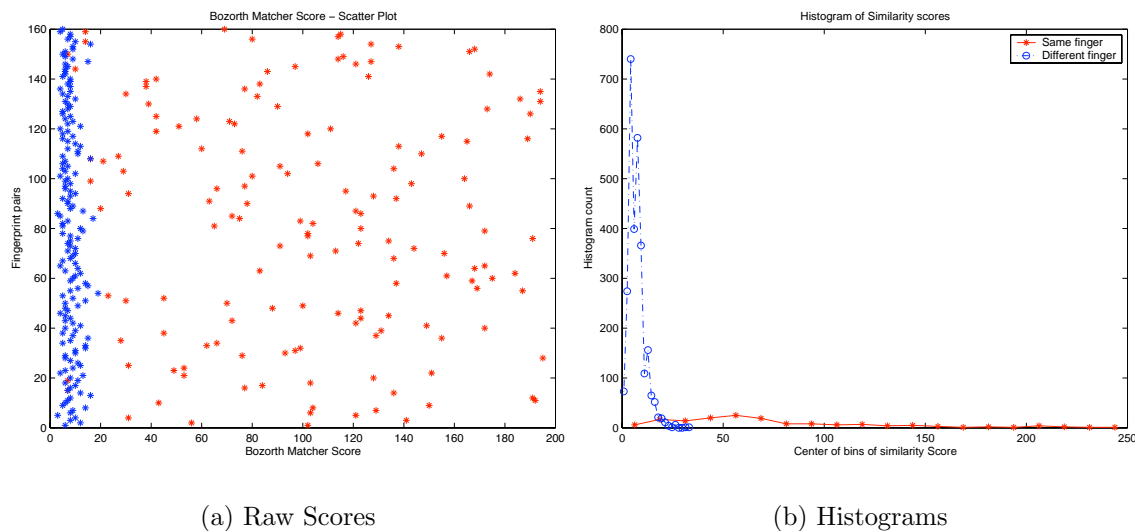


Figure 2.23: Likelihood Ratio Method: (a) Raw scores corresponding to different fingerprint pairs, and (b) histogram of the distribution of scores of same and different finger pairs. The fingerprint scores were first binned into 20 equally spaced bins. The centers of these bins are the x-axis values. The y-axis is the count of how many scores fell in that bin.

2.3. RESULTS

CHAPTER 2. FINAL REPORT NARRATIVE

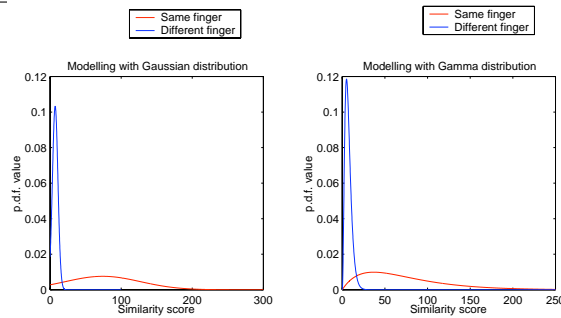
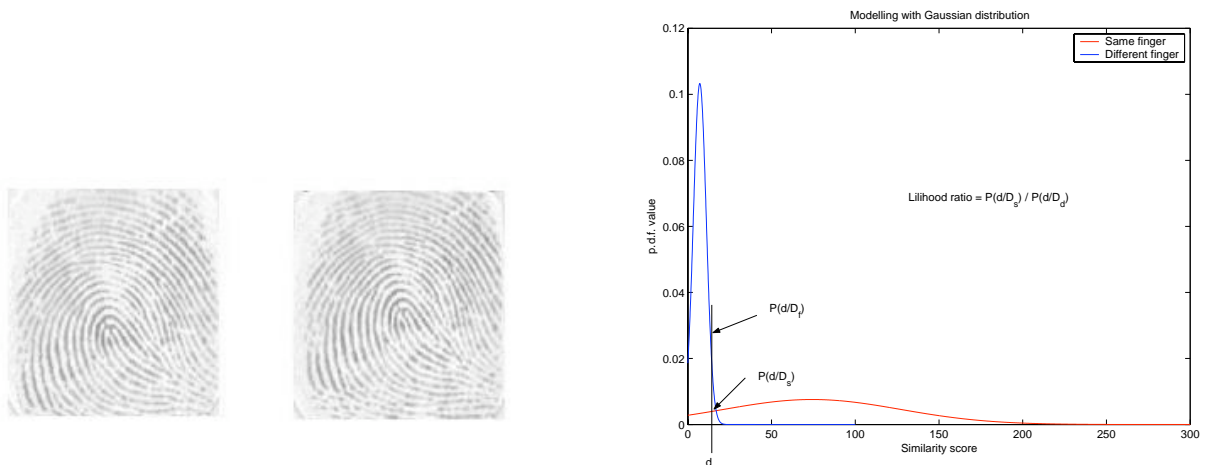


Figure 2.24: Two plots show modeling the histogram in Figure 2.23 using Gaussian(left) and Gamma(right) distributions.



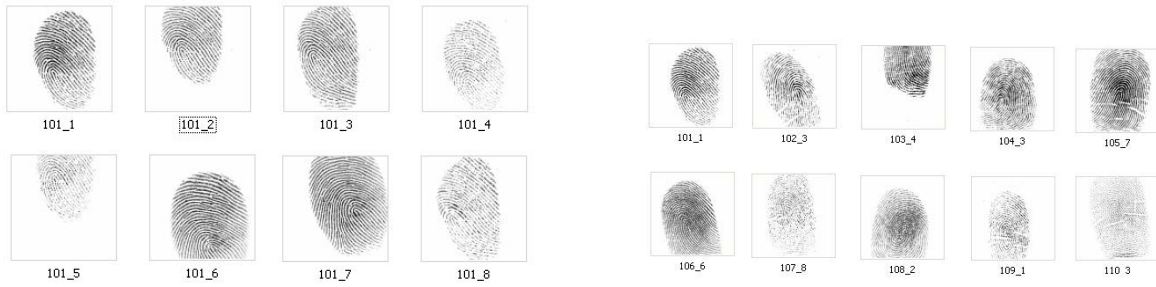
(a) Verification: Two finger print samples are verified whether they belong to the same finger.

(b) PDF value of the Gaussian distributions at  $d$

Figure 2.25: The score between the two samples to be verified is obtained from the Bozorth matcher to be  $d$ . The p.d.f. value of the two distributions at  $d$  is calculated.

2.3. RESULTS

CHAPTER 2. FINAL REPORT NARRATIVE



(a) 8 samples for one finger.

(b) One sample from each of 10 different fingers.

Figure 2.26: (a) Samples from one finger. (b) Samples from different fingers. All these samples were from database 1 of the FVC2002 dataset.

2.3. RESULTS

CHAPTER 2. FINAL REPORT NARRATIVE

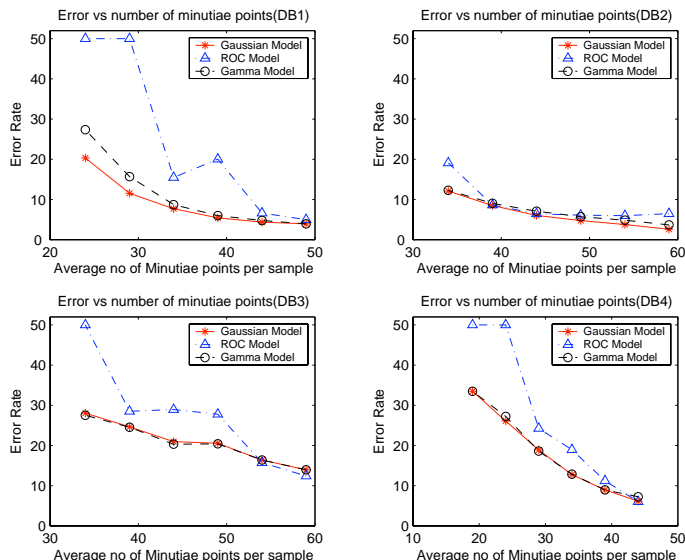


Figure 2.27: Variation in the error rates for 1:1 verification for each of the 4 databases with the average number of minutiae available per sample (after random removal). The last data point in each of the database corresponds to the case where no minutiae were removed.

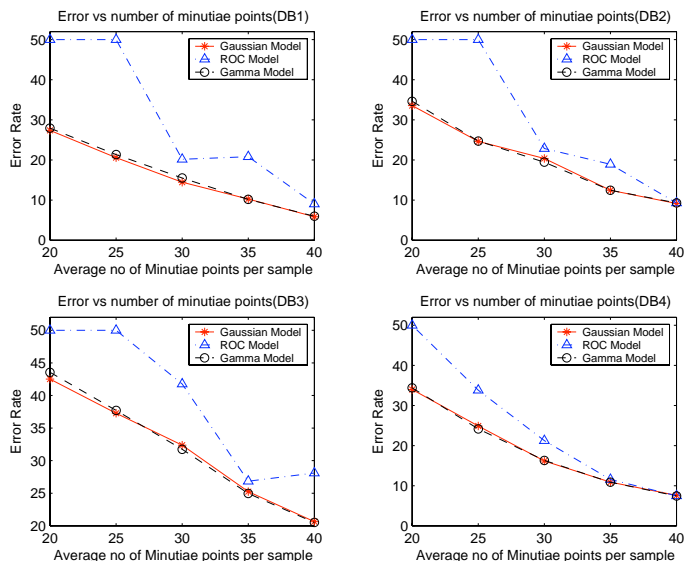


Figure 2.28: Variation in the error rates 1:1 verification for each of the 4 databases with the average number of minutiae available per sample (corresponding to a region).

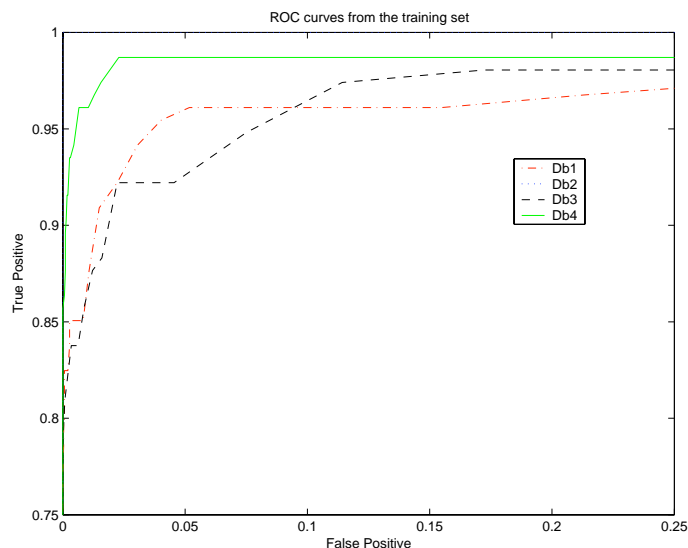


Figure 2.29: ROC curves obtained from the training set for each of the 4 databases.

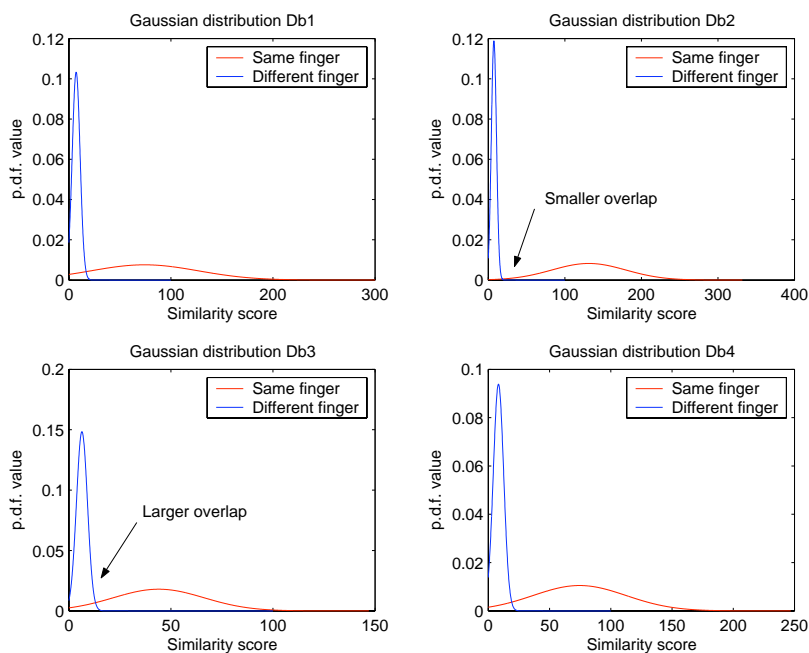
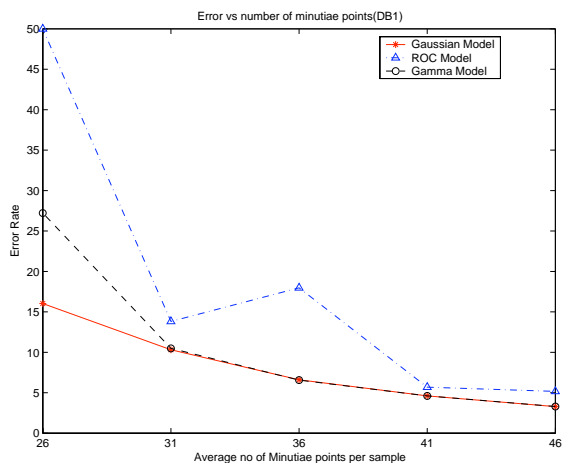
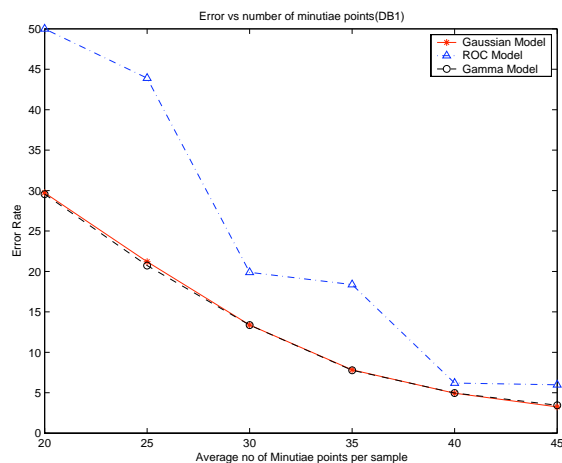


Figure 2.30: The distribution of similarity scores for each of the 4 databases modelled with Gaussian distribution.



(a) Variation in the error rates for all available 800 images after randomly removing minutiae



(b) Variation in the error rates for for all available 800 images after considering minutiae from a region

Figure 2.31: Error rates for a database of 800 fingerprint images

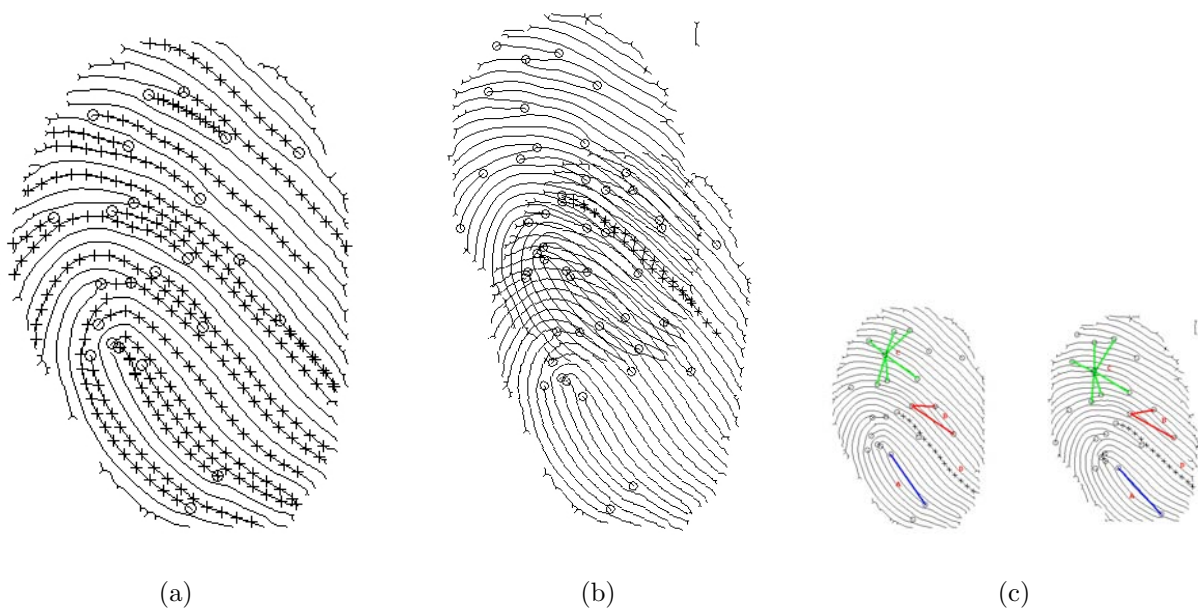
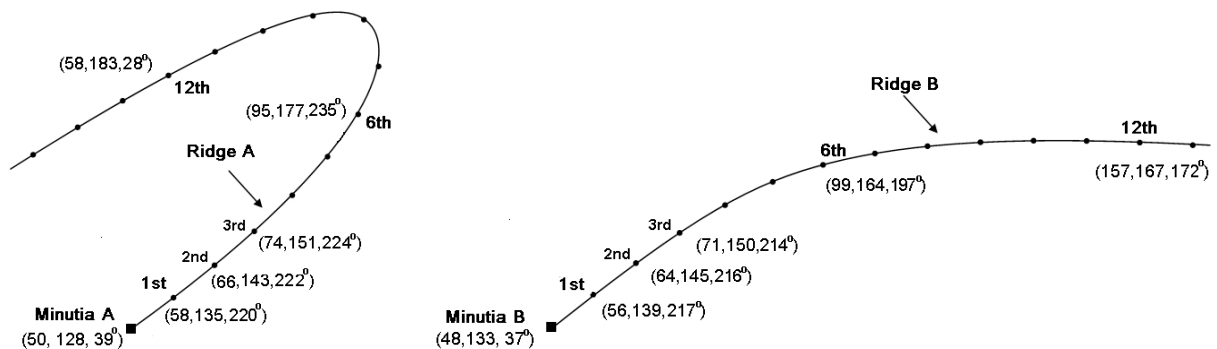


Figure 2.32: Ridge similarity: (a) minutiae and associated ridges (represented by points sampled at average inter-ridge distance), (b) false alignment with similar ridge pair (beyond the tolerance of an adaptively compensating minutiae matching algorithm), and (c) region sizes of local similarity models of three minutiae matchers: A(lower left blue box): Bozorth minutiae pair, B(small red box): triplet model [52], C(top green box): k-minutiae model. D(black): labels a ridge.



(a) A ridge in Fingerprint I.

(b) A ridge in Fingerprint II. (After aligned to Fingerprint I. through affine transformation)

Figure 2.33: Importance of using ridge information in addition to minutiae. Ridge A and Ridge B are respectively from two fingerprints I and II. After fingerprint II is aligned to fingerprint I through affine transformation, minutia B and minutia A share very similar location and orientation (the  $(x, y, \theta)$  values are within tolerance  $(5, 5, 10^\circ)$ ). The first three ridge point pairs on the two ridges are also similar (within tolerance  $(5, 5, 10^\circ)$ ). However, because the shapes of Ridge A and Ridge B are totally different from each other (also could be sensed from the large differences of the 6<sup>th</sup> ridge point pair and the 12<sup>th</sup> ridge point pair), we should reject these two ridges as being identical.

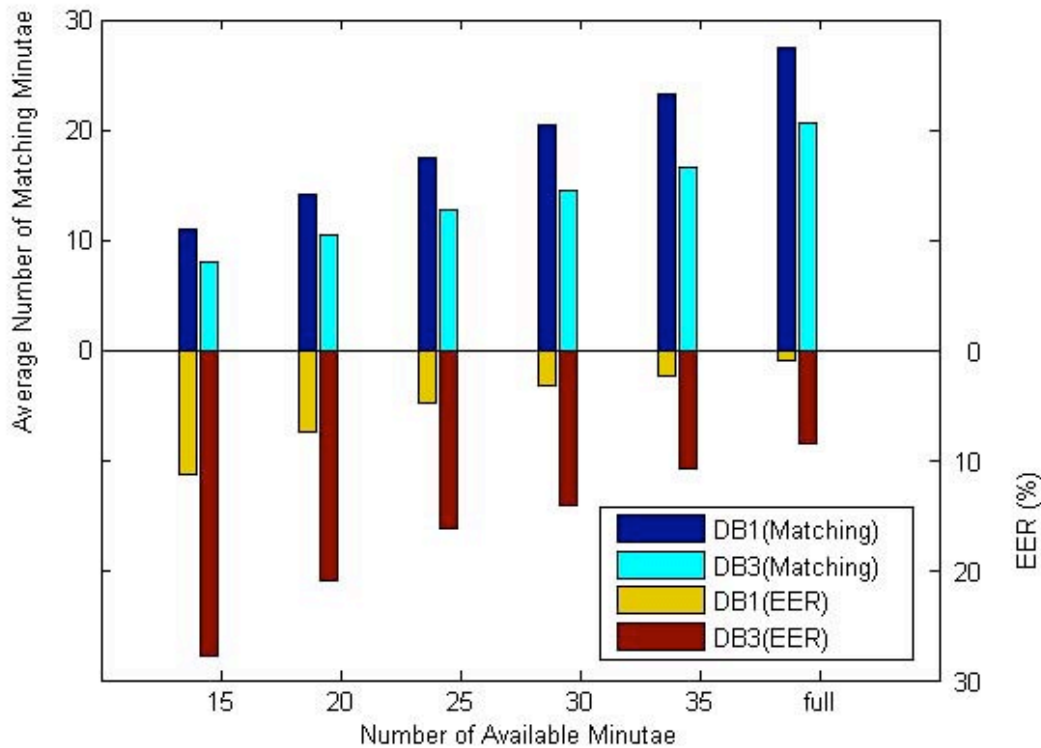


Figure 2.34: Effect of number of input minutiae on: (i) number of minutiae that match with the genuine full print (top half of chart), and (ii) equal error rate (EER) (bottom half of chart). As the number of minutiae increases, the number of matched minutiae increases and the EER decreases. The partial images were generated from images in FVC2002– data sets DB1 and DB3. The average number of minutiae of full fingerprints in DB1 and DB3, as detected by MINDTCT [11], were 43 and 53 respectively.

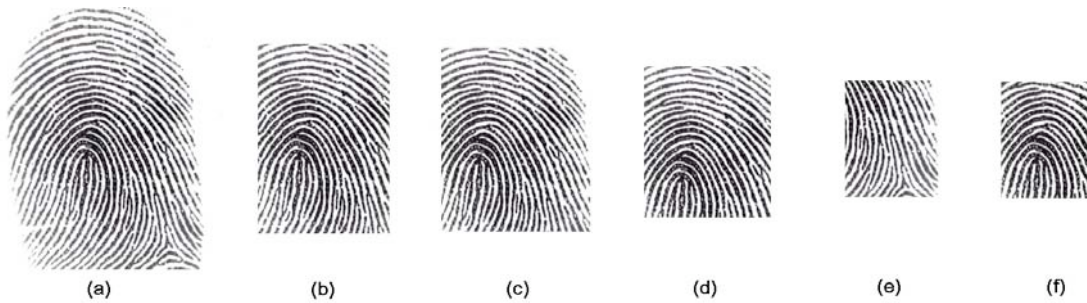


Figure 2.35: Partial fingerprints: (a) a full fingerprint image, and (b)-(f) partial fingerprint images cut from the full fingerprint with decreasing numbers of minutiae (35, 30, 25, 20, and 15). Note: In this paper, we are focusing on the effectiveness of using RRP for fingerprint matching when number of available minutiae decreases in partial fingerprints with fair image quality, but not coping with the latent partial fingerprints in real forensic cases with very poor quality. So, we simulate partial fingerprints by cropping full-sized images with fair image quality.

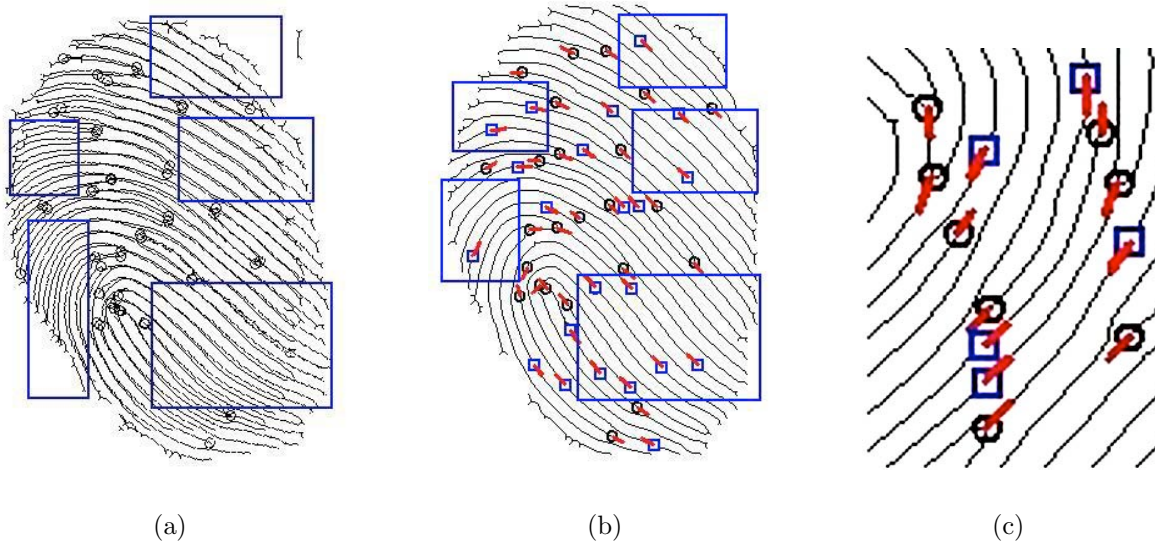


Figure 2.36: Representative Ridge Points: (a) genuine fingerprints have overlapping minutiae and ridges, (b) minutiae (circles) and RRPs (squares). As an example, the 6<sup>th</sup> and 12<sup>th</sup> RRPs are shown; regions without minutiae are now characterized by RRPs. (c) Ridge endings, ridge bifurcations and RRPs.

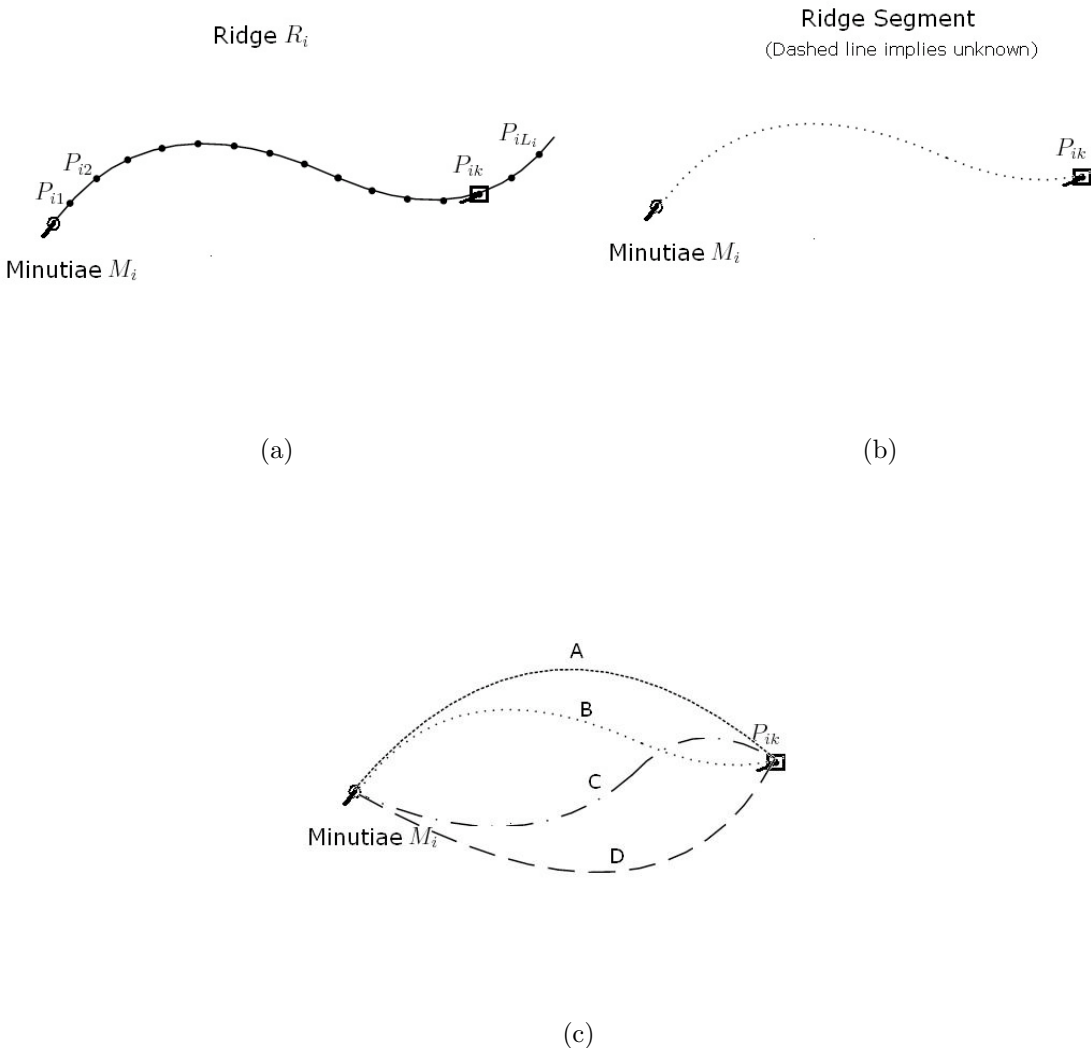


Figure 2.37: Implication from minutiae and the  $k^{th}$  ridge points to ridge segment. (a) a ridge with minutiae and ridge points, (b) the  $k^{th}$  ridge point is selected as RRP, (c) four possible candidate shapes of the ridge segment with fixed segment length  $kd$  and fixed positions of both the two end points. Please note that, in (c), we are only considering the four possible candidates because we only care about the approximate ridge shape types. Slight shakes on ridge shapes are not interesting here because, given the existence of non-linear deformation in fingerprint impressions, it is irrational and impossible to use a strict criterion such as ridge similarity to say whether two ridges are identical or not. Instead, we use the basic ridge type (e.g. one/two turn) to classify all possible ridges connecting a minutia and a ridge point. Admittedly, there might be other possible ridge shape types, e.g. in core and delta region, ridges may have very sharp turns or more than two turns. However, in most cases, fingerprint ridges are smooth flowing patterns with seldom sharp turns, and unlikely have more than three turns. So, we are only considering the four possible candidates here.



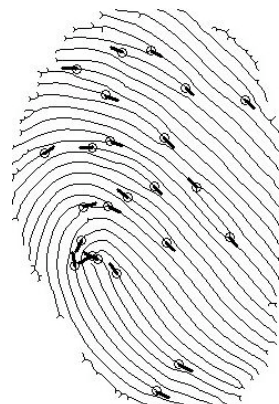
(a) Original fingerprint image



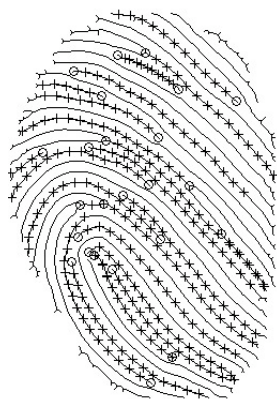
(b) Enhancement and binarization



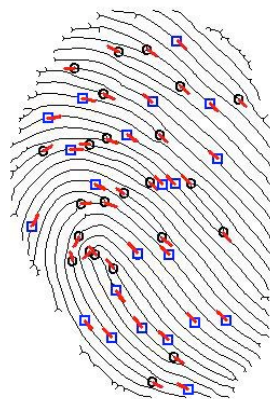
(c) Thinning



(d) Minutiae detection



(e) Ridge points detection



(f) RRP selection

Figure 2.38: Processing steps in extracting RRP from original fingerprint images.

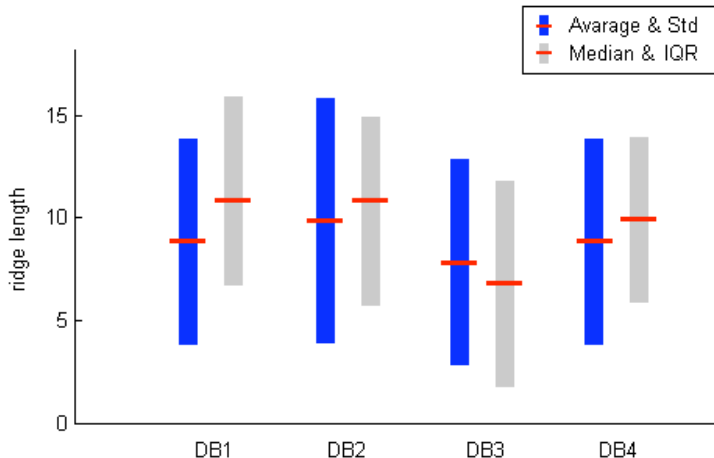
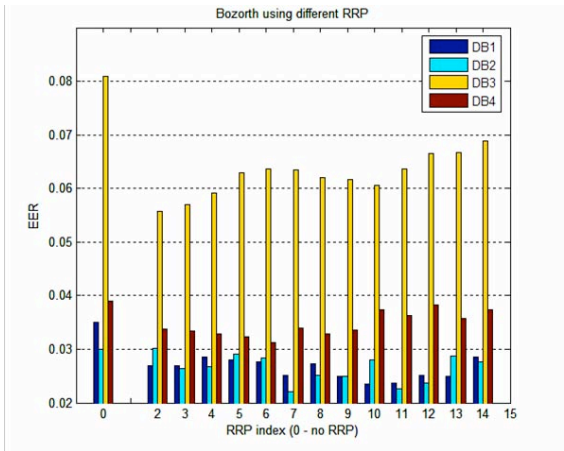
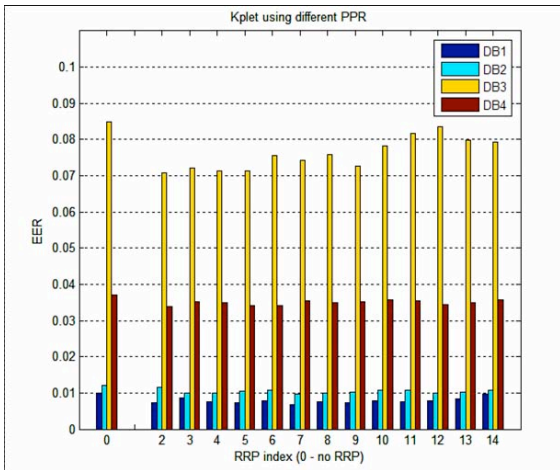


Figure 2.39: Ridge length statistics for the FVC2002 data sets. For each dataset, mean and standard deviation(Std),median and interquartile range(IQR) are shown. The horizontal line for each bar marks the average length or the median of ridge length, and the vertical bar depicts plus and minus the Std or the IQR (the range between 75% quartile (upper quartile) and 25% quartile (lower quartile)).



(a) Bozorth

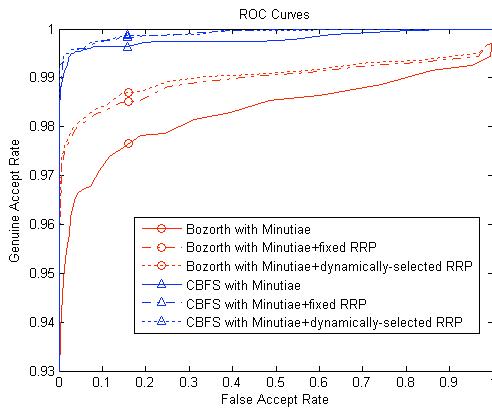


(b) K-minutiae

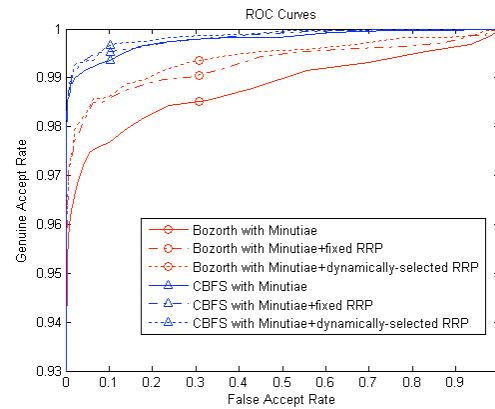
Figure 2.40: Equal Error Rate comparison using single RRP with pre-determined index on FVC2002 data set (this result is corresponding to Table 2.11). For all data sets, RRP index ranges from 2 to 14. Compared with only minutiae are used (RRP index = 0), both Bozorth and k-minutiae are improved by adding RRP.

### 2.3. RESULTS

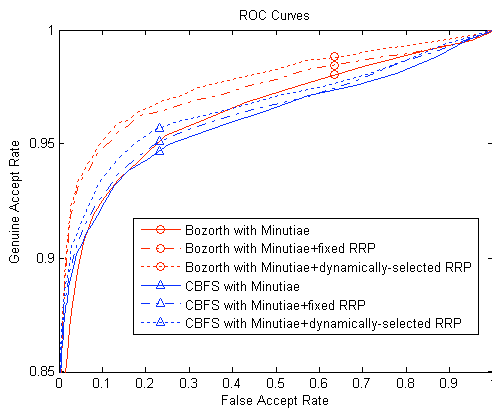
### CHAPTER 2. FINAL REPORT NARRATIVE



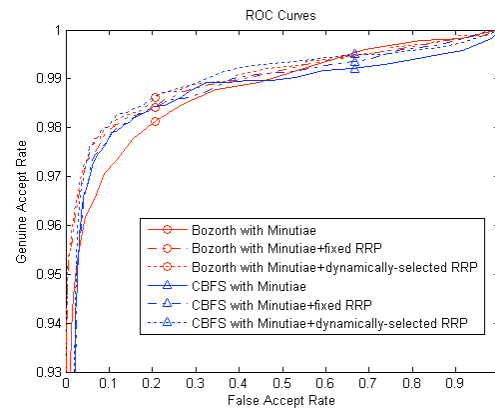
(a) DB1



(b) DB2



(c) DB3



(d) DB4

Figure 2.41: ROCs of full fingerprint matching with the four databases DB1-DB4 in FVC2002. The four curves correspond to pairwise matching (Bozorth) and  $k$  minutiae matching (CBFS) with and without RRP. In each case the ROC of minutiae+RRPs (dot and dashdot) is fully above the ROC of minutiae only (solid).

2.3. RESULTS

CHAPTER 2. FINAL REPORT NARRATIVE

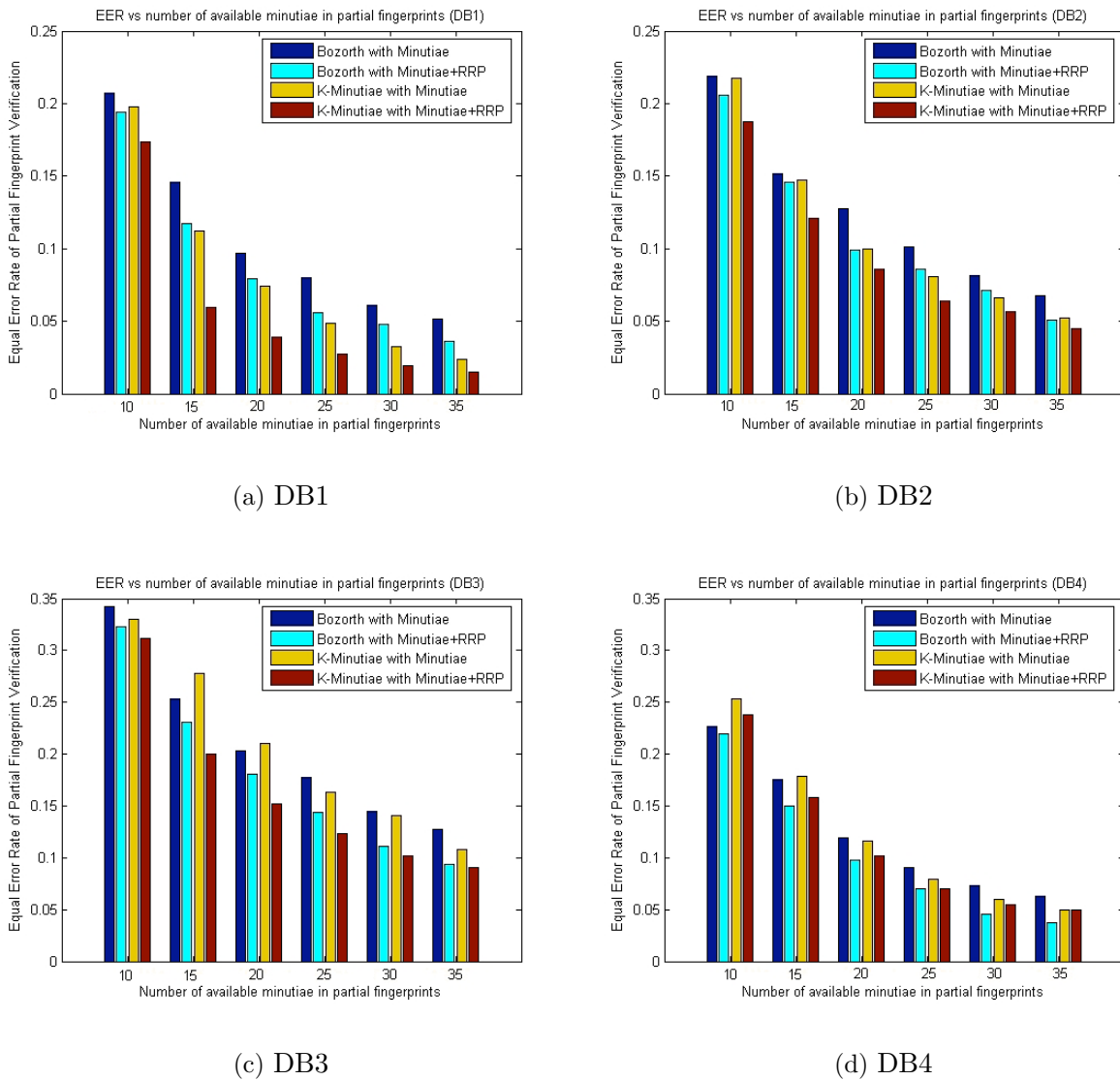


Figure 2.42: EER vs Number of Available Minutiae in Partial Fingerprint Matching.

## 2.4 Conclusions

### 2.4.1 Discussion of Findings

There is more similarity between friction ridges of corresponding fingers of twins than in the case of two arbitrary fingers. However, such pairs of twin fingerprints can be successfully discriminated using minutiae-based fingerprint algorithms. There is no significant difference between the fingerprints of identical and fraternal twins.

The probability of random correspondence between fingerprints can be characterized in terms of the number of available minutiae and the number of matching minutiae. For instance In the case of both input and template having 36 minutiae with 16 matching minutiae, this probability is 1.4 in 10 billion. This probability was calculated using both minutiae and ridge information which is much lower than using minutiae alone. The probabilities can also be expressed in terms of some pair of matching fingerprints in databases of given size. Given a database of 100,000 fingerprints, and for specific fingerprints the probabilities were calculated and were found to be very small, e.g., for a fingerprint with 26 minutiae the probability of matching 12 minutiae in a database of 100,000 fingerprints is  $10^{-45}$ .

The use of likelihood methods results in noticeable improvement over decision based on ROC curves.

Ridge points can be represented in a manner similar to minutiae, using  $x, y$  and  $\theta$  values, thereby improving the performance of matching algorithms

### 2.4.2 Implications for Policy and Practice

The net result of both the twin's study and the generative model study is that the argument for the individuality of fingerprints is strengthened. The probability of random correspondence can be used in support of admitting fingerprint evidence in courts provided the fingerprints are clear enough to have a certain number of features (minutiae and ridges) in them.

AFIS algorithms can get a small improvement in performance by utilizing likelihood ratios derived from distributions of scores rather than directly using ROC curves.

AFIS algorithms can get significant improvement in performance by using ridge points in addition to minutiae without significant degradation in matching speed.

### 2.4.3 Implications for Further Research

The twin's study can be extended to larger data sets and to palm prints.

The generative model can be derived from a larger data set and compared to the present model.

Further improvement in likelihood decision performance is possible by using mixture models or more robust distributions such as Student- $t$  distributions.

## Chapter 3

### References

The references in the Program Narrative are given below. The references are in the order in which they are referred to in the text.

# Bibliography

- [1] U. S. Supreme Court: *Daubert v. Merrell Dow Pharmaceuticals*. (1993) US 579.
- [2] U. S. District Court Eastern District of Pennsylvania: *United States of America v. Byron Mitchell*. (1999) July 7, Action No. 96-407.
- [3] Galton, F.: *Fingerprints*. McMillan, London (1892) pp.100
- [4] Henry, E.: *Classification and uses of fingerprints*. Routledge & Sons London (1900) pp.54
- [5] Wentwort, B., Wilder, H.: *Personal Identification*. Richard G. Badger, Boston (1918)
- [6] Moenssens, A.: *Fingerprint Techniques*. Chilton Book Company, Radnor, PA (1971)
- [7] Loesch, D.: *Quantitative Dermatoglyphics*. Oxford University Press, New York (1983)
- [8] Ashbaugh, D.: *Quantitative-Qualitative Friction Ridge Analysis*. CRC Press, Boca Raton, FL (1999)
- [9] of Investigation, F.B.: *The Science of Fingerprints: Classification and Uses*. Washington, D.C.: U.S. Government Printing Office (1984)
- [10] H.C.Lee, Gaensslen, R.: *Advances in Fingerprint Technology*. New York: Elsevier (1991)
- [11] Watson, C., Garris, M., Tabassi, E., Wilson, C., McCabe, R., Janet, S.: *User's Guide to NIST Fingerprint Image Software 2 (NFIS2)*. NIST (2004)
- [12] Maio, D., Maltoni, D.: *Direct gray scale minutia detection in fingerprints*. *IEEE Transactions on PAMI* **19** (1997)
- [13] Jain, A., Hong, L., Bolle, R.: *On-line fingerprint verification*. *IEEE Trans. Pattern Analysis and Machine Intelligence* (Vol.19, NO.4,pp.302-314, April 1997)
- [14] Luo, X., Tian, J., Wu, Y.: *A minutiae matching algorithm in fingerprint verification*. *Proceedings. 15th International Conference on Pattern Recognition* **4** (2000) 833–836
- [15] Cheng, J., Tian, J., Chen, H.: *Fingerprint minutiae matching with orientation and ridge*. *Proc. of International Conference on Biometric Authentication* (2004) 351–358

*BIBLIOGRAPHY*

*BIBLIOGRAPHY*

- [16] Marana, A., Jain, A.: Ridge-based fingerprint matching using hough transform. Proc. of 18th Brazilian Symposium on Computer Graphics and Image Processing (2005) 112–119
- [17] Feng, J., Ouyang, Z., Cai, A.: Fingerprint matching using ridges. Pattern Recognition **39(11)** (2006) 2131–2140
- [18] Dass, S., Jain, A., Russ, A.: Fingerprint warping using ridge curve correspondences. IEEE Transactions on Pattern Analysis and Machine Intelligence **28(1)** (2006) 19–30
- [19] Hickin, R., Korves, H., Ulery, B., Zoepfl, M., Bone, M., Grother, P., Michaels, R., Otto, S., Watson, C.: Fingerprint vendor technology evaluation (fpvte) nistir 7123. NIST, Gaithersburg MD (2003)
- [20] Evans, A., Caroline, G., Baal, M.V.: The genetics of coronary heart disease: the contribution of twin studies. In: Australian Academic Press. Volume 6(5). (2003) 432–441
- [21] Rubocki, R., McCue, B., Duffy, K., Shepard, K., Shepherd, S., Wisecarver, J.: Natural dna mixtures generated in fraternal twins in utero. In: Journal of Forensic Science. Volume 46(1). (2001) 120–125
- [22] Splitz, E., Mountier, R., Reed, T., Busnel, M.C., Marchaland, C., Robertoux, P.L., Carlier, M.: Comparative diagnoses of twin zygosity by sslp variant analysis, questionnaire, and dermatoglyphics. Behavioral Genetics **26** (1996) 56–63
- [23] Goldberg, S., Perrotta, M., Minde, K., Corter, K.: Maternal behaviour and attachment in low birthweight twins and singletons. In: Child Development. Volume 57. (1986) 34–46
- [24] S. N. Srihari, C.H., Srinivasan, H.: On the the discriminability of the handwriting of twins. Journal of Forensic Sciences **53** (2008) 430–446
- [25] A.K.Jain, S.Prabhakar, S.Pankanti: Twin test: On discriminability of fingerprints. Proceedings of third international conference on audio and video based person authentication. (2001) 211–216
- [26] Stoney, D., Thornton, J.: A critical analysis of quantitative fingerprint individuality models. Journal of Forensic Sciences **31** (1986) 1187–1216
- [27] Stoney, D.: Measurement of fingerprint individuality. In: Advances in Fingerprint Technology, 2nd Ed. By Henry C Lee, R. E Gaensslen, CRC Press (2001)
- [28] Osterburg, J.: Development of a mathematical formula for the calculation of fingerprint probabilities based on individual charectiristics. Journal of American Statistical Association **vol.772** (1997) pp.72
- [29] Roxburgh, T.: Galton’s work on the evidential value of fingerprints. Sankhya: The Indian Journal of Statistics **vol.1** (1933) pp. 62

*BIBLIOGRAPHY*

*BIBLIOGRAPHY*

- [30] Roxburgh, T.: On the evidential value of fingerprints. *Sankhya: The Indian Journal of Statistics* **vol.1** (1933) pp. 89
- [31] BaltHazard, V.: De l'identification par les empreintes digitales. *Comptes Rendus, des Academies des Sciences* **vol.152** (1911) pp.1862
- [32] Champod, C., Margot, P.: Computer assisted analysis of minutiae occurrences on fingerprints. *Proc. International Symposium on Fingerprint Detection and Identification*, J. Almog and E. Spinger, editors, Israel National Police, Jerusalem (1996) pp. 305
- [33] Trauring, M.: Automatic comparison of finger-ridge patterns. *Nature* (1963) 197, 938
- [34] Bishop, C.: *Pattern Recognition and Machine Learning*. Springer, New York (2006)
- [35] Srihari, S.N., Cha, S., Arora, H., Lee, S.: Individuality of handwriting. *Journal Of Forensic Sciences* **47** (2002) 856–872
- [36] Pankanti, S., Prabhakar, S., Jain, A.K.: On the individuality of fingerprints. *IEEE Transactions on Pattern Analysis and Machine Intelligence* **24(8)** (2002) 1010–1025
- [37] Dass, S., Zhu, Y., Jain, A.K.: Statistical models for assessing the individuality of fingerprints. *Fourth IEEE Workshop on Automatic Identification Advanced Technologies* (2005) pp.3–9
- [38] Fang, G., Srihari, S., Srinivasan, H.: Use of ridge types in generative models for fingerprint individuality. In: *Proc. International Symposium on Information Assurance and Security/ Workshop on Computational Forensics*. (2007) 423–428 Manchester, U.K.
- [39] Maltoni, D., Maio, D., Jain, A., Prabhakar, S.: *Handbook of Fingerprint Recognition*. Springer, New York (2003)
- [40] Press, W.H., Flannery, B.P., Teukolsky, S.A., Vetterling, W.T.: *Numerical Recipes in C: The Art of Scientific Computing*. Cambridge University Press (1992)
- [41] Mardia, K.V., Jupp, P.E.: *Directional Statistics*. Wiley (2000)
- [42] Chen, J., Moon, Y.S.: A minutiae-based fingerprint individuality model. *Computer Vision and Pattern Recognition, 2007. CVPR '07.* (2007)
- [43] Hsu, R.V., Martin, B.: An analysis of minutiae neighborhood probabilities. *Biometrics: Theory, Applications and Systems, 2008.* (2008)
- [44] Tabassi, E., Wilson, C., Watson, C.I.: Fingerprint image quality. *NISTIR 7151, National Institute of Standards and Technology* (2004)
- [45] Banerjee, A., Dhillon, I., Ghosh, J., Sra, S.: Generative model-based clustering of directional data. In: *Proceedings of the Ninth ACM SIGKDD International Conference on Knowledge Discovery and Data Mining.* (2003)

*BIBLIOGRAPHY*

*BIBLIOGRAPHY*

- [46] Ralph B. D'Agostino, M.A.S.: Goodness-of-fit Techniques. CRC Press (1986)
- [47] Maio, D., Maltoni, D., Cappelli, R.: Fingerprint verification competition. <http://bias.csr.unibo.it/fvc2002/> (2002)
- [48] Green, D., Swets, J.A.: Signal Detection Theory and Psychophysics. Wiley, New York (1974)
- [49] Neyman, J., Pearson, E.: On the problem of the most efficient tests of statistical hypotheses. Philosophical Transactions of the Royal Society, London **231** (1928) 289–337
- [50] Jain, A., Hong, L., Bolle, R.: Online fingerprint verification. IEEE Transactions on Pattern Analysis and Machine Intelligence **19** (1997) 302–314
- [51] Ratha, N.K., Pandit, V.D., Bolle, R.M., Vaish, V.: Robust fingerprint authentication using local structure similarity. Workshop on applications of Computer Vision (2000) 29–34
- [52] Jea, T., Govindaraju, V.: A minutia-based partial fingerprint recognition system. Pattern Recognition (Vol.38, NO.10 pp. 1672-1684, 2005)
- [53] Chikkerur, S., Cartwright, A., Govindaraju, V.: K-plet and cbfs: A graph based fingerprint representation and matching algorithm. International Conference on Biometrics (2006)
- [54] Jiang, X., Yau, W.: Fingerprint minutiae matching based on the local and global structures. International Conference on Pattern Recognition (2000) 1038–1041
- [55] Cormen, T., Leiserson, C., Rivest, R.: Introduction to Algorithms. New York: McGraw-Hill (1990)
- [56] Kingston, C., Kirk, P.: Historical development and evaluation of the '12 point rule' in fingerprint identification. International Criminal Police Review (1965)
- [57] Putte, T., Keuning, J.: Biometrical fingerprint recognition don't get your fingers burned. Fourth Working Conference on Smart Card Research and Advanced Applications (2000) 289–303
- [58] Ashbaugh, D.: Quantitative-Qualitative Friction Ridge Analysis: An Introduction to Basic and Advanced Ridgeology. CRC Press (1999)
- [59] Jain, A., Chen, Y., Demirkus, M.: Pores and ridges: High-resolution fingerprint matching using level 3 features. IEEE Transactions on Pattern Analysis and Machine Intelligence **29(1)** (2007) 15–27
- [60] Hrechak, Mchugh: Automated fingerprint recognition using structural matching. Pattern Recognition (1990) 23,no: 8

*BIBLIOGRAPHY*

*BIBLIOGRAPHY*

- [61] Ross, A., Shah, J., Jain, A.K.: Towards reconstructing fingerprints from minutiae points. Proc. of SPIE Conference on Biometric Technology for Human Identification II (2005) 68–80
- [62] Chikkerur, S., Govindaraju, V.: Fingerprint image enhancement using stft analysis. International Workshop on Pattern Recognition for Crime Prevention, Security and Surveillance (ICAPR 05) **20-29** (2005)
- [63] B.G.Sherlock, D.M.Monro, K.Millard: Fingerprint enhancement by directional fourier filtering. IEEE Proceedings of Visual Image Signal Processing **141** (1994) 87–94
- [64] Hong, L., Jain, A.K., Pankanti, S., Bolle, R.: Fingerprint enhancement. IEEE Workshop on Applications of Computer Vision (1994) 202–207
- [65] Wen, C.Y., Yu, C.C.: Fingerprint enhancement using am-fm reaction diffusion systems. Journal of Forensic Science **48** (2003)
- [66] Haralick, R., Shapiro, L.: Computer and Robot Vision, Volume I. Addison-Wesley (1992)
- [67] Pratt, K, W.: Digital Image Processing. John Wiley & Sons, Inc. (1991)
- [68] Inc., M.: Matlab image processing toolbox. Ver. 3.2, Natick, MA (2002)
- [69] Ross, A., A.K.Jain: Information fusion in biometrics. Pattern Recognition Letters (Vol.24, pp.2115-2125, 2003)
- [70] Duda, R., Hart, P., Stork, D.: Pattern Classification, Second Edition. New York: John Wiley and Sons (2000)

# Chapter 4

## Dissemination

### 4.1 Publications

#### 4.1.1 Journal Papers

1. H. Srinivasan and S. N. Srihari, “Comparison of ROC-based and Likelihood Methods in Fingerprint Verification,” in *International Journal of Pattern Recognition and Artificial Intelligence*, 22(3) 2008: 535-553.
2. S. N. Srihari, and H. Srinivasan, “Discriminability of the Fingerprints of Twins,” *Journal of Forensic Identification.*, 58(1), January 2008: 109-127.

#### 4.1.2 Papers in Conference Proceedings

1. H. Srinivasan, S. N. Srihari, M. Beal, P. Phatak and G. Fang, “Comparison of ROC-based and likelihood methods for Fingerprint Verification,” in *Biometric Technology for Human Identification III: Proceedings of SPIE Defense and Security Symposium*, Kissimmee, FL, April 17-18, 2006, pp. 620209-1 to 620209-12.
2. G. Fang, S. N. Srihari, H. Srinivasan, and P. Phatak, “Use of Ridge Points in Partial Fingerprint Matching,” in *Biometric Technology for Human Identification IV: Proceedings of SPIE*, Orlando, FL, April 9-10, 2007, pp. 65390D-1 to 65390D-9.
3. G. Fang, H. Srinivasan and S. N. Srihari, “Use of Ridge Types in Generative Models of Fingerprint Individuality,” in *Proc. Int. Symposium on Information Assurance and Security/ Int. Workshop of Computational Forensics (IWCF 2007)*, Manchester, England, Aug. 2007, IEEE-CS Press, pp. 423-428.
4. S. N. Srihari and C. Su, “Computational Methods for Determining Individuality,” in *Computational Forensics: Proceedings Second International Workshop*, Washington D.C., 2008, Springer LNCS 5158, pp. 11-21.

5. C. Su and S. N. Srihari, "Generative Models for Fingerprint Individuality using Ridge Models," in *Proceedings International Conference on Pattern Recognition*, Tampa, FL, 2008. IEEE Computer Society Press, 2008

## 4.2 Presentations

### 4.2.1 Conferences

Portions of this research were presented at the following conferences:

1. Biometric Technology for Human Identification III, Society of Photo-instrumentation Engineers, Orlando, Florida, April 2006
2. International Association for Identification, Boston, MA: July 2006
3. Int. Symposium on Information Assurance and Security/ Int. Workshop of Computational Forensics (IWCF 2007), Manchester, England, Aug. 2007
4. International Association for Identification, San Diego, CA: September 2007
5. International Workshop on Computational Forensics, Washington DC, August 2008
6. International Conference on Pattern Recognition, Tampa, Florida, December 2008

### 4.2.2 General

The individuality work was presented as part of a talk on *Computational Forensics* given at the following venues:

1. Kripas in Oslo, Norway on May 26, 2008. Kripas is the official forensic center for the Norwegian government.
2. Gjøvik University in Norway on May 27, 2008.
3. *Netherlands Forensic Institute (NFI)* in the Hague on June 2, 2008.